WOOD AND FIBER SCIENCE

The Sustainable Natural Materials Journal

Volume 54, Number 2_2022 *(ISSN 0735-6161)*

Open Access

JOURNAL OF THE

SWST – International Society of Wood Science and Technology

WOOD AND FIBER SCIENCE

Wood and Fiber Science is published quarterly in January, April, July, and October by the Society of Wood Science and Technology, P.O. Box 6155, Monona, WI 53716-6155

There are three classes of membership (electronic only) in the Society: Members – dues $150; Retired Members – dues $75; Student Members – dues $50. We also have membership category for individuals from Emerging Countries where individual members pay $30, individual students pay $10; Emerging Group of 10 pay $290, and Student Groups of 10 pay $90. Institutions and individuals who are not members pay $300 per volume (electronic only). Applications for membership and information about the Society may be obtained from the Executive Director, Society of Wood Science and Technology, P.O. Box 6155, Monona, WI 53716-6155 or found at the website http://wwww.swst.org.

Site licenses are also available with a charge of:

- $300/yr for single online membership, access by password and email
- $500/yr for institutional subscribers with 2–10 IP addresses
- $750/yr for institutional subscribers with 11–50 IP addresses
- $1000/yr for institutional subscribers with 51–100 IP addresses
- $1500/yr for institution subscribers with 101–200 IP addresses
- $2000/yr for institutions subscribers with over 200 IP addresses.

New subscriptions begin with the first issue of a new volume. All subscriptions are to be ordered through the Executive Director, Society of Wood Science and Technology.

The Executive Director, at the Business Office shown below, should be notified 30 days in advance of a change of email address.

Business Office: Society of Wood Science and Technology, P.O. Box 6155, Monona, WI 53716-6155.
Editorial Office: Susan LeVan-Green, sue.levangreen@gmail.com

SWST STUDENT CHAPTERS: A VALUABLE MEANS OF BROADENING STUDENT PERSPECTIVES IN WOOD SCIENCE AND TECHNOLOGY

*Francesco Negro**†

Assistant Professor
Department of Agricultural, Forest and Food Sciences (DISAFA)
University of Torino
Largo Paolo Braccini 2
10095 Grugliasco, Italy
E-mail: francesco.negro@unito.it

Tamara Filgueira Amorim Franca†

Assistant Professor
Department of Sustainable Bioproducts
Mississippi State University
Mississippi State, MS 39762-5724
E-mail: tsf97@msstate.edu

Eric Hansen†

Professor
Forest Products Marketing
Department Head of Wood Science and Engineering
Oregon State University
119 Richardson Hall
Corvallis, OR 97331
E-mail: eric.hansen@oregonstate.edu

(Received March 2022)

Abstract. SWST Student Chapters exist to broaden student perspectives in wood science and technology. This is pursued through the organization of various activities, including seminars, site visits, and practical experiences. Over the years, chapters have proven to be beneficial to students, first and foremost, and also to faculty advisors and involved institutions. To encourage the activation of new chapters, the know-how of faculty advisors of the existing chapters is here shared. The details on constituting and running SWST Student Chapters are illustrated, the opportunities that chapters offer are discussed, and a list of possible activities is provided for guidance.

Keywords: Education, SWST, wood science, wood technology.

INTRODUCTION

The Society of Wood Science and Technology (SWST) Student Chapters provide unique opportunities for undergraduate and graduate students to network and to broaden their perspectives in wood science. Chapters are a valuable means of professional development, and of fostering lifelong members of the society. Student Chapters can be activated by any SWST member and can be hosted, upon approval of the Executive Board, by any institution of higher education worldwide.

The main goal of SWST Student Chapters is to organize activities focused on wood science and technology, including seminars, experimental activities, site visits, and discussions with professionals and others. In general terms, through interactions among students, advisors, and industry, the chapter is an interesting educational method that in the last decade has become considerably more oriented toward practical experiences, practice of soft skills, and a learning-by-doing approach (Wachenheim 2007).

* Corresponding author
† SWST member

https://doi.org/10.22382/wfs-2022-08

SWST is aspiring to extend the number of Student Chapters. Of note, constituting and running SWST Student Chapters is free of charge. Currently, three are active, at the Department of Wood Science and Engineering, Oregon State University (OSU), at the Department of Sustainable Bioproducts, Mississippi State University (MSU), and at the Department of Agricultural, Forest and Food Sciences (DISAFA), University of Torino, Italy. Although SWST has a constitution and bylaws that should be followed by the chapters, each chapter has the opportunity to customize and adapt the activities accordingly to its needs.

Because students represent the future of both the field of wood science and the society, we as faculty advisors of existing chapters would like to share our experience in advising SWST Student Chapters, and encourage other wood science programs to reopen or activate their Student Chapter. In this view, we intend to: 1) share the know-how on constituting and running SWST Student Chapters, and 2) discuss the opportunities inherent in operation of Student Chapters.

HOW TO CONSTITUTE AN SWST STUDENT CHAPTER

The process of constituting a Student Chapter is presented as follows, based on the SWST Constitution and Bylaws and on the experience gained by running chapters. The constitution process can be divided into five steps, followed by an annual organizational step (Fig 1).

After the initial idea, the proponent should 1) preliminarily define the characteristics of the proposed Student Chapter. Vision, mission, available facilities, eventual funding, etc. can be considered in this phase. Constitutions of existing Student Chapters are available on the SWST website and can be consulted for framing this initial design. Once the main outline is defined, checking 2) with SWST, hosting institution, students, and students' associations can be recommended. This enables the assessment of the overall feasibility and to refine the elements to be included in the Constitution. Afterward, the most straightforward way to draft the Constitution 3) consists of downloading the Constitutions of Student Chapters active to date and taking them as a model. The proponent can modify or integrate the Constitution according to the specific needs of the proposed Student Chapter; SWST Bylaws on Student Chapters on the SWST website can also be consulted (https://www.swst.org/wp/education/student-chapters/ [10 Mar 2022]). Next, the Constitution and the Faculty advisor must be approved 4) both by the hosting institution and by the SWST executive board. Exchange of official attestations of approval finalizes formation of the Student Chapter. Once the Student Chapter is active, a kick-off meeting 5) can be held. In this occasion, Student officers are nominated and the overall setting is shared with participating students. From then on, an annual organizational meeting 6) shall be organized to nominate new officers, to review the past year and to set goals for the new one.

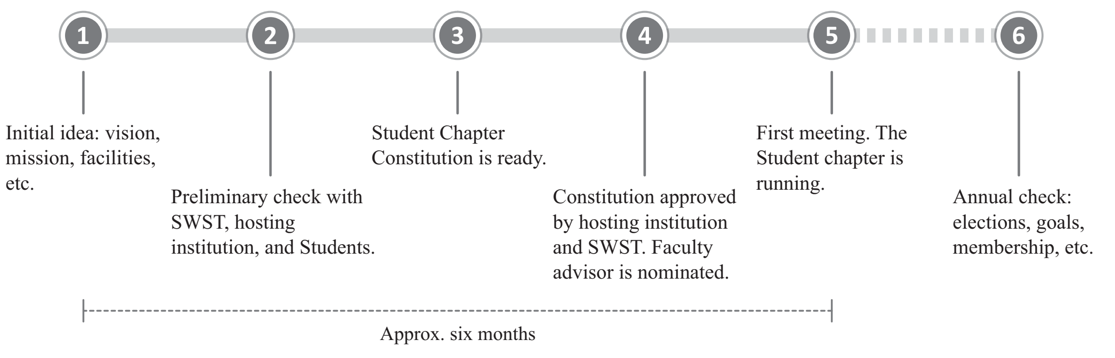

Figure 1. Outline of the constitution process of a SWST Student Chapter.

INSIGHT INTO SWST STUDENT CHAPTERS

SWST Student Chapters are intended as flexible organizations that can be set according to the specific needs of the context in which they operate. Relations with existing student associations should be managed to collaborate and to differentiate the initiatives.

Within the broad range of possible set-ups, the main considerations regarding students, faculty advisors, and institutions are presented in the following.

Students

Enrollment in Student Chapters is free of charge and can be a way for students to obtain SWST membership (see Membership in Table 1). A structured chapter can benefit undergraduate and graduate students by facilitating the organization of seminars, external visits, networking with professionals, lab/experimental activities, and team building. Chapters can ease contacts with associations and students from other sectors, like engineering, and with industries, from which internships or job opportunities can arise. Overall, chapter activities represent an alternative learning pathway, beyond formal teaching in the classroom, where students can embrace new information in an informal setting without exams, homework, etc. In addition, students have the opportunity to develop organizational and leadership skills via serving as an officer of the chapter.

Faculty Advisors

Depending on the interests of the faculty advisor, the chapter can provide an opportunity to test innovative teaching, fine tune research presentations, and build a strong service element into their CV. Although the role can be demanding, there are no specified time investments. Depending on the support given by the home institution, the faculty advisor may need to be especially in tune with issues around insurance coverage, liability, etc. Of course, an active Student Chapter can help with student recruiting, benefiting the home department, and indirectly the advisor.

Institutions

By hosting a Student Chapter, institutions acquire a valuable means of promoting practical experiences and innovative education. In addition, they increase their networking opportunities at national and international levels, and also enhance their image as international bodies. The activity of the chapter can also help in recruiting new students and in achieving higher student retention.

Table 1 provides examples of activities commonly realized by active Student Chapters. Activities can be a single event (a meeting, a seminar) or extended over time (ie the design and realization of a wooden object), and can be proposed both by the faculty advisor and by students. Goals can be directly related to wood science and technology, such as in the case of an experimental activity, or to the development of transferable skills, ie practicing English language or acquiring organizational competencies.

CONCLUSIONS

Teaching methods considerably evolved in the last decade, aiming at increased interaction, inspiring learning, innovative experiences, etc. SWST Student Chapters offer a valuable opportunity to broaden student perspectives in wood science and technology by providing a dynamic environment that favors practical experiences, team building, networking, international perspectives, etc. Actually, experience has shown that Student Chapters not only have positive impacts on students by broadening their network with professionals and promoting leadership and team-building skills, but also, they are beneficial to faculty advisors and involved institutions.

The main factors that lead to having a successful Student Chapter are the amount of time spent by advisors and students, providing high quality activities and meetings, fostering networking opportunities, and educating students to

Table 1. Example of activities realized in the past years, or already scheduled, by existing Student Chapters.

Activity	Overview	Goal	Challenge	Suggestion
Mill visits/site visits/ visit at fairs	Visit to facilities and sites, even multiple day long, combined with parallel recreational activities such as hiking and camping.	Build a team-oriented organization.	Find activities that will be interesting to all students. Eg a sawmill visit can be not attractive to students that do not want to work or do research related to this area.	Educate and motivate students to go beyond their field and show how these experiences will enrich their views.
Development of a wooden item	Guided by the faculty advisor, students design a wooden object, and realize it using the facilities of the institution.	Learning the development process (Technology Readiness Levels); practical working of wood.	The activity can be time-consuming; logistics has to be scheduled.	The activity should have a well-defined time window. Multiple units of the item should be realized so that each student can take one after the activity. The activity can also be structured as a contest.
Volunteering	Collaboration in volunteering activities that are somehow related to the curricular disciplines.	Volunteering per se; testing one's skills and learning transferable competences.	Technical aspects have to be managed, eg drafting of a formal agreement with the volunteering association.	Adequate scheduling is needed. A reference person of the volunteering association should be clearly identified.
Making of a scientific article	A scientific article authored by the speaker is presented, both to discuss the content and to show its "making of."	Deepening into a specific argument at scientific level, and introducing the research environment.	Topics and methods can be complex, especially for students enrolled in first years.	Forward the article in advance; keep the overview simple.
Book review	Parts of a book are read and discussed.	Activate the students' interest toward specific themes.	Parts to be read have to be selected to give a suitable overview of the book.	The author can be invited, in person or online, to present her/his work. The book should be made available in the institution's library.
Seminars	Seminars are held by the faculty advisor or by academics and professional.	Deepening specific topics in wood science. If the presentation is held in English, students can test their listening.	Topics and methods can be complex, especially for students enrolled in first years of course.	Keep the overview simple; double-check in advance with the speaker.

(*continued*)

Table 1. Example of activities realized in the past years, or already scheduled, by existing Student Chapters. (cont.)

Activity	Overview	Goal	Challenge	Suggestion
Thesis presentations	Students practice their Bachelor's or Master's degree presentation in front of their colleagues, prior to the final discussion; the faculty advisor comments on it.	See specific topics; candidates have the opportunity to practice their discussion in a realistic environment; students see how to work on a presentation.	Ensure that the candidate's presentation is clear; fine-tuning of the presentation can result flat.	Set the meeting just before the discussion, so that the candidate is adequately prepared; keep the fine-tuning short, just to show how the process works; encourage students to ask questions.
Organizational meeting	Once a month during spring and fall semester the Student Chapter receives a guest speaker, from industry, research institutions, and other guests.	Interaction with experienced professionals from industries, professional associations, research agencies/institutions, and others.	Maintain student engagement to the end of each term.	Schedule a day/time that fits guests' availability and that most students can attend. Meals are provided.
Membership	The chapter pays the SWST membership for students that attend at least three meetings per semester and collaborate on at least one activity.	To measure attendance and record of which students will earn the membership.	Keep students engaged to participate in the meetings after they meet the criteria to earn the membership.	Attendance is taken at the end of every meeting using an app with questions from the presentation given at the meeting. This promotes interaction between students and keeps their attention.
Financing	There is a cost involved in paying SWST memberships (see above row) and meals provided during the meetings, and any other activities that the students decide to pursue.	Pay for expenses related to SWST memberships, meals, and other activities.	Ensure that all students participate.	Fundraisings, sponsorships and services to the department. For example, MSU department needed wooden boxes for the wood anatomy collection, and the chapter received money to fabricate them.
Others	The students may come up with extra activities or clubs derived from the chapter.	Promote a deeper interaction between students outside the student's chapter.	Activate the students' interest toward specific themes.	MSU Chapter has created a "wood club" where students come together in mini-projects to learn practical work in the woodshop.

understand the value of participating in the activities promoted by the chapter. The main benefits of serving as a faculty advisor are: 1) satisfaction derived from mentoring and developing new professionals (students); 2) opportunities for the advisor to interact with stakeholders, creating opportunities for future academia-industry collaboration; and 3) contribution to tenure and promotion, as advising chapters can be listed as teaching and/or service. Being a faculty advisor does consume time, but the benefits overflow its downside. We strongly encourage other wood science programs to reopen or activate their Student Chapter.

ACKNOWLEDGMENTS

Alberto Falaschi, Jacob Atkins, Detlef Laughery, Jacob Gradwohl, Mia Craig, Alan Sherrington, Adam Wade, and Noah Babik, to date enrolled and/or officers in the active chapters, are thanked for their feedback that contributed in refining the text.

REFERENCE

Wachenheim CJ (2007) Growing and maintaining viable student chapters of professional organizations: The case of the National Agri-Marketing Association. NACTA J 51(2):60-64.

COMPARISON OF RESISTANCE AND BIODEGRADABILITY PROPERTIES OF WOOD-PLASTIC COMPOSITES FROM WOOD FLOUR/PHB/HDPE/STARCH

Hoda Norouzpour

PhD Student
E-mail: hananoroozpoor@yahoo.com

*Amir Hooman Hemmasi**

Full Professor
E-mail: h_hemmasi@srbiau.ac.ir

Mohammad Talaeipour

Associate Professor
E-mail: m.talaeipoor@srbiau.ac.ir

Behzad Bazyar

Associate Professor
Department of Wood and Paper Industry Engineering
Faculty of Natural Resources and Environment
Science and Research Branch
Islamic Azad University
Tehran, Iran
E-mail: mmh1832@gmail.com

Majid Abdouss

Department of Chemistry
Amirkabir University of Technology
Tehran, Iran
E-mail: phdabdouss44@aut.ac.ir

Amir Hooman Hemmasi

Full Professor
Department of Wood and Paper Industry Engineering
Faculty of Natural Resources and Environment
Science and Research Branch
Islamic Azad University
Tehran, Iran
E-mail: h_hemmasi@srbiau.ac.ir

(Received March 2022)

Abstract. In this study, mechanical and biodegradability properties of wood-plastic composite were investigated. Beech wood flour (WF) 40 wt% was used as a reinforcing base material, maleic anhydride (MA) as a coupling agent, and nano clay to improve the properties were added. The polymer studied was polyhydroxybutyrate (PHB) and the other polymer was high-density polyethylene (HDPE). Three groups of composites were produced, in two groups each of the polymers alone and in the third group a combination of two types of polymers was used as a matrix. Starch 8 wt% and 12 wt% was used instead copolymer. The specimens were mixed using a twin-screw extruder, made with an injection-molding machine, and subjected to mechanical tests: tensile strength and modulus, bending strength and modulus, impact resistance tests and

* Corresponding author

https://doi.org/10.22382/wfs-2022-09

biodegradability tests. In mechanical properties, it was observed that wood-plastic composite with PHB base material has lower resistance properties than composites containing HDPE. With the addition of starch, all resistance properties were significantly reduced compared with the control sample without starch in all three groups of composite samples. Starch could not play the role of copolymer well in any of the groups. The third group of samples showed better results in terms of mechanical strength resistance properties than the first group. Tensile strength and Modulus, bending strength and Modulus, impact resistance increased compared with the first group. In the biodegradability test, the samples were buried at a height of 25 cm for three months. Weight loss was due to the destruction of WF, starch, and natural polymers by soil microorganisms. The weight loss trend of the samples was increasing until the end of the second month and then decreasing.

Keywords: Wood-plastic composite, biodegradability, PHB, HDPE, starch.

INTRODUCTION

Reinforced plastic composites are a class of composites in which high-modulus fibers are added to a polymer matrix to overcome the low modulus and thermal instability of the plastic. However, today they use organic fillers such as lignocellulosic fibers. These low-cost materials are low weight, renewable, available, and biodegradable. On the other hand, the use of these composites is a good alternative to wood and polymeric materials in different applications. With the increase of environmental awareness and interest of the international community and new environmental and oil consumption regulations, the use of environment-friendly materials has increased, and this is also true for wood-plastic composites (Casarin et al 2017).

To prevent environmental damage, high cost savings, and replacement of synthetic polymers, natural polymers were used in composite fabrication. In this regard, we examined the production of wood-plastic composites based on natural polymer. The largest group of biodegradable polymers are polyhydroxy alkanoates (PHAs). Despite the higher cost of production, these materials are probably much cheaper than traditional plastics because the cost of environmental degradation and postproduction recycling costs have never been calculated (Ienz and Marchessault 2005; Chen et al 2015). PHAs are generally made up of a subunit called β-hydroxy alkanoate by a simple pathway with three enzymes of acetyl coenzyme A, the most famous of which is polyhydroxybutyrate (PHB). PHB is a short-chain biological of PHA. Its advantages include availability, biocompatibility, and physical properties comparable to plastic thermoplastics (Isola et al 2017). This polymer is a good option for making the target composite (Chan et al 2020). Investigated the mechanical stability of PHA-based wood-plastic composite and used PLA/wood flour (WF) and polyethylene (PE)/WF composites as a comparison reference. PHA-containing biocomposites were degraded when continuously submerged, unlike PE- and PLA-containing composites. The specimens were mechanically stable indoors but a decrease in stability in mechanical properties was observed outdoors. Nikushi et al (2018) investigated the improvement of compatibility of physical-mechanical properties of polymer composites based on natural materials and biodegradability. They used polylactic acid (PLA), PHB, PHB with polyhydroxyvalerate copolymer (PHBV), bioflex (PLA blend) and solanyl (Starch-based). Biocomposites show poor mechanical properties due to the weak bond between the fibers and the matrix.

Vandi et al (2019) produced PHBV-based plastic wood composite by extrusion method and investigated its mechanical properties. In the mechanical properties of the composite containing 40% of wood, it showed higher strength, which showed a 73% increase in modulus and 80% in tensile strength compared with pure PHBV. Panaitescu et al (2020) investigated the thermal and mechanical properties of PHB composite and cellulose from wood waste. Composites showed better thermal stability than PHB. In composites with 5% fiber content, 13% and 10% fiber content increased by 25%. The highest rate of increase in the composite was 10% fiber, ranging from 25% at room temperature to 90% at 125°C. The best mechanical and thermal properties of the composite compared with PHB were when lignin was present on the fiber surface. Gunning et al (2019) produced PHB-based biocomposites and three types of natural fibers by extrusion and compression injection. PHB was evaluated with hemp, jute, and lyocell with 10 wt% to 30 wt%. This study was performed to investigate the effect of fibers on the matrix. Tensile properties and impact resistance showed a significant decrease. Adding 30 wt% of hemp and jute fibers changed the modules. This value was very high in the flexural modulus. A value of about 591% was observed in hemp and 246% in jute compared with pure PHB. On the other hand, PHB/Lyocell composites showed the lowest flexural modulus. In total, the modulus values increased with fiber loading for all types of fibers.

Casarin et al (2017) to investigate the biodegradability, they made two types of composites: a composite with PHB/WF (80/20) composition and a composite with combination of PHB/fibers of sisal plants (80/20). They produced extruded plastic pipes by injection. Samples were placed in three degradation test devices for 30, 60, and 90 da. At the end of each experiment, the samples were weighed to measure the degree of degradation. Based on the results, it was observed that all samples lost their mass during the degradation test. Both types of composites lost more weight than pure PHB because of the adsorption of water due to the presence of natural fibers, which in turn creates a faster rate for PHB degradation. In flexibility tests, the modulus of elasticity decreased after composite degradation. After 30 and 60 da, the modulus of elasticity did not change much, but after 90 da, the amount of modules decreased by half. This indicates that the destruction is slow and accelerates over a period. Nicoleta Frone et al (2020), investigated the morphological structure, thermal and mechanical properties of biodegradable PLA/PHB/nanocellulose (NC) nanocomposites. They used three methods of injection, extrusion, and three-dimensional (3D) printing. The composites were fabricated by a combined single-step reaction process using dicumyl peroxide (DCP) as a bonding agent. They used plum seed shells to produce cellulose nanocrystals. Nanocrystals with a diameter between 30 and 80 nm were used. The results showed that with the addition of DCP the surface adhesion improved. The carbonyl index was calculated by infrared (IR) spectroscopy, which showed an increase in crystallinity after DCP was added to the composite mixture. This was confirmed by differential calorimetric scanning. The presence of NC and DCP caused nuclear activity and increased PLA crystallinity.

PLA/PHB composite crystallinity increased from 16% to 38% and NC/PLA/PHB composite crystallinity up to 34% because of the addition of DCP, which increased crosslinking. In addition, DCP, due to low molecular weight product production increased with mobility, also affects melting processes and recrystallization. In the study of production method, the values of higher storage modulus were for extrusion films, 3D scan, and then injection mold, respectively. The best thermal stability and high degradation temperature belonged to biocomposites containing DCP. Torres-Tello et al (2017), used agave plant to produce green biocomposite with two types of polymers PHB and PHBV. Biocomposites were produced by compression molding with two purposes, first to reduce the amount of biopolymer used (because of high cost) in the final product and second to improve the mechanical properties of the material. To evaluate the effect of fiber content, 10 wt%, 20 wt%, and 30 wt% were used to prepare the composite. The results showed that the addition of fiber at 30 wt% in both matrices increased the tensile modulus by 80% compared with PHB and by 30% compared with PHBV and also the bending modulus by about 36% and 41% for both composites, respectively, shows. In addition, tensile strength and flexural strength did not have a negative effect and the impact strength increased significantly, which was 44% and 66% for the two matrix, respectively. Koller and Owen (1996) investigated the structure and mechanical properties of PHB/corn starch and PHB/HV copolymer. To make the samples, they used the compression molding method at 190 degrees. In the PHB/starch, composite, brittle cracks were observed below 1% of the pressure, indicating that the starch fails in the PHB, reduces the strength and increases the modulus. In another part of composite fabrication, starch was treated with water, heat, and cut. This starch found better properties than the previous starch grains. However, there was not much change in the composite. Bledzki and Jaszkiewicz (2010) investigated the mechanical properties of natural fiber-reinforced PLA and PHBV composites in comparison with polypropylene (PP).

They used cellulose, jute, and abaca fibers plant as reinforcing fibers. Samples were made using injection molding. Resistance tests were performed to evaluate the mechanical performance of the composites. Electron microscopy was also used to examine the adhesion between the fibers and the matrix. In other samples, PP-containing composite was made with the same fibers studied for comparison. Fiber reinforcement significantly increased stiffness and tensile strength. However, depending on the type of fiber, there were differences in mechanical properties. Impact strength and tensile strength for composites containing cellulose fibers; the highest value was seen. In scanning electron microscope (SEM) images, matrix fiber bonding in PLA and PHBV composites was very different from PP composites. These bonds were much weaker in PHBV because of the very crystalline structure of PHBV. As a result, the bonding phase between the fiber and the matrix is reduced. As a result, the fibers are not well embedded in the matrix and a weak bond is created. The best fiber dispersion in the field belonged to Abaka fibers.

The purpose of this study is to use PHB to create the biodegradability of the composite after the service period for recycling in the natural cycle and to investigate the effect of the starch and combination of PHB and HDPE to increase the strength properties and degrade the composite after waste.

MATERIALS AND METHODS

PHB made by the British company Good fellow and HDPE purchased from Shazand Petrochemical Company of Iran was used as the base material. PHB was in the form of granules with a size of 5 mm. Persian beech flour was used as a matrix reinforcing fibers. The starch was purchased from the German Merck brand under the brand name starch 101252soluble GR, Maleic Anhydrid as a coupling agent graft with polyethylene (Pe-g-MA) from Aria polymer pioneer under the brand name Aria couple1141 as compatible and nanoclay with grade 20A of the company American Saturn was produced under the brand name Cloisite 20A. In this research, extrusion and injection molding methods were used to make samples. The WF was placed in an oven at 90°C for 24 h to dry. The studied samples were made in three different categories in terms of composition and each group had 12 samples with different percentages of materials (Table 1).

To make each sample, a specified combination of raw materials and additives was alternately poured into an extruder with twin-screw nonaligning. The extruder has six areas for heating from 145 to 165 degrees with a distance of one temperature every 5 degrees. The rotation speed of the device was 60 RMP. Ingredients of the samples were hot extruded out of the extruder and after cooling were milled to become suitable granules for the injection machine. The raw materials were turned into test samples by injection machine. The samples were made according to the standard and tested. Beech flour was used as a matrix reinforcer in 80-mesh particle size with 40 wt%. Starch with an 8 wt% and 12 wt% was used as a copolymer. To improve the strength properties of 1 wt% nano and to improve the bonds of polymer and WF, 5 wt% maleic anhydride (MA) was used.

Mechanical Tests

Tensile strength and modulus test, bending strength and modulus test, and impact resistance test were

Table 1. Percent weight of sample compositions. Beech WF/ MA/ PHB/HDPE/nano clay/starch.

1	40%WF / 5%MA/8% starch/1% nano/46% PHB
2	40%WF/5%MA/12% starch/1% nano/42% PHB
3	40%WF/5% MA/8% starch/1% nano/46% HDPE
4	40% WF/5% MA/12% starch/1% nano/42%HDPE
5	40% WF/5% MA/8% starch/1% nano/46% PHB+HDPE
6	40% WF/5% MA/12% starch/1% nano/42% PHB+HDPE

WF, wood flour; MA, maleic anhydride; PHB, polyhydroxybutyrate; HDPE, high-density polyethylene.

performed according to ASTM D638, ASTM D790, and ASTM D250 standards, respectively. The results are shown in Table 2. The test of each sample was repeated three times.

According to the results (Table 2), a decrease in strength, especially in tensile strength, was observed in samples containing PHB alone. With the addition of HDPE to the samples, all resistances increased. This is because of the mixing of two polymers in combination with WF. HDPE by adding to the composite composition increases the strength and reduces the weakness and brittleness of PHB. However, the presence of WF is effective in improving the strength. Starch and its percentage increase showed a noticeable decrease in strengths, which produced weaker composites than nonstarch samples. Compared with mechanical properties, composites containing 1% nanoclay showed better mechanical properties than pure PHB. Addition of nanoclay to the polymer matrix increased the degree of crystallinity and increased the amorphous degree of the semicrystalline PHB.

Biodegradability Test

This test is one of the main objectives of this study. Soil burial test was performed according to ASTM G160 standard. The samples were buried at a height of 25 cm for 3 mo. The soil used is the soil of Aradkooh waste processing and disposal complex located at 23 km of the old Tehran-Qom road. This soil was collected in the required amount and transferred to the test environment under natural environmental conditions. The required amount of soil was poured into 12 plastic boxes with dimensions of 18 × 35 × 50 cm. The samples were placed in each box according to the group and the time period of getting out of the soil. Soil characteristics of this center: 3% granules, 30% sand, 45% silica, and 22% clay.

The samples were placed horizontally in the soil and after certain periods, the first 2 wk, the first month, the second month, and the third month were taken out of the soil and cleaned with a soft brush to completely remove dust from their surface and then weighed. The results of each weighing step and the amount of weight loss were recorded. This weight loss is because of the destruction of WF, starch, and natural polymers by microorganisms that use these substances as food. In the samples of the second group, which contained HDPE as a synthetic polymer, the degradation was very small, which was done in WF and starch, and the polymer was not degraded, but in the first and third groups, because of the presence of PHB, in addition to WF and starch, weight loss and destruction also occurred in PHB. The amount of destruction in the first group was more than all groups. In the first 2 wk, the destruction took place slowly, but after a month, the percentage of destruction accelerated and after 2 mo, it decreased. The results are given in Tables 3 and 4.

Weathering Test

Wood-plastic composite samples were transferred to the weathering tester for weathering test. In this device, according to the standard, the samples were exposed to moisture and light rays and were tested during different hours as shown in the results diagram (2000, 1000, 500, 250 h). In the early stages, small but large cracks were seen on the surface of the samples, which due to ultraviolet (UV) radiation and exposure of the samples to

Table 2. Samples mechanical resistances (MPa).

N	Tensile strength	Tensile modulus	Bending strength	Bending modulus	Impact resistance
1	14.8	3321.5	21.7	1451.6	45.3
2	12.6	3301.09	18.87	1364.7	41.2
3	29	3633.6	36.1	1945.4	70.1
4	26.3	3477.3	27.86	1773.4	64.12
5	21.6	3385.4	27.3	1582.3	65.23
6	20.13	3314.1	26.1	1502.1	58.4

Table 3. Samples weight (gr).

N	Initial weight	2 wk	1 mo	2 mo	3 mo
1	8.902	8.853	8.786	8.714	8.672
2	8.989	8.938	8.856	8.783	8.740
3	7.22	7.203	7.189	7.186	7.180
4	7.333	7.325	7.315	7.311	7.308
5	7.827	7.800	7.761	7.729	7.703
6	8.213	8.185	8.154	8.127	8.110

moisture caused the wood fibers to swell and create surface cracks. In the later stages, the cracks increased and were larger because of radiation. Light degradation occurred in cellulose, hemicellulose, and lignin. Because the samples also contained starch, degradation also occurred in starch. Starch swells and bursts because of the presence of glucose units due to water and heat and their semicrystalline structure is destroyed so that under weathering conditions the starch in the samples is destroyed, Griffin (1994). However, its sensitivity to moisture and poor mechanical stability are the main disadvantages when compared with other commercial bioplastics, which increased with increasing weathering time. As a result, the polymer chains in the inner layers are also broken and shortened and degradation occurs in the crystalline region. Therefore, with the increase of weathering time, the amount of degradation increased. This degradation was more in the first group. In this group, PHB was degraded earlier because of its fragile structure. The results can be seen in Figs 1-5.

RESULTS AND DISCUSSION

In this study, natural PHB polymer was used to investigate the strengths and biodegradability of composites. Starch was used instead copolymer to compare and create a new combination of HDPE, and MA was added as a coupling agent and nano was added to improve the resistance properties and beech WF 40 wt% was added to reinforce the matrix. One of the main bottlenecks of PHB/lignocellulosic fibers biocomposites is the poor affinity between lignocellulosic fibers and PHB resulting in limited tensile properties. Natural fibers have polar and hygroscopic properties, whereas plastics are mostly nonpolar and hydrophobic Therefore, because of the molecular structure, there is no bond between them. A coupling agent is used to make the connection. MA has a polar end and a nonpolar end that forms an ester bond from the hydrocarbon head by nonpolar bonding to the matrix and from the other end by carboxylic groups with hydroxyl groups maleic anhydrid as a coupling agent graft with polyethylene (MAPE) connects natural fibers with polymer. In previous research, various researchers have reported the properties of nanoclay on the increase of mechanical strengths in wood-plastic composites except for impact resistance (Wang et al 2006; Chowdhury et al 2006; Wu 2007; Han et al 2008; Abdous et al 2010). Nanoclays are layered. These layers can be quadrilateral or octagonal, which are attached to

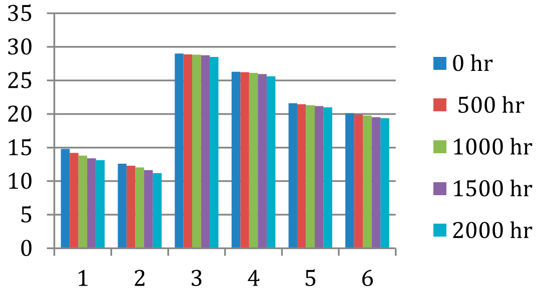

Figure 1. Mean tensile strength after weathering.

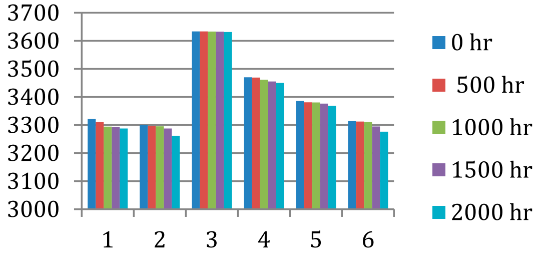

Figure 2. Mean tensile modules after weathering.

Table 4. Weight loss of samples (%).

N	2 wk	1 mo	2 mo	3 mo
1	%0.0055	%0.013151	%0.021534	%0.026568
2	%0.0057	%0.015018	%0.023432	%0.028484
3	%0.0024	%0.004312	%0.004731	%0.005571
4	%0.0011	%0.002461	%0.003009	%0.003421
5	%0.0035	%0.008504	%0.01268	%0.016098
6	%0.0034	%0.007236	%0.010582	%0.0127

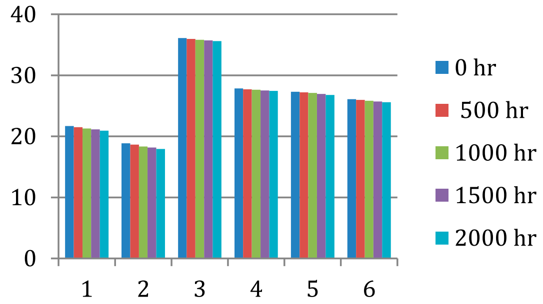

Figure 3. Mean bending strength after weathering.

the raw materials in three ways and to the other layers of nanoclay in one way. Because of the plate structure, they are placed between the raw materials and bond with van der Waals and hydrogen bonds, increasing the mechanical properties.

In mechanical properties, it was observed that plastic wood composite with PHB base material, which is a family of natural polymers, has lower strength properties than synthetic polymer base composites containing HDPE. With the addition of starch, all resistance properties showed a significant decrease compared with the control sample without starch in all three groups of composite samples. Starch could not play the role of copolymer well in any of the groups. The internal bonds between the polymer and the WF were weakened and in some cases prevented from forming a proper bond. Therefore, in terms of tensile strength, the composite showed low mechanical strength. The results showed poor mechanical properties because of insufficient adhesion and nonbinding effect and heterogeneous morphology of PHB/starch composition. This has been stated in other studies (Innocentini-mei et al 2003; Thire et al 2006; Jorres-Giner et al 2018; Gunning et al 2019).

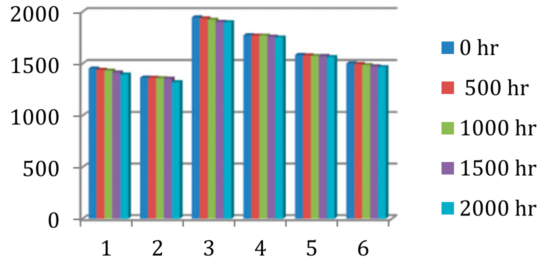

Figure 4. Mean bending modules after weathering.

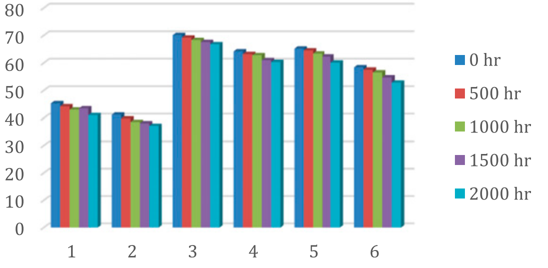

Figure 5. Mean impact resistance after weathering.

This weakness was also seen in the second group, which did not contain PHB. PHB has a high crystallinity structure. When a composite is made due to melting, its structure changes to amorphous, which is why the bonds it make with other raw materials, are weak. These bonds are nonchemical. After cooling the resulting composite, the PHB structure returns to the crystalline state and as a result, the composite shows poor mechanical properties. As a result, the bonding phase between the fiber and the matrix is reduced. We divided the polymer 50 wt%-50 wt% between PHB and HDPE. In this way, we can form a stronger internal structure and stronger bonds. PHB breaks down quickly because of its brittle structure and has less tensile strength. Combining HDPE with a composite containing PHB and spreading it during the initial melting in different parts of the composite creates stronger bonds and increases the strengths.

Accelerated weathering test was performed on the samples by Atlas Xenon. The accelerated weathering process was performed for 2000 h. In the early stages, fine cracks were seen on the surface of the samples; in the later stages, the cracks were larger and larger in size. In general, the rate of water absorption and the rate of biodegradation of polymers are the main factors controlling the mechanical stability over time, so the composite is constantly moving toward the loss of mechanical properties. These factors cause cracks and crevices, which in turn weaken the performance of the material under mechanical load. The composite showed a reduction in mass by weathering exposure. The molecular weight of PHB polymer and WF decreased steadily with increasing weathering.

During the biodegradability test, the samples were removed from the soil for 2 wk, 1 mo, 2 mo, and 3 mo after burial in the soil. Weight loss is because of the degradation of WF, starch, and natural polymers by microorganisms that use these substances as food. The weight loss trend of the samples was increasing until the end of the second month and then decreasing. With the addition of nano to the samples, the interlayer distribution of nanojoints improved. In composite specimens, the polymeric materials and additives are more compact, so that PHB and HDPE combine to form better fibers.

CONCLUSIONS

In mechanical properties, it was observed that wood-plastic composite with PHB base material has lower resistance properties than composites containing HDPE. With the addition of starch, all resistance properties were significantly reduced compared with the control sample without starch in all three groups of composite samples. Starch could not play the role of copolymer well in any of the groups. The third group of samples presented better results in terms of resistance properties than the first group. All mechanical properties increased compared with the first group. In the biodegradability test, the samples were buried at a height of 25 cm for 3 mo. Weight loss was because of the destruction of WF, starch, and natural polymers by soil microorganisms. The weight loss trend of the samples was increasing until the end of the second month and then decreasing.

REFERENCES

Abdous M, Raisi Nafgi H, Kazemi Najafi S (2010) The use of nanoclay particles in improving the functional properties of wood-plastic composites made of wood fibers-polypropylene–nanoclay. First National Conference on Nanoscience and Nanotechnology, Yazd, Iran.

Bledzki AK, Jaszkiewicz A (2010) Mechanical performance of biocomposites based on PLA and PHBV reinforced with natural fibers–A comparative study to PP. Compos Sci Technol 70(12):1687.

Casarin SA, Rodrigues CP, Souza OF Jr., De Rosario F, Agnelli JAM (2017) Biodegradation in soil of the PHB/wood flour (80/20) and PHB/Sisal fibe (80/20) tubes. Mater Res 20:47-50.

Chan CM, Vandi LJ, Pratt S, Halley PD, Richardson D, Werker A, Laycock B (2020) Mechanical stability of polyhydroxy alkanoate based wood plastics composites. Polym Environ 28:1571-1577.

Chen GQ, Hajnal I, Wu H, Lv L, Ye J (2015) Engineering biosynthesis mechanisms for diversifying polyhydroxyalkanoates. Trends Biotechnol 33:564-574.

Chowdhury FH, Hosur MV, Jeelani S (2006) Studies on the flexural and thermomechanical properties of woven carbon/nanoclay-epoxy laminates. Mater Sci Eng A 421:298-306.

Frone AN, Batalu D, Chiulan L, Oprea M, Gabor AR, Nicolae C-A, Raditioiu V, Trusca R, Panaitescu DM (2020) Morpho-structural, thermal and mechanical properties of PLA/PHB/cellulose biodegradable nanocomposites obtained by compression molding extrusion and 3D printing. Nanomater 10(1):51.

Griffin GJL (1994) Particulate starch based products. In chemistry and technology of biodegradable polymers. Blackie Academic and Precessional, London, UK.

Gunning MA, Geever LM, Killion JA, Lyons JO, Higginbotham CL (2019) Mechanical and biodegradation performance of short natural fiber poly hydroxybutyrate composites. Polym Test 32:1603-1611.

Han G, Lei Y, Wu Q, Kojima Y, Suzuki S (2008) Bamboo–fiber filled high density polyethylene composites: Effect of coupling treatment and nanoclay. J Polym Environ 21:1567-1582.

Ienz RW, Marchessault RH (2005) Bacterial polyesters: Biosynthesis, biodegradable plastics and biotechnology. Bromacromolecules 6:1-8.

Innocentini-mei LH, Bartoli RJR, Baltieri C (2003) Mechanical and thermal properties for poly (3-hydroxybutyrate) blend with starch and starch derivatives. Macromol Symp 197:77-88.

Isola C, Sieverding HL, Raghunathan R, Sibi MP, Webster DC, Sivaguru J, Ston JJ (2017) Life cycle assessment of photo degradable polymeric material derived from renewable bioresources. J Clean Prod 42:2935-2944.

Jorres-Giner S, Hilliou L, Melendez-Rodriguez B, Figueroa-Lopez KJ, Madalena D, Cabedo L, Cavas JA, Vicente AA, Logaron JM (2018) Melt process ability, characterization and antibacterial activity of compression molded green composite sheets mode of poly (3-hydroxybutyrate-co-3-hidroxyValverate) reinforced with coconut fiber impregnated with organo essential oil. Food Packag Shelf 17:39-49.

Koller I, Owen AJ (1996) Starch filled PHB and PHB/HV copolymer. Polym Int 39:175-181.

Nikushi S, Yutigala A, Bajwa S, Sreekala G (2018) Compatibilization improves physico-mechanical properties of biodegradable biobased polymer composites. Compos, Part A Appl Sci Manuf 107:315-325.

Panaitescu DM, Nicolae AC, Gabor AR, Truscam R (2020) Thermal and mechanical properties of (3-polyhydroxybutirate) reinforced with cellulose fibers from wood waste. Ind Crops Prod 145:112071.

Thire RMSM, Ribeiro TAA, Rade CT (2006) Effect of starch addition on compression-molded poly (3-hydroxybutyrate)/starch blend. J Appl Polym Sci 100:4338-4347.

Torres-Tello EV, Robledo-Ortiz JR, Gozalez-Garcia Y, Prez-Fonseca AA, Gasso-Gastinel GMF, Mendizable E (2017) Effect of agave fiber content in the thermal and mechanical properties of green composites based on polyhydroxybutyrate or (hydroxybutyrate-co-hydroxyvalerate). Ind Crops Prod 99:117-125.

Vandi LJ, Chan CM, Werker A, Richardson D, Laycock B, Part S (2019) Experimental data for extrusion processing and tensile properties of poly (hydroxybutyrate-co-hydroxyvalerate) (PHBV) polymer and wood fiber rein forced PHBV Biocomposites. Data Brief 22:687-692.

Wang L, Wang K, Chen L, Zhang Y, He C (2006-11) Preparation, morphology and thermal/mechanical properties of epoxy/nanoclay composite. Composites Part A: Applied Science and Manufacturing 37(11):1890-1896.

MOE DISTRIBUTION IN VISUALLY GRADED PONDEROSA PINE LUMBER HARVESTED FROM RESTORATION PROGRAMS IN SOUTHERN OREGON AND NORTHERN CALIFORNIA

Sina Jahedi†

Graduate Research Assistant
E-mail: jahedisina@gmail.com

Lech Muszynski†

Professor
E-mail: lech.muszynski@oregonstate.edu

Mariapaola Riggio†

Associate Professor
Department of Wood Science and Engineering
Oregon State University
Corvallis, OR 97331
E-mail: mariapaola.riggio@oregonstate.edu

Benjamin Brice Blengino

Undergraduate Student
Ecole Supérieure du Bois
Nantes, France
E-mail: benjamin.blengino@etu.es-campus.fr

Sujit Bhandari†

Graduate Research Assistant
Department of Wood Science and Engineering
Oregon State University
Corvallis, OR 97331
E-mail: sujit.bhandari@oregonstate.edu

(Received December 2021)

Abstract. Every year, restoration programs in Southern Oregon and Northern California produce large amounts of low-value ponderosa pine, *Pinus ponderosa* (PP) lumber. This material has a limited market in the United States. Engineered wood products, such as cross-laminated timber (CLT) and glulam, are expected to provide a value-added market to offset the high costs of restoration programs. However, restoration program lumber has larger amounts of juvenile wood and visual grades are reported to show lower mechanical properties compared with commercially harvested material, on which the National Design Specification (NDS) design values are based. This research addresses a knowledge gap on the impact of juvenile wood and visual strength-affecting characteristics on the mechanical performance of PP lumber generated in the region of interest. The purpose of this study was to assess this impact based on dynamically measured MOE of samples of visually graded and ungraded restoration program PP lumber. The material used in this study was intended for fabrication of CLT for another project, hence it could not be used for destructive tests to measure MOR. The results were compared with previous studies and published values for commercially harvested PP as reflected in the NDS Western Woods (WW) species group. The results show that characteristic MOE values of visual grade Nos. 1 and 2 of PP from restoration programs were lower than respective design values for NDS WW group. However, the mean MOE values of all groups considered individually as well as pooled together were higher than NDS WW grade No. 3. MOE

* Corresponding author
† SWST member

https://doi.org/10.22382/wfs-2022-10

distributions for all groups, except for the visual grade No. 1, were remarkably similar. The average MOE of PP harvested in Southern Oregon and Northern California were higher than those reported for Columbia PP harvested in North Idaho.

Keywords: Forest restoration programs, ponderosa pine, juvenile wood, visual grades, modulus of elasticity.

INTRODUCTION

The forestlands in Western United States are prone to catastrophic wildfires and pest outbreaks. Restoration programs are implemented to prevent or mitigate such events. USDA Forest Service is seeking value-added markets for logs harvested from thinning operations to offset the high costs of these programs. While utilization in structural engineered products have been proposed (Hernandez et al 2005; Larkin 2017; Lawrence 2017a, 2017b), most such products require lumber graded for structural uses. There are two common lumber grading systems used in the United States (Entsminger et al 2020). The first is visual grading, where the grade is assigned based on the characteristics that are visible to the naked eye, eg size and location of knots, grain angle, wane, etc. This task is done by either a trained lumber grader or an automated scanning system. The second system is machine grading which includes machine stress rated (MSR) and machine evaluated lumber. For machine grading system, a property of the material, commonly MOE, or density is measured as a predictor of other properties of the material, in combination with some visual limiting criteria, eg rejecting pieces with large edge knots (Entsminger et al 2020). In addition to machines that bend lumber to measure stiffness, other machines use dynamic measurements, including transverse vibration to measure stiffness from the fundamental frequency of the flatwise vibration of a piece of lumber supported at the ends.

The most common approach for restoration programs is "thinning from below," meaning that the lower crown classes or canopy layers are harvested to preserve upper crown classes or layers (Powell 2013). Pacific Northwest restoration programs consist of removing trees smaller than 0.5 m (22 in.) in diameter as well as dead trees (Smith 2021). The lumber obtained from these small diameter trees contains substantial presence of knots, wane, warp, and twist, which results in lower fractions of the higher structural grades, compared with the yield from commercial stands (Erikson et al 2000; Hernandez et al 2005; Smith 2021).

One of the species harvested in forest restoration operations in substantial quantities is ponderosa pine, *Pinus ponderosa* (abbreviated as PP in this paper; Shinneman et al 2016). Commercially harvested PP is listed among structural softwoods in the National Design Specification (NDS) supplement handbook (FPL 2010). Substantial portion of the material harvested in Southern Oregon and Northern California does not meet the requirements of structural grade lumber and is turned into chips to be used as biofuel or for fabrication of hardboards and particleboards (Smith 2021). A comparison of visual grade yield of PP in typical restoration programs to commercial harvest is presented in Table 1. One of the main causes of reduced mechanical properties in small diameter logs is the high amount of juvenile wood, which has higher microfibril angle and thinner cell walls, resulting in higher longitudinal shrinkage, lower specific gravity, and lower strength compared with mature wood (FPL 2010). The transition from juvenile wood to mature wood is gradual (Moore and Cown 2017), and it is not easy to determine the proportion of juvenile wood content in individual pieces of lumber by macroscopic visual clues. Currently, the presence of juvenile wood is not among grade-defining criteria in visual grading systems (WWPA 2017); hence, the effect of juvenile wood on the design characteristics of graded lumber is not considered. Those characteristics are mainly determined based on commercially harvested logs and cannot represent the properties of the lumber obtained from small diameter trees having high contents of juvenile wood.

Table 1. Typical ponderosa pine visual grade yield in "thinning from below" operations and comparison with commercial harvest.

References	Region	Grade No. 2 or better	Grade No. 3	Other
Erikson et al (2000)	Grangeville, ID (thinning)	47.4%	3.2%	49.4%[a]
Hernandez et al (2005)	Flagstaff, AZ (thinning)	34.0%	32.2%	33.7%[a]
This study	Lakeview, OR (thinning)	50.0%[b]	34.0%	16.0%[c]
Smith (2021)	Lakeview, OR (commercial)	70.0%	20.0%	10.0%[a]

[a] Includes economy.
[b] Includes 2% No. 1.
[c] Includes ungraded lumber.

The characteristic values of MOE and MOR of commercially harvested PP lumber were determined as a part of in-grade testing programs (Green and Evans 1987). These data were collected from approximately 80 specimens for each grade obtained from various mills around the country. No information could be found on specific locations the specimens were obtained from. Also, NDS supplement handbook provides the design values of commercially harvested PP lumber grouped with similar species as Western Woods (WW). The design values for the whole group were derived based on the weakest species for that specific property. Applying WW design values or in-grade data to restoration program PP lumber that contains a high proportion of juvenile wood is likely to result in overestimating mechanical properties. The major design values used for engineering purposes include MOE, bending strength (F_b), tension strength parallel to grain (F_t), shear strength parallel to grain (F_v), and compression perpendicular to grain ($F_{c\perp}$). Although among these properties only MOE can be measured nondestructively, it is commonly accepted that there are correlations between MOE and other properties (Green and Kretschmann 1991). As per ASTM D2915, the sample mean is used for deflection-related design values, while a 5th percentile tolerance limit is considered for derivation of strength-related design values.

A study on PP lumber obtained from restoration programs in Arizona showed that MOE of straight grained small clear specimens increases with cambial age, which is an indication of the amount of juvenile wood present in the material (Vaughan et al 2021). Detrimental effects of juvenile wood on material mechanical properties are confirmed for other pine species. A study on Loblolly pine lumber with high content of juvenile wood showed that approximately 20% of the material did not conform to the design values (MOE and ultimate tensile stress) of the assigned visual grades in NDS (Kretschmann and Bendtsen 1992). Another study collected data on 2 × 4 PP lumber harvested from restoration programs in North Idaho (Erikson et al 2000) and the results showed that PP lumber from thinning operations visually graded as No. 2 had lower MOE compared with the data published for that grade of commercially harvested PP. The subspecies (PP subsp. *ponderosa*, Columbia ponderosa pine) studied by Erikson et al 2000 is different from Pacific PP trees growing in West Oregon and Northern California (PP subsp. *critchfieldiana* Callaham, subsp. nov., Pacific ponderosa pine) investigated in this study (Callaham 2013). However, regardless of the potential differences between subspecies, there seems to be mounting evidence that the design values established for commercially harvested ponderosa pine may overestimate the actual properties of the lumber obtained from forest restoration thinning. The magnitude of the effect for PP lumber generated in the region of interest is the research gap addressed partially in this study.

A study on utilization of thinning program PP lumber (Hernandez et al 2005) showed that approximately 28% of the material can be used to produce a new PP glulam beam combination better than all PP L3-grade combinations published in the standards. The authors of this study reported that the major factors for rejection of lumber were wane and skip. A study conducted at Oregon State University suggested that lumber harvested in restoration programs in the Pacific Northwest could also be used for production of cross-laminated timber (CLT), adding to the diversity and resilience of the current schemes of utilization (Lawrence 2017a). CLT is a massive, engineered wood panel consisting of three or more orthogonally arranged plies of lumber bonded with an adhesive. ANSI APA PRG-320 (ANSI/APA 2019) specifies the requirements for fabrication, performance, and quality assurance of CLT panels in North America. Experimental studies (Larkin 2017; Lawrence 2017b) demonstrated that acceptable structural performance may be achieved in hybrid CLT layups including low-value PP lumber in the cores, however both studies failed to meet the resistance to cyclic delamination criteria. An example of the interest in using PP in construction may be a small-scale CLT manufacturer in Colorado fabricating non-structural restoration program PP panels since 2018, with the prospect to produce structural panels in the near future (Timber Age 2018).

Using restoration program PP lumber in all laminations of CLT is intended to maximize the utilization of the material in the value-added structural product. However, to predict the design properties of such layups, the design values of PP lumber generated in restoration program thinning in the Pacific Northwest must be known first. The necessary step toward structural utilization of this material is collecting representative data on the properties of the lumber. The objective of this study was to determine the distribution of the MOE in visually graded and ungraded PP lumber harvested from restoration programs in Southern Oregon and Northern California. This study is part of a broader project aimed at utilizing ungraded restoration program PP lumber in all laminations of structural CLT. The target use of the proposed CLT layup is in low-rise modular construction, identified as a potential market for such large outlet of restoration program lumber (Bhandari et al 2020).

Limitation

The PP lumber obtained for this study was intended for fabrication of CLT, performance tests on CLT elements, and construction of a demonstration CLT unit in parallel projects conducted at the Oregon State University. This precluded destructive test procedures, such as determination of MOR. Therefore, in this study, only the MOE and specific gravity distributions, which could be measured nondestructively, were determined and used for comparisons and analysis.

MATERIALS AND METHODS

While the common species harvested in Southern Oregon and Northern California restoration operations include White Fir (*Abies concolor*), and PP, only PP was the focus of this project. The lumber for this project was obtained from "thinning from below" harvest, aimed at preserving the healthy trees with a diameter larger than 560 mm. The material was harvested, sawn to 2 × 6 nominal dimension lumber (actual dimension 38 mm by 152 mm), kiln-dried to 19% MC, and visually graded by Collins Co. (Lakeview, OR). The length of the lumber was 2.44, 3.05, 3.66, or 4.88 m (8, 10, 12, or 16 ft.).

Out of the 18 units of PP lumber donated for the fabrication of prototype CLT layups for a parallel project conducted at OSU, seven units were randomly selected for nondestructive testing. A total of 810 pieces was obtained from the units, of which 84% were visually graded by the lumber company based on the standard (WWPA 2017) as following: No. 1 (2%), No. 2 (48%), and No. 3 (34%), while the rest (16%) remained ungraded (last row of Table 1). The ungraded lumber was mostly blue-stained pieces acquired from dead trees. Although this portion of the material potentially could be visually graded, there is hardly any demand for blue-stain lumber in the region, therefore, it is typically converted into chips.

Upon the arrival at OSU, the material was stored outdoors in the original tight units without any spacers between pieces and protected from rain and water exposure (July-November 2019). All pieces were visually inspected for the presence of selected grade-defining features that were easily identifiable by an untrained operator. Table 2 presents a summary of the inspection. Wane was the most frequent grade-defining feature, appearing in 54% of the specimens, followed by saw skips (29%), and dead knots (25%). The size, position and grouping of these features have not been marked.

Specific gravity and MOE of the material were determined using Metriguard E-computer Model 340 dynamic tester (Raute Metriguard 2011). The MOE calculation is based on the first mode natural frequency of the simply supported lumber (Ross 1994), where transverse vibration was induced by gently tapping the lumber at the center and data were recorded by a load cell integrated in one of the supports (Fig 1). The proprietary firmware also takes the distance between supports and cross section dimensions (assuming a perfect prismatic shape) as input data, but the documentation does not explain whether the values are actually converted to static MOE values (Raute Metriguard 2011).

MC was measured using a resistance moisture meter (Delmhorst, model RDM3) on every 10th lumber pulled from the unit in sequence, one layer at a time. Since the MC in the layers of units stored for 5 mo in sheltered outdoor condition is not expected to vary much from one piece to another, the measured MC was assigned to the next nine unmeasured pieces in the same layer. Specific gravity and modulus of elasticity of the individual lumber pieces were adjusted to the reference MC of 12% used in NDS tables based on those measured and assigned local MC values. At the time of test, the overall average MC of all pieces was 12.9% ± 0.3%.

Each specimen was marked with an ID, and the data related to grade-defining features along with MOE and specific gravity were recorded, so that the lumber could be traced in the prototype CLT production stage for future analysis. MOE design values for the sample groups were calculated following the ASTM D2915 standard procedure (ASTM International 2017), which covers "evaluation of allowable properties of specified populations of stress-graded structural lumber." As per ASTM D2915 section 5.4, the sample mean MOE is considered as the design value for serviceability.

Table 2. Frequency of pieces with selected grade-defining features (810 specimens).

Defect	No. of pieces by grade			
	No. 1	No. 2	No. 3	Ungraded
Wane	—	40%	73%	52%
Saw skips	—	24%	37%	27%
Dead knot	—	26%	24%	27%
Resin pocket	—	9%	8%	8%
Bow	—	9%	7%	5%
Blue stain	—	2%	6%	22%
Twist	—	10%	3%	4%
Crook	—	3%	6%	1%
Hole	—	0%	4%	2%
Total no. pieces	Not significant	388	271	132

RESULTS

The MOE distribution of all four groups (grade Nos 1-3 and the ungraded sample) is presented as boxplots in Fig 2. The gray clouds demonstrate the distribution of data points in each sample. The mean MOE values for grade Nos. 2, 3, and ungraded lumber were remarkably similar to each other (6.47, 6.54, and 6.42 GPa, respectively). Grade No. 1 showed a significantly higher average MOE than the other groups (7.11 GPa), but still lower than the NDS value for No. 1 in WW (7.58 GPa, marked as the top horizontal line in Fig 2). Visually comparing the data clouds and the boxplots, the MOE distributions of grade Nos

Figure 1. MOE and specific gravity measurement using Metriguard E-computer Model 340 dynamic tester.

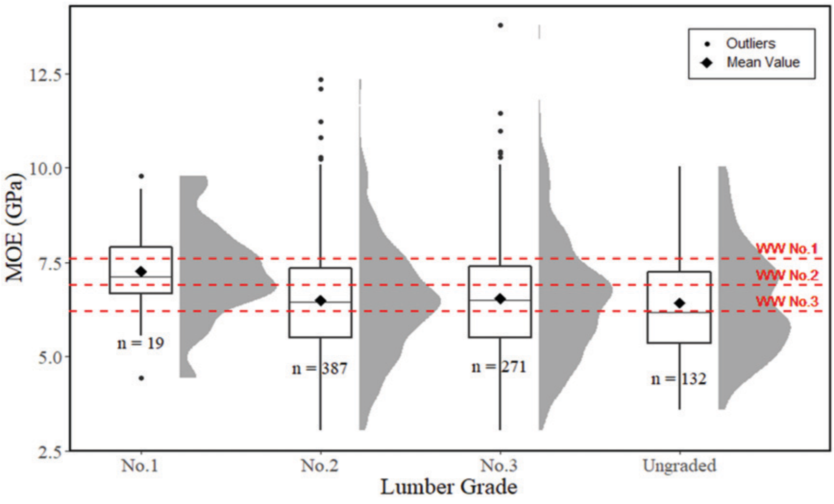

Figure 2. MOE distributions and derived design values for restoration harvested Pacific *Pinus ponderosa* compared with the design values published for Western Woods species.

2, 3, and ungraded lumber were also very similar to one another (<2% difference in average values).

While the mean MOE values of grade Nos. 1 and 2 fall below the respective NDS design values for WW (7.58 and 6.90 GPa, respectively, marked as horizontal lines in Fig 2) all mean MOE values were higher than WW grade No. 3. This means that, if the data are pooled together, the mean MOE value for the pooled group would be higher than WW grade No. 3 as well. The effect of grade No. 1, constituting just 2% of the population on the overall average MOE was negligible. Figure 3 represents the cumulative distribution of MOE for the pooled group. Based on the mean and standard deviation values, a normal distribution line was fitted to the data and a good visual match can be appreciated in the graph. The average MOE of the material for all grading groups pooled together is 6.50 GPa, which is lower than WW No. 2 but higher than WW No. 3.

Table 3 summarizes the specific gravity and MOE design value of PP individual grade groups obtained in this study compared with WW species and previous studies. Mean specific gravity of all individual grade groups of restoration program PP were similar. Following NDS format, average specific gravity of all groups combined were calculated as 0.38 ± 0.04 at the MC of 12%, which was higher than 0.36 assigned to WW species in NDS supplement handbook, and higher than the values reported for PP harvested from Northern Idaho (Erikson et al 2000). Grade Nos. 1 and 2 restoration program PP had lower MOE compared with similar grades for WW and in-grade data. However, grade No. 3 PP had higher MOE compared with grade No. 3 WW.

DISCUSSION

The fact that grade Nos. 1 and 2 restoration harvested PP lumber had lower MOE compared with the same grades for lumber harvested from commercial stands is likely a result of the presence of higher proportion of juvenile wood in the restoration program material compared with lumber generated in commercial harvesting. As mentioned in the introduction, the presence of juvenile wood reduces the mechanical properties of lumber. However, it is not easy to detect a transition line between juvenile and mature wood on a macroscale (Moore and Cown 2017); hence the proportion of juvenile wood in individual pieces of lumber cannot be easily determined by bulk visual clues (such as those used in visual grading).

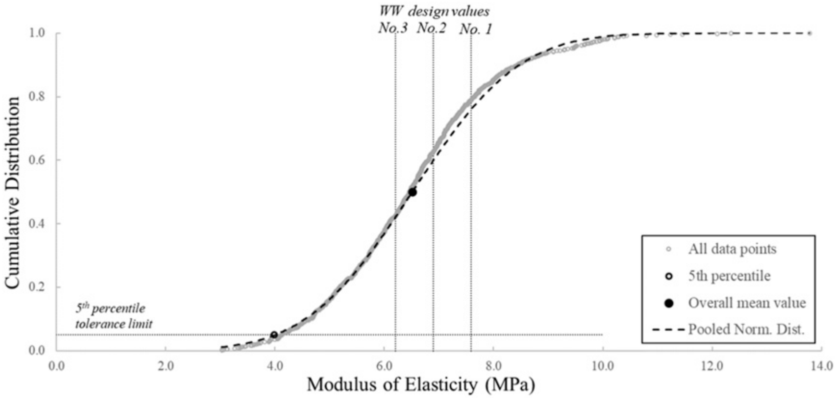

Figure 3. Pooled MOE data values for restoration harvested Pacific *Pinus ponderosa* compared with the design values published for Western Woods species.

Currently, the presence of juvenile wood is not considered a grading criterion for structural lumber.

According to in-grade data (Green and Evans 1987) commercially harvested PP has the second lowest mechanical properties among WW species, followed only by Sugar pine (*Pinus lambertiana*). All grades of restoration harvested PP lumber evaluated in this study had higher mean MOE values compared with the NDS design value for WW species grade No. 3. The material was needed for production of prototype CLT specimens and could not be subjected to destructive tests to determine strength-related properties. The exact correlation between MOE and other properties of restoration program Pacific PP could not be determined in this study and must be assumed unknown. Determination of this correlation should be a subject of a future study.

If for practical purposes it can be assumed that other properties of the lumber are directly correlated with MOE, we might also assume that the other design properties of restoration harvested PP should exceed the corresponding NDS WW No. 3 design values as well. With this assumption, the design values of WW grade No. 3 could be considered conservative approximations of design values for Southern Oregon and Northern California restoration harvested PP lumber, until exact correlations are determined.

Given the close similarities of the MOE distributions in visual grade Nos. 2 and 3 with the ungraded lumber and a marginal representation of

Table 3. Summary of specific gravity and average MOE of restoration harvested Pacific *Pinus ponderosa* (PP) lumber adjusted to 12% MC and the comparison with previous studies and commercially harvested PP.

	Location		SG	No. 1	No. 2	No. 3	Other	Pooled data
This study	SOR and NCA	MOE (GPa)	0.38	7.11	6.47	6.54	6.42[a]	6.50
		STD	(0.04)	(1.01)	(1.56)	(1.61)	(1.54)	(1.54)
Erikson et al (2000)	NID	MOE (GPa)	0.36	6.48	5.90	5.81	NA[b]	6.06[c]
		STD	—	(1.35)	(1.28)	(1.50)	—	—
Green and Evans (1987)	Mixed	MOE (GPa)	—	—	7.05	—	—	—
		STD	—	—	(1.34)	—	—	—
WW NDS	Mixed	MOE (GPa)	0.36	7.58	6.89	6.20	—	—

SOR, southern Oregon; NCA, northern California; NID, northern Idaho (N, ID); mixed, commercially harvested lumber acquired from various US mills with unknown specific locations.

[a] Ungraded.

[b] MOE values for economy not measured.

[c] Pooled data do not include economy.

No. 1, there is a potential of pooling all grades of restoration harvested PP lumber as one class of material. This might reduce complexities in the production lines of engineered wood panels utilizing lumber from restoration thinning.

One limitation of this study is that the MOE were measured by a dynamic tester machine. The manufacturer's description of the output provided by proprietary firmware does not specify any correction factors used to determine the static MOE from the dynamic modulus. In this study, it has been assumed that the output produces unadjusted dynamic MOE values, which typically overestimates the static MOE. Previous studies using the same device reported a linear correlation ($R^2 \approx 0.85$) between dynamic and static MOE measurements (Wang et al 2008; França et al 2018). The difference between these values for PP dimension lumber obtained from small diameter trees in North Idaho was approximately 4% (Erikson et al 2000). Applying similar adjustments to the dynamic MOE measured in this study does not reduce the characteristic MOE values of any group below WW grade No. 3, therefore the conclusions remain valid.

Although it is shown that the mechanical characteristics related to design values cannot be effectively differentiated by visually grading of the restoration harvested PP, by principle, grading cannot be avoided because standards for engineered wood products, such as CLT, does not permit utilization of ungraded lumber. If MSR grading is considered as an alternative for visual grading, it should be noted that the mean MOE of the restoration program PP lumber pooled in one group does not meet the MOE qualifications of any currently established standard MSR grade. One solution that can be investigated in future studies is to define a new MSR grade specifically for restoration program PP. This is also beneficial since presence of juvenile wood is not considered in the current visual grading standards, therefore performing MOE measurements is a more accurate mean for determination of the properties of restoration program lumber.

Lastly, although grade-defining features such as wane, bow, and twist do not influence mechanical properties of the restoration harvested material, excessive presence of such defects can be unfavorable for the use in engineered wood products. For instance, significant wanes that cannot be removed by surfacing the lumber cause gaps between lamellas of CLT which can accelerate moisture penetration when exposed to precipitation during open construction periods (Schmidt et al 2019) and reduce acoustic and fire performance. Substantial twist in large number of laminations may be hard to overcome in pressing CLT layups. Therefore, it is suggested to apply visual limiting criteria to the restoration harvested material accordingly.

CONCLUSIONS

MOE distribution determined on a sample of visually graded PP lumber harvested from restoration programs in Southern Oregon and northern California was compared with design values for corresponding grades determined in previous studies and with published values for commercially harvested PP as reflected in the NDS WW species group.

Characteristic MOE values of visual grade Nos. 1 and 2 of PP from restoration programs considered in this study were lower than respective design values for NDS WW group. However, the mean MOE values of all groups considered individually as well as pooled together were higher than NDS WW grade No. 3. MOE distributions for all groups, except for the visual grade No. 1, were remarkably similar, showing negligible differences in the mean values.

The design values published for WW grade No. 3 in NDS supplement handbook were suggested as provisional conservative representation of the restoration program Pacific PP lumber, until proper correlations between MOE and the other design values for the material are experimentally determined.

ACKNOWLEDGMENTS

This research is supported by the United States Department of Agriculture Wood Innovation Grants Program 2017—(17-DG-11062765-742) and 2018—(18-DG-11062765-738). The material used in the study was donated by Collins Co. (Lakeview). Special thanks to Dr. Rakesh Gupta and Lucas Walter.

REFERENCES

ANSI/APA (2019) ANSI/APA PRG 320:2019 standard for performance-rated cross-laminated timber. APA—The Engineered Wood Association, Tacoma, WA.

ASTM International (2017) ASTM D2915 standard practice for sampling and data-analysis for structural wood and wood-based products. American Society for Testing and Materials, West Conshohocken, PA.

Bhandari S, Jahedi S, Riggio M, Muszynski L, Luo Z, Polastri A (2020) CLT modular low-rise buildings: A prototype for deployable structures using low grade timber *in* World Conference on Timber Engineering (WCTE), Santiago, Chile.

Callaham RZ (2013) *Pinus ponderosa*: A taxonomic review with five subspecies in the United States. U.S. Department of Agriculture, Forest Service, Pacific Southwest Research Station Research Paper PSW-RP-264, Albany, CA. 52 pp.

Entsminger ED, Brashaw BK, Seale RD, Ross RJ (2020) Machine grading of lumber—Practical concerns for lumber producers. General Technical Report FPL-GTR-279. U.S. Department of Agriculture, Forest Service, Forest Products Laboratory, Madison, WI. 66 pp.

Erikson RG, Gorman TM, Green DW, Graham D (2000) Mechanical grading of lumber sawn from small-diameter lodgepole pine, ponderosa pine, and grand fir trees from northern Idaho. Forest Prod J 50(7/8):59-65.

FPL (2010) Wood handbook: Wood as an engineering material. General Technical Report FPL-GTR-190. U.S. Department of Agriculture, Forest Service, Forest Products Laboratory, Madison, WI. 508 pp.

França FJN, Seale RD, Ross RJ, Shmulsky R, França TSA (2018) Using transverse vibration nondestructive testing techniques to estimate stiffness and strength of Southern pine lumber. U.S. Department of Agriculture, Forest Service, Forest Products Laboratory Research Paper FPL-RP-695, Madison, WI. 8 pp.

Green D, Kretschmann D (1991) Lumber property relationships for engineering design standards. Wood Fiber Sci 23(3):436-456.

Green DW, Evans JW (1987) Mechanical properties of visually graded lumber: A summary. Vol. 1. U.S. Department of Agriculture, Forest Service, Forest Products Laboratory, Madison, WI.

Hernandez R, Green DW, Kretschmann DE, Verrill SP (2005) Improved utilization of small-diameter ponderosa pine in glulam timber. U.S. Department of Agriculture, Forest Service, Forest Products Laboratory Research Paper FPL-RP-625, Madison, WI. 36 pp.

Kretschmann D, Bendtsen B (1992) Ultimate tensile stress and modulus of elasticity of fast-grown plantation loblolly pine lumber. Wood Fiber Sci 24(2):189-203.

Larkin B (2017) Effective bonding parameters for hybrid cross-laminated timber (CLT). MS thesis, Oregon State University, Corvallis, OR. 184 pp.

Lawrence B (2017a) Utilization of low-value lumber from small-diameter logs harvested in Pacific Northwest Forest Restoration Programs in hybrid cross laminated timber (CLT) core layers: A market response. MS thesis, Oregon State University, Corvallis, OR. 114 pp.

Lawrence C (2017b) Utilization of low-value lumber from small-diameter timber harvested in Pacific Northwest Forest Restoration Programs in hybrid cross laminated timber (CLT) core layers: Technical feasibility. MS thesis, Oregon State University, Corvallis, OR. 166 pp.

Moore JR, Cown DJ (2017) Corewood (juvenile wood) and its impact on wood utilisation. Curr For Rep 2(3): 107-118.

Powell DC (2013) Silvicultural activities: Description and terminology. White Paper F14-SO-WP-Silv-34. USDA Forest Service. Pendleton, OR.

Raute Metriguard (2011) Metriguard Model 340 E-computer user manual. Pullman, WA. https://www.raute.com/ (12 November 2021).

Ross RJ (1994) Nondestructive testing for assessing wood members in structures: A review. General Technical Report FPL-GTR-70. U.S. Department of Agriculture, Forest Service, Forest Products Laboratory, Madison, WI. 40 pp.

Schmidt EL, Riggio M, Barbosa AR, Mugabo I (2019) Environmental response of a CLT floor panel: Lessons for moisture management and monitoring of mass timber buildings. Build Environ 148:609-622.

Shinneman DJ, Means RE, Potter KM, Hipkins VD (2016) Exploring climate niches of ponderosa pine (*Pinus ponderosa* Douglas ex Lawson) haplotypes in the western United States: Implications for evolutionary history and conservation. PLoS One 11(3):e0151811.

Smith G (2021) Personal communication. Collins Co., Lakeview, OR.

Timber Age (2018) Working with ponderosa. https://www.timberage.com/ (12 October 2021).

Vaughan D, Auty D, Dahlen J, Sánchez Meador AJ, Mackes KH (2021) Modelling variation in wood stiffness of *Pinus ponderosa* using static bending and acoustic measurements. Forestry 94(2):232-243.

Wang SY, Chen JH, Tsai MJ, Lin CJ, Yang TH (2008) Grading of softwood lumber using non-destructive techniques. J Mater Process Technol 208:149-158.

WWPA (2017) Western lumber grading rules. Western Wood Products Association, Portland, OR.

EVALUATING LOG STIFFNESS USING ACOUSTIC VELOCITY FOR MANUFACTURING STRUCTURAL ORIENTED STRAND BOARD

Tracye M. Murphy

Warnell School of Forestry and Natural Resources
University of Georgia
Athens, GA 30602
E-mail: tmurphy@uga.edu

L. Schimleck†

Department of Wood Science and Engineering
Oregon State University
Corvallis, OR 97331
E-mail: laurence.schimleck@oregonstate.edu

Albert Landers

Huber Engineered Woods
Commerce, GA 30538

(Received December 2021)

Abstract. Oriented strand board (OSB) is an engineered panel product formed by layering strands of resinated wood in specific orientations into a mat, then pressing the mat at a high temperature to form a panel of desired strength and stiffness. OSB manufacturing facilities utilize small diameter logs from thinning operations and waste from harvesting. Considerable variation exists in the wood properties of the raw material and ideally the OSB industry would take advantage of such variation, however, it lacks the technology required to rapidly assess log quality on-site. Nondestructive evaluation (NDE) techniques based on acoustics have the potential to rapidly segregate logs in the field, however, the influence of acoustic-based log segregation on OSB panel properties is unknown. The aims of this project were to determine whether log quality affects panel properties and if acoustic NDE technology is a satisfactory tool for determining log stiffness before entering the manufacturing process. It was found that low-velocity (stiffness) logs produced panels with low stiffness whereas high- and medium-velocity (stiffness) logs produced panels with similar properties. The Director HM 200 was a satisfactory tool for determining log stiffness. Further studies are required to determine how to incorporate NDE tools into the manufacturing process.

Keywords: Acoustics, log stiffness, oriented strand board, log sorting, log quality, engineered wood products.

INTRODUCTION

Oriented strand board (OSB) is an engineered panel product formed by layering strands of resinated wood in specific orientations into a mat, then pressing the mat at a high temperature to form a panel of desired strength and stiffness. The mat consists of approximately 90–95% soft or hardwood, 3-8% exterior grade resins, and 1-5% wax products. OSB manufacturing facilities are able to utilize small diameter logs from thinning operations and waste from harvesting while maintaining equivalent strength and stiffness to plywood. Owing to the use of low-value raw materials OSB competes with plywood on a cost basis and in the early-2000s US production of OSB exceeded production of structural plywood (Howard 2002). In 2021, North American OSB panel production was approximately 25.5 billion square feet (Forisk 2021).

Using low-quality, small-diameter logs, some OSB manufacturers are able to produce high-quality, specialty products for high-end structural uses, such as I-joists, and engineered flooring and roofing systems. However, if low-quality logs with

* Corresponding author
† SWST member

https://doi.org/10.22382/wfs-2022-11

inherently low stiffness are used to develop high-quality specialty products, then manufacturing facilities must compensate for the low stiffness furnish with more expensive materials such as resin and wax to achieve desired product properties. Considerable variation exists in the wood properties of the raw material and ideally the OSB industry would take advantage of such variation, however, it lacks the technology required to rapidly assess log quality.

Interest in the area of nondestructive wood evaluation has seen the emergence of several new techniques: acoustics (Wang et al 2007), near IR spectroscopy (Schimleck and Evans 2002), and SilviScan (Evans 2006), which are suitable for the prediction of log quality, specifically, stiffness. Of the three technologies, acoustics has been favored for on-site evaluation owing to the development of robust, inexpensive, field-based tools (Huang 2000; Carter and Lausberg 2001; Chauhan et al 2006; Wang et al 2013; Schimleck et al 2019).

Log stiffness is derived from green log density, which can be measured but is often assumed to be constant (Schimleck et al 2019), and acoustic velocity. Several studies have used acoustics to evaluate log stiffness and have examined what impact log segregation, based on acoustics, has on sawn lumber grade recovery (Ross et al 1997; Carter and Lausberg 2001; Wang et al 2002; Dickson et al 2004; Grabianowski et al 2006; Raymond et al 2008; Wang et al 2013; Butler et al 2017; Simic et al 2019). However, few studies have examined the influence of acoustic-based log segregation on composite wood products. Ross et al (1999) examined acoustics for assessing the potential quality of veneer obtained from ponderosa pine (*Pinus ponderosa* Douglas ex C.Lawson) logs and found that a strong relationship existed between log and veneer nondestructive measurements. Carter and Lausberg (2001) also reported that several trials have been conducted to examine the effectiveness of acoustics, for segregating logs for veneer production. In a study based on logs from the Central North Island of New Zealand, high stiffness logs resulted in production of 51.9% premium DT veneer product, compared against unsegregated logs of only 24.1%. Segregation using acoustics resulted in substantially higher proportions of higher stiffness veneer being produced. Ross and Pellerin (1988) also found stress wave speed to correlate well with certain mechanical properties of wood composite panels. To the best of our knowledge no studies exist that report the effects of acoustic-based log segregation on OSB panel properties.

The objective of this study was to determine whether acoustic technology could be used to presort logs for manufacturing high stiffness OSB products. The overall hypothesis is that presorting logs using acoustic technology will give manufacturers a means of optimizing their current wood use by identifying high-quality logs for structural products.

MATERIALS AND METHODS

Sample Origin

This study was based on samples from the southeast Oklahoma-Arkansas area, where samples were taken from an area having a radius of approximately 250 miles. Wood having different origins, naturally grown shortleaf pine (*Pinus echinata* Mill.) and plantation grown loblolly pine (*Pinus taeda* L.), were investigated. Preliminary velocity measurements were taken on logs from different sites to determine how it varied. A minimum of 30 measurements from both natural and plantation types were taken. All baseline data were compiled, keeping the two growth types separate. Interquartile ranges and 95% confidence intervals for the mean were calculated using Minitab Statistical Software (version 15). Based on this information, three velocity groups (high, medium, and low) were identified for the plantation and natural groups. All measurements were in imperial units.

Sample Selection

Trucks entered the manufacturing facility and stand locations along with plantation or natural type were recorded for identifying velocity trends by site. A grapple load of logs (approximately 5-10 logs) was unloaded from each truck and set aside in a pile (the truck continued further to complete unloading as standard for the manufacturing facility). Log lengths were measured in the pile as accurately as possible, and the Director HM 200 acoustic tool used to measure velocity. Logs were assigned to the appropriate velocity group and were marked with a sequential number. A total of 368 logs were tested for velocity with the distribution of velocities for logs from plantation and natural forests shown in Fig 1. The logs came from 72 trucks from 21 different counties in Texas, Arkansas, Louisiana, and Oklahoma.

Logs were spread out on the ground and measured a second time to record an accurate length. Velocity was also remeasured and if it was still within one of the target groups, the log was labeled with a color code (Table 1), in addition to the log number, and was sampled for further testing as follows:

- The first 4-6" of wood was trimmed from the butt giving a clean surface for the Director HM 200 as well as to eliminate the air-dried butt;
- Two 1-2" thick disks were cut after the butt was trimmed. One was used for MC, age, and diameter determination, the second used for specific gravity determination;
- The following 2′ of log after the disks were cut was sampled for clear lumber testing;
- Following the clear lumber sample, a 10′ bolt was cut for OSB manufacture; and
- Sampling continued along the length of the tree in the same manner: 2" disks then 2′ bolts, and finally 10′ logs. Most of the logs sampled were long enough to provide 2-10′ bolts, 2-2′ bolts, and 3 sets of disks.

Flake Manufacture

The 10′ bolts were sent to the University of Maine (UM) for debarking, stranding, and drying. Debarking was done by hand using a draw knife once the logs arrived at UM, and then the debarked logs were sprayed periodically with

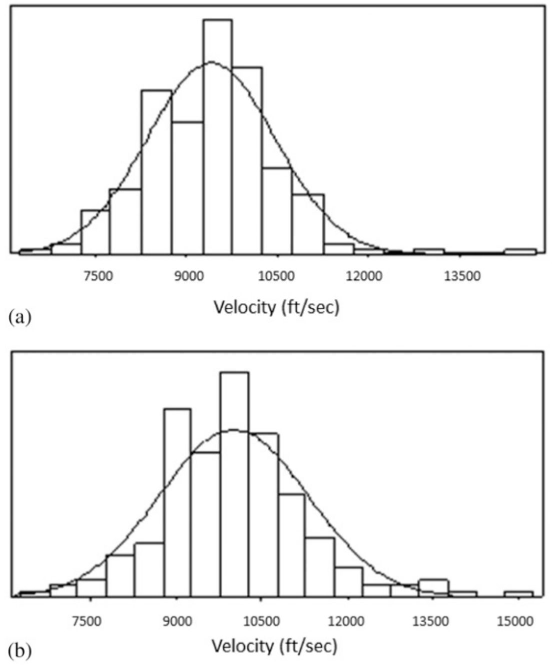

Figure 1. Distribution of velocities for logs from (a) plantation (186 logs) and (b) natural forests (182).

Table 1. Summary of stiffness groups.

Source	Color code	Velocity group	Velocity min (ft/sec)	Velocity max (ft/sec)	# Logs sampled	Av. length (ft.)
Plantation	Red	1	7480	8957	7	40.6
	Green	2	9416	11,089	11	38.6
	Purple	3	11,122	14,731	9	37.8
Natural	Orange	4	7054	8432	13	27.5
	None	5	8530	10,827	3	42.3
	Blue	6	11,089	14,961	7	30.9

water to keep them from drying out prior to stranding. Stranding was completed using a Carmanah 12/48 ring strander capable of processing logs up to 13" diameter to a target flake thickness of 0.025". Flake length was targeted at approximately 6", whereas width was difficult to control owing to variable log diameter, so only a visual target was used (acceptable or not acceptable). Prior to drying, fines (material less than 0.125") were screened out using an Acrowood Trillium Diamond Roll screen. A Koch Bros. Low Temperature Conveyor Dryer was used to dry strands to approximately 8-10% MC. Strands were passed through the dryer at 340°F at 3′ per minute, giving a 3.3 min residence time for the 10′ long dryer.

OSB Manufacture

The strands (in approximately 50 plastic-lined Gaylord boxes) were sent to the Alberta Research Council (ARC) test facility located in Edmonton, Canada, for OSB manufacture. Strands were redried upon arrival at the ARC facility in a hot air box dryer to 8% MC. After drying, strands were batch blended in a coil blender and a liquid isocyanate resin was applied with a single atomizing head; emulsified wax was applied with an air atomization system at loadings typical to a high-strength OSB product. Three-layer panels were produced on a single opening hot oil press at 420°F with the surface orientation being parallel and the core orientation perpendicular, ie typical orientation for OSB production. After pressing for approximately 4 min, panels were trimmed to final size, density was calculated, and panels were allowed to hot stack overnight prior to OSB panel testing at a private testing lab.

OSB Testing

Panels were tested according to Table 2. Properties evaluated were full panel stiffness in both the parallel and perpendicular strength directions (Panel flexure-QL-3), small sample bending for strength and stiffness (MOE and MOR, respectively, along with bending strength in parallel and perpendicular panel directions (FbS)), dimensional stability parallel and perpendicular (linear expansion ≤), and water absorption and thickness swell on edge (water absorption (ABS) and thickness swell (TS), respectively).

Statistical Analysis

All log and full panel data analysis was performed using Minitab Statistical Software version 15 (Student edition). Dynamic MOE (DMOE) was calculated from the measured log velocities. Variables considered from the raw stem data were site location (site), inside bark butt diameter in inches (IBD), green and basic specific gravity (GSG and BSG, respectively), and tree age (age). All data were analyzed for relationships with either log velocity (V) or DMOE. All data were analyzed using naturally and plantation grown wood as separate groups.

RESULTS

Full Panel Testing

Full panel bending, panel flexure, was tested according to ASTM D 3043 method C (2000). A summary of the results by velocity group is shown in Table 3. Group 1, the low-velocity (stiffness) plantation group, gave parallel EI values from 423,683 to 507,755 lb-in^2/ft with an average of 468,460 lb-in^2/ft. In comparison, group

Table 2. OSB Panel testing matrix.

Test	Method	Conditions (vel. group[a])	Panels per condition	Samples per panel	Total samples
Panel flexure (QL-3) EI	ASTM D 3043-C	6	7	2	84
Small sample bending - MOE, EI, MOR, FbS	ASTM D 3043-D	6	7	4	168
Dimensional stability - LE	PS2	6	7	4	168
Water absorption	ASTM D 1037	6	7	4	168
Thickness swell	ASTM D 1037 PS2	6	7	4	168

LE, linear expansion; OSB, oriented strand board.
[a] See Table 1 for the six velocity groups.

4, the low-velocity natural group gave parallel EI values from 353,406 to 476,419 lb-in^2/ft with an average of 437,345 lb-in^2/ft. The high-velocity groups had similar performance with an average of 511,802 lb-in^2/ft. (range of 454,787 to 558,726 lb-in^2/ft) for plantation grown wood and an average of 519,783 lb-in^2/ft (range from 400,182 to 596,165 lb-in^2/ft) for naturally grown wood. Perpendicular EI results were similar for the plantation and natural groups. The middle velocity logs of the parallel and perpendicular EI groups of both growth types had slightly higher averages than the other groups with higher minimum and maximum values.

Small Sample Testing

Small sample bending was tested according to ASTM D 3043 (2000) method D: three-point bending using an MTS universal test machine. A summary of results is given in Table 4. Plantation grown trees resulted in parallel small sample stiffness of 1.045×10^6 psi, with 441,042 in*lbf EI for the low log velocity group, a MOE of 1.193×10^6 psi, with an EI of 503,311 in*lbf for the middle group, and a MOE of 1.224×10^6 psi with a EI of 516,767 in*lbf for the high log velocity group. Naturally grown trees had similar parallel small sample stiffness with 1.023×10^6 psi, with 431,950 in*lbf EI for the low log velocity group, a MOE of 1.208×10^6 psi, with 509,773 in*lbf EI for the middle group, and 1.278×10^6 psi MOE with an EI of 539,283 in*lbf for the high log velocity group.

Perpendicular small sample stiffness ranged from 396,382 psi (167,224 in*lbf EI) to 355,637 psi (150,035 in*lbf EI) for plantation grown trees, and 360575 (152,118 in*lbf EI) to 341,855 psi (144,221 in*lbf EI) for the low and high log velocity groups, respectively. Strength results were similar for all groups with high standard deviations for both the naturally grown and the plantation grown trees. The low-velocity plantation group resulted in a parallel MOR of 7657 psi with an FbS of 8614 lbf*in; the high-velocity group resulted in a MOR of 8196 psi (9221 lbf*in FbS) with the middle group resulting in a MOR of 8444 psi and a FbS of 9500 lbf*in and standard deviations ranging from 1543 to 887 psi and 1736 psi to 997 lbf*in FbS for the low- and high-velocity groups, respectively. The low-velocity naturally grown trees showed a parallel MOR of 7535 psi with an FbS of 8477 lbf*in. The middle

Table 3. Summary of full panel bending test results.

Velocity group	Avg. Para EI lb-in^2/ft	St. Dev. Para EI	Min. Para EI lb-in^2/ft	Max. Para EI lb-in^2/ft	Avg. Perp EI lb-in^2/ft	St. Dev Perp EI	Min. Perp EI lb-in^2/ft	Max. Perp EI lb-in^2/ft	*N*
1	468,460	27,506	423,683	507,755	200,382	14,131	181,587	228,351	10
2	519,123	29,340	476,882	570,536	191,164	8928	177,956	208,963	14
3	511,802	35,237	454,787	558,726	183,089	8276	169,557	193,269	12
4	437,345	38,018	353,406	476,419	177,304	11,185	161,751	197,359	14
5	531,667	30,269	491,763	577,644	196,799	11,096	180,342	207,987	8
6	519,738	59,678	400,182	596,165	180,973	13,099	160,865	206,298	12

Table 4. Summary of small sample test results.

Velocity group	1	2	3	4	5	6
Avg. Para MOE (psi)	1,045,430	1,193,030	1,224,925	1,023,879	1,208,349	1,278,298
Avg. Para MOR (psi)	7657	8444	8196	7535	7734	8031
Avg. Para FbS (lbf*in)	8614	9500	9221	8477	8701	9035
Avg. Perp MOE (psi)	396,382	396,392	355,637	360,575	377,605	341,855
Avg. Perp MOR (psi)	3158	3261	3098	2936	3112	2936
Avg. Perp FbS (lbf*in)	3552	3668	3.485	3303	3501	3304
Avg. Para % LE	0.174	0.178	0.190	0.190	0.210	0.195
Avg. Perp % LE	0.352	0.351	0.368	0.375	0.438	0.400
Avg. % Water Abs.	17.3	17.9	18.5	17.8	20.9	18.9
Avg. % Edge Swell	10.7	11.5	11.5	11.3	12.4	12.0

LE, linear expansion.

log velocity group resulted in a MOR of 7734 psi (8477 lbf*in FbS) with the high-velocity group resulting in a MOR of 8031 psi (9035 lbf*in FbS) with similarly high standard deviations.

Dimensional stability was tested in the parallel and perpendicular strength axis using the LE wet/redry method of Voluntary Product Standard PS2-04 (2004). None of the samples in either machine direction were above the expansion limit of 0.5%. The parallel direction resulted in 0.174-0.190% expansion for the plantation groups and 0.190-0.195% for the natural growth groups (low-to high-velocity groups).

Water absorption and thickness swell were evaluated using the 24-h water soak/oven dry method in ASTM D 1037 (1999). Data for both properties were very similar for all groups and growth types.

Relationships were observed between the log velocity groups of plantation grown trees and full panel stiffness (EI) in both longitudinal and transverse directions, small sample bending stiffness parallel and perpendicular (MOE/EI), dimensional stability parallel and perpendicular (LE), and edge swell. For naturally grown trees, relationships were observed between the velocity groups and parallel full panel stiffness (EI), small sample bending stiffness parallel and perpendicular (MOE/EI), and perpendicular dimensional stability. Analysis of variance (ANOVA) was conducted to determine which velocity groups were significantly different for each of the tests that showed correlations with the log velocity groups. Analysis of parallel EI showed that the low-velocity plantation and natural groups performed poorly compared with the middle- and high-velocity groups (Fig 2). Perpendicular EI only showed a significant difference in the plantation grown trees with the high-velocity group performing poorly compared with the middle- and low-velocity groups (Fig 3).

ANOVA of small sample bending results showed the low-velocity groups for both growth types did not perform as well as the middle- and high-velocity groups for parallel stiffness, whereas the high-velocity groups did not perform as well in the perpendicular panel directions. Figures 4 and 5 show boxplots of the parallel and perpendicular results, respectively.

An ANOVA of dimensional stability showed the high-velocity group in the plantation growth type did not perform as well as the other velocity groups in the parallel and perpendicular directions (Figs 6 and 7). However, in the natural growth condition for perpendicular dimensional stability, the performance of each group was significantly different from each other, with the low-velocity group showing the best results, followed by the high- and middle-velocity groups.

No significant differences were seen in water absorption, but for the plantation grown trees the low stiffness group performed better than the middle- and high-velocity groups. No differences were seen in the naturally grown trees (Fig 8).

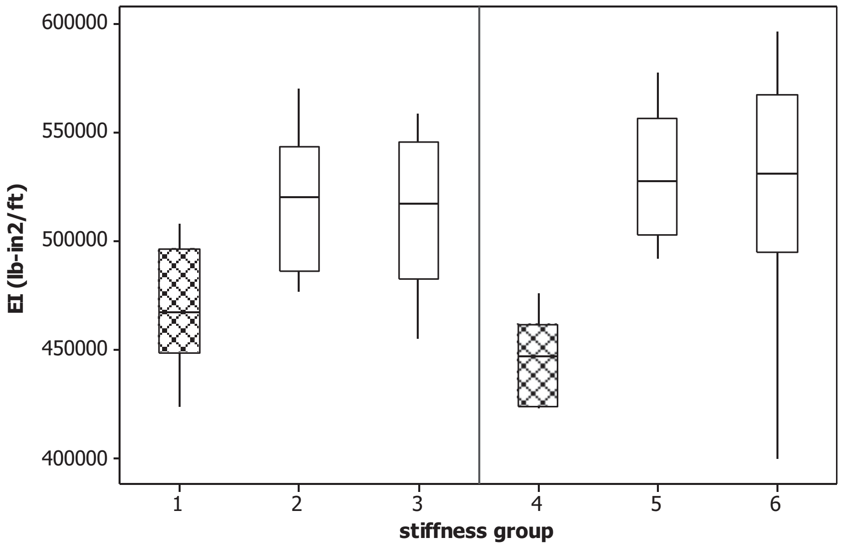

Figure 2. Plot of parallel full panel bending EI. Significant differences are denoted by the patterned boxes.

DISCUSSION

Relationships were observed between log velocity (stiffness) groups and full panel stiffness, small sample bending stiffness, dimensional stability, and edge swell. Analysis showed that, in general, the low log velocity groups had poor full panel and small sample stiffness in the parallel machine direction with better dimensional stability and edge swell. The middle and high log velocity groups rarely performed differently from each other, while the low-velocity groups negatively influenced OSB panel stiffness. The high log velocity groups showed the poorest results in perpendicular panel stiffness and dimensional

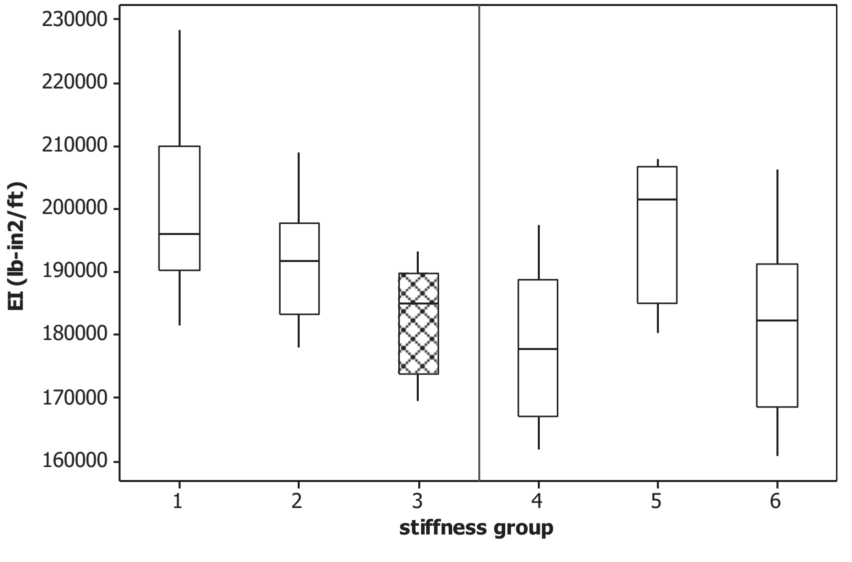

Figure 3. Plot of perpendicular full panel bending EI. Significant differences denoted by patterned boxes.

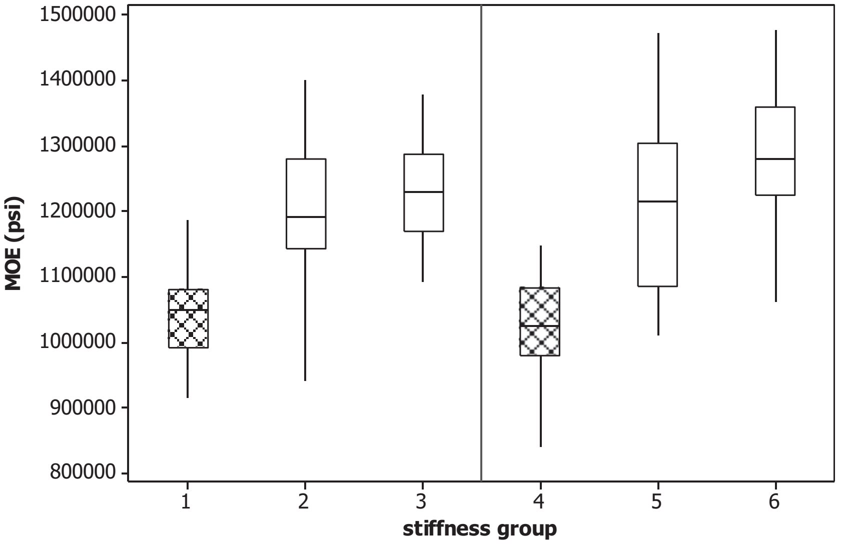

Figure 4. Plot of parallel small sample bending MOE. Significant differences denoted by patterned boxes.

stability. Typically, perpendicular panel properties are controlled more by manufacturing operations than by raw material quality, so poor performance along the perpendicular strength axis is not a concern for quality.

Plantation and naturally grown trees from the area sampled do not need to be segregated; log quality indicated no difference between growth types. The most important factor for segregation in the region analyzed was log velocity. The lowest velocity groups negatively impacted panel stiffness, which is the most important and the most difficult panel property to control by manipulating manufacturing parameters (Wu 1998; Wang and Winistorfer 2000). If low-velocity (stiffness) logs

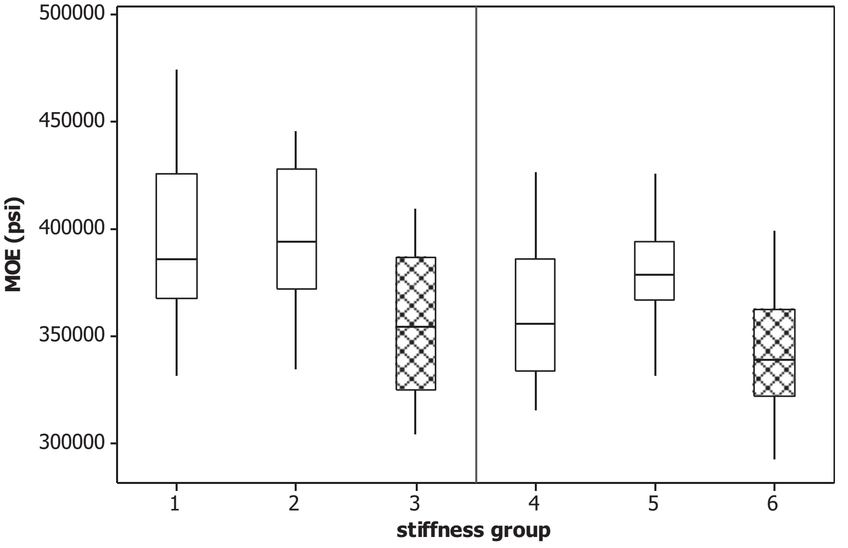

Figure 5. Plot of perpendicular small sample bending MOE. Significant differences denoted by patterned boxes.

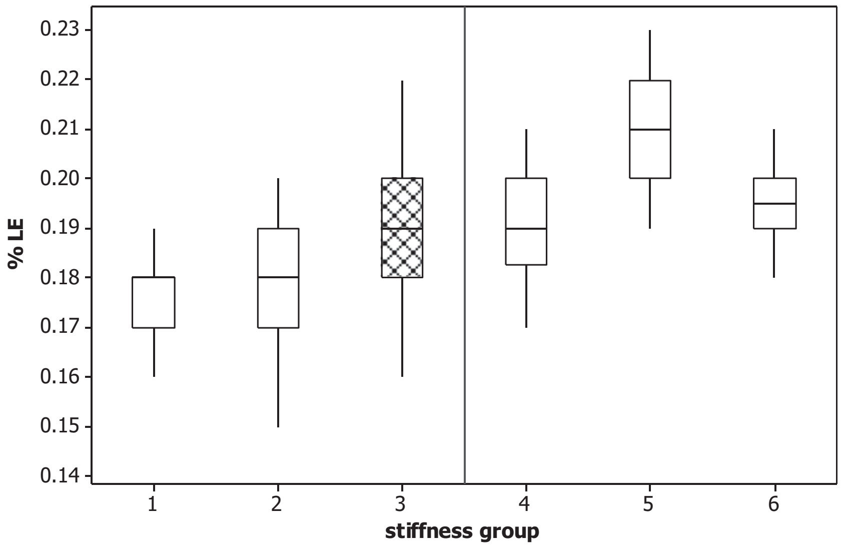

Figure 6. Plot of parallel linear expansion (%LE). Significant differences denoted by patterned boxes.

can be excluded before processing, panel stiffness should go up and ideally the amount of rejected material due to low quality would go down. Similar results have been seen in the lumber, plywood, and veneer industries using acoustic-based techniques (Carter and Lausberg 2001; Dickson et al 2005; Ross et al 2005; Moore et al 2013; Butler et al 2017; Simic et al 2019).

It was noted during processing that larger logs produced wider flakes due to the limitations of the laboratory flaker used. More of the lower stiffness material came from logs of larger diameter, which in turn had wider flakes. It was hoped that flake width would adjust itself by breakage of the flakes during the drying and blending processes, but the laboratory equipment was extremely gentle with

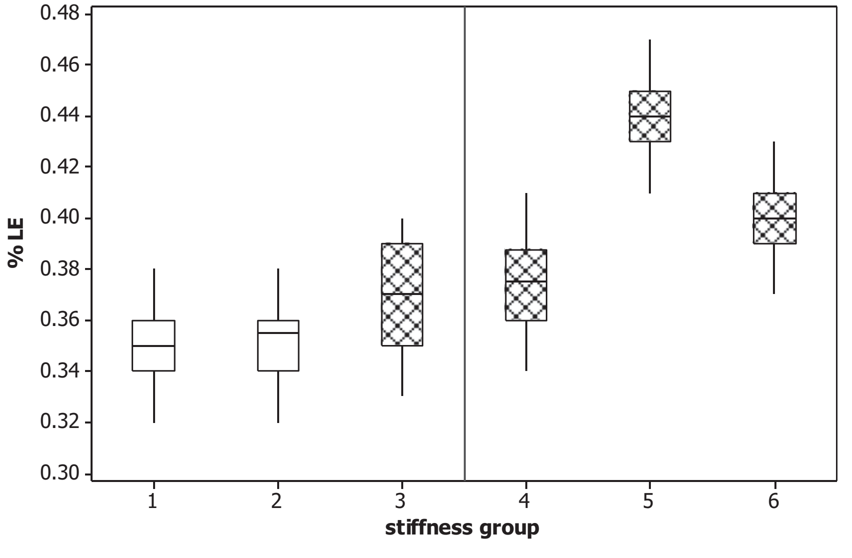

Figure 7. Plot of perpendicular linear expansion (%LE). Significant differences denoted by patterned boxes.

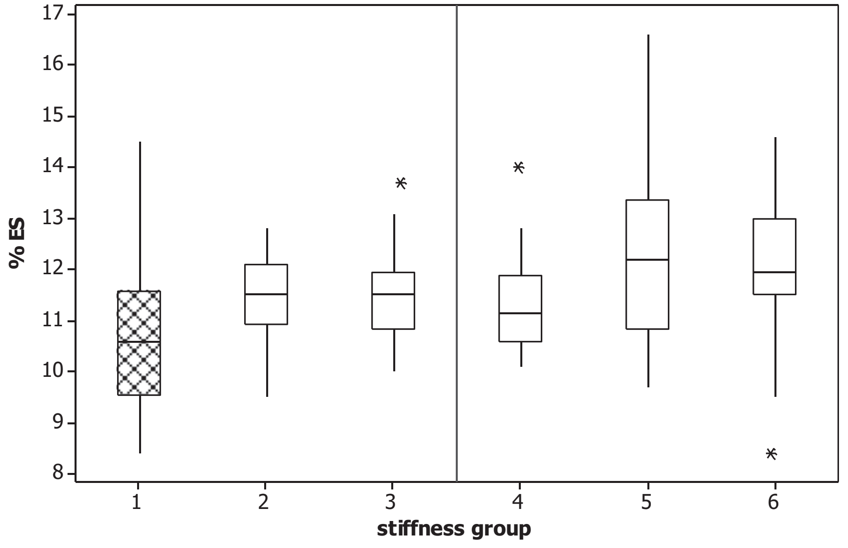

Figure 8. Plot of percent edge swell (%ES). Significant differences denoted by patterned boxes.

material (as the aim was to produce the best furnish possible), however, this is not true for manufacturing facilities. Perpendicular strength and stiffness as well as dimensional stability and water properties are significantly affected by wider flakes (Shuler and Kelly 1976; Wu 1998).

Low log velocity groups also showed significantly better dimensional stability and edge swell likely due to the wider flakes. In terms of this study, there was a lot of variation in the test results for edge swell and LE, so the difference detected might have been related to the relatively small sample size.

Overall, differences in log velocity (or stiffness calculated from velocity) had little or no effect on OSB panel properties other than stiffness, the single most important panel property. One explanation is that the logs were generally young and probably had a high proportion of juvenile wood which will lower OSB panel performance (Pugel et al 1990; Cloutier et al 2007). In general, acoustic velocity is an indicator of log quality. If low-velocity logs are segregated from the higher quality material, a stiffer panel should be made under normal operations. If producing a stiffer panel is not a problem for the manufacturing facility, using only higher velocity logs could result in the ability to lower panel densities, lower resin, and overall reduce raw material costs. If a plant does not make lower stiffness products, the purchase of low-velocity/stiffness material could be avoided by eliminating it at procurement sites. This approach would require some additional studies and would require the manufacturing facility to buy mostly procured logs, not gatewood, which is the current practice.

This study showed that log quality can affect OSB panel properties and that acoustic-based technology can be used to presort logs prior to processing to identify and remove low-velocity/stiffness logs from the high-velocity/stiffness material for high-strength structural panel production. However, the incorporation of acoustic tools into a manufacturing facility was not investigated. Important components to consider if acoustics were to be utilized for log segregation include the development of a sampling strategy and an examination of financial feasibility.

CONCLUSIONS

Relationships were observed between log velocity (stiffness) groups and full panel stiffness as well as small sample stiffness. Analysis showed that, in general, the low log velocity groups had poor full panel and small sample stiffness in the parallel machine direction. The middle and high log velocity groups rarely performed differently, hence the low-velocity groups negatively influenced OSB panel stiffness. This indicates that by removing low-velocity logs from the material used to produce high-quality structural panels, a higher stiffness panel will be produced. This creates opportunities to lower panel densities and reduce resin usage, as well as reducing downgrade.

Relationships were also observed between log velocity groups and dimensional stability, internal bond, and edge swell. The low log velocity groups generally showed low internal bonding, better dimensional stability, and edge swell.

The high log velocity groups showed the poorest results in perpendicular panel stiffness and dimensional stability. Typically, these panel properties are controlled more by manufacturing operations than by raw material quality, so poor performance along the perpendicular strength axis is not a major concern for quality.

ACKNOWLEDGMENTS

The authors thank Huber Engineered Woods for acoustic instrumentation, sample collection, small sample testing, and financial support. The authors would also like to thank University of Maine and Alberta Research Council staff for the manufacture of OSB flakes and panels.

REFERENCES

ASTM (1999) D1037: Standard test methods for evaluating properties of wood-base fiber and particle panel materials. ASTM, West Conshohocken, PA.

ASTM (2000a) D3043: Standard test methods for testing structural panels in flexure - Method C, pure moment test. ASTM, West Conshohocken, PA.

ASTM (2000b) D3043: Standard test methods for testing structural panels in flexure - Method D, flexure test for quality assurance. ASTM, West Conshohocken, PA.

Butler MA, Dahlen J, Eberhardt TL, Montes C, Antony F, Daniels RF (2017) Acoustic evaluation of loblolly pine tree- and lumber-length logs allows for segregation of lumber modulus of elasticity, not for modulus of rupture. Ann Sci 74:1-15.

Carter P, Lausberg M (2001) Application of Hitman® acoustic technology—The Carter Holt Harvey Experience. FIEA paper *in* Proc 4th Wood Quality Workshop: Tools & Technologies to Improve Log & Wood Products Segregation. Forest Industry Engineering Association, Rotorua, New Zealand, 29-30th October 2001.

Chauhan S, Donnelly R, Huang CL, Nakada R, Yafang Y, Walker J (2006) Wood quality: Multifaceted opportunities. Pages 159-202 *in* JC Walker, ed. Primary wood processing, principles and practice, 2nd edition. Springer, Dordrecht, The Netherlands.

Cloutier A, Ananias R, Ballerini A, Pecho R (2007) Effect of radiata pine juvenile wood on the physical and mechanical properties of oriented strandboard. Holz Roh Werkst 65:157-162.

Dickson R, Joe B, Harris P, Holtorf S, Wilkinson CA (2004) Acoustic segregation of Australian-grown *Pinus radiata* logs for structural board production. Aust For 67(4):261-266.

Dickson R, Joe B, Johnston D, Austin S, Ribton-Turner F (2005) Pre-processing prediction of wood quality in peeler logs and saw logs. Aust For 68(3):186-191.

Evans R (2006) Wood stiffness by X-ray diffractometry. Pages 138-146 *in* DD Stokke and LH Groom LH, eds. Characterization of the cellulosic cell wall. Blackwell Publishing, IA.

Forisk (2021) Top 10 North American Structural Panel Producers. https://forisk.com/blog/2021/03/23/top-10-north-american-structural-panel-producers/ (4 December 2021).

Grabianowski M, Manley B, Walker JCF (2006) Acoustic measurements on standing trees, logs and green lumber. Wood Sci Technol 40:205-216.

Huang CL (2000) Predicting lumber stiffness of standing trees. *In* Proc 12th International Nondestructive Testing and Evaluation of Wood Symposium, September 13-15, 2000, Sopron, Hungary.

Moore JR, Lyon AJ, Searles GJ, Lehneke SA, Ridley-Ellis DJ (2013) Within- and between-stand variation in selected properties of Sitka spruce sawn timber in the UK: Implications for segregation and grade recovery. Ann Sci 70:403-415.

Pugel AD, Price EW, Hse CY (1990) Composites from southern yellow pine juvenile wood. Part 1. Panel fabrication and initial properties. Forest Prod J 40(1):29-33.

Raymond CA, Joe B, Anderson DW, Watt DJE (2008) Effect of thinning on relationships between three measures of wood stiffness in *Pinus radiata*: Standing trees vs. logs vs. short clear specimens. Can J Res 38:2870-2879.

Ross R, Pellerin R (1988) NDE of wood-based composites with longitudinal stress waves. Forest Prod J 38(5):39-45.

Ross RJ, McDonald KA, Green DW, Schad KC (1997) Relationship between log and lumber modulus of elasticity. Forest Prod J 47(2):89-92.

Ross RJ, Willits SW, von Segen W, Black T, Brashaw BK, Pellerin RF (1999) A stress wave based approach to NDE of logs for assessing potential veneer quality. Part 1. Small-diameter ponderosa pine. Forest Prod J 49(11/12):60-62.

Ross R, Zerbe J, Wang X, Green D, Pellerin R (2005) Stress wave nondestructive evaluation of Douglas-fir peeler cores. Forest Prod J 55(3):90-94.

Schimleck LR, Evans R (2002) Estimation of wood stiffness of increment cores by near infrared spectroscopy: The development and application of calibrations based on selected cores. IAWA J 23(3):217-224.

Schimleck L, Apiolaza L, Dahlen J, Downes G, Emms G, Evans R, Moore J, Pâques L, Van den Bulcke J, Wang X (2019) Non-destructive evaluation techniques and what they tell us about wood property variation. Forests 10:728.

Shuler CE, Kelly RA (1976) Effect of flake geometry on mechanical properties of eastern spruce flake-type particleboard. Forest Prod J 26(6):24-31.

Simic K, Gendvilas V, O'Reilly C, Harte AM (2019) Predicting structural timber grade-determining properties using acoustic and density measurements on young Sitka spruce trees and logs. Holzforschung 73:139-149.

Voluntary Product Standard PS2-04 (2004) Performance standard for wood-based structural-use panels. https://www.nist.gov/system/files/documents/2017/06/13/ps2-04.pdf (4 December 2021).

Wang S, Winistorfer PM (2000) Fundamentals of vertical density profile formation in wood composites. Part II. Methodology of vertical density formation under dynamic conditions. Wood Fiber Sci 32(2):230-238.

Wang X, Ross RJ, Green DW, Englund K, Wolcott M (2002) Nondestructive evaluation for sorting red maple logs. *In* Proc 13th Int Sym on Nondestructive Testing of Wood, August 19-21, 2002, Berkeley, CA.

Wang X, Carter P, Ross RJ, Brashaw BK (2007) Acoustic assessment of wood quality of raw forest materials - a path to increased profitability. Forest Prod J 57:6-14.

Wang X, Verrill S, Lowell E, Ross RJ, Herian VL (2013) Acoustic sorting models for improved log segregation. Wood Fiber Sci 45(4):343-352.

Wu Q (1998) In-plane stability of oriented strandboard: Layer properties in relation to processing variables. Wood Fiber Sci 31(1):28-40.

COMPARISON OF THE EFFECT OF TMP PITCH CONTROL AGENTS WITH DIFFERENT MECHANISMS

Chul-Hwan Kim
Professor
E-mail: jameskim@gnu.ac.kr

*Min-Seok Lee**
Graduate Student
E-mail: symara9@naver.com

Ji-Young Lee
Professor
E-mail: paperyjy@gnu.ac.kr

Jeong-Heon Ryu
Graduate Student
E-mail: aof05@naver.com

Jin-Hwa Park
Graduate Student
E-mail: wlsghk2332@naver.com

Jin-Hong Park
Undergraduate Student
Department of Forest Products
IALS, Gyeongsang National University
Jinju, 52828, Korea
E-mail: skyeowl12@naver.com

(Received December 2021)

Abstract. The pitch contained in thermomechanical pulp (TMP) negatively affects paper quality, pulp, and the papermaking process. Serious pitch and stickies problems may occur in paper recycling processes. In this study, the effects of chemicals used to control the pitch in the TMP process were compared. The method used to analyze the pitch control effect was to perform image analysis after using a reagent that selectively stains only the hydrophobic pitch. Three different mechanisms, namely fixation, detackification, and dispersion, were applied to solve the pitch problem from TMP. All the control agents were effective in pitch control, and, in particular, the agents related to fixation and dispersion were found to be more effective in reducing the number and area of tacky particles per unit area in sheets and white water. However, it was difficult to clearly identify the effect of both the detackifiers and the dispersant agents through image analysis after staining except for the fixative agent.

Keywords: Pitch, stickies, TMP, fixing agent, detackifier, dispersing agent.

INTRODUCTION

In the pulp and paper industry, pitch problems often occur, primarily in the form of the precipitation of organic tacky material escaping from water suspensions as spots on papermaking equipment or in the paper web itself (Guéra et al 2005). A significant part of the pitch exists in a colloidally dispersed form. The tacky components originating from the resins and extractives of wood consist of a mixture of different components

* Corresponding author

https://doi.org/10.22382/wfs-2022-12

having similar physical characteristics. The low-molecular-weight substances they are practically insoluble in water under alkaline or acidic conditions (Putz 2000).

The pitches can bond with each other to become larger particles, or they can remain suspended in the process water (Gutiérrez et al 2004). When recycling postconsumer paper, stickies are tacky substances contained in the paper pulp and process water systems of paper machines. Contaminations of paper that are classified as tacky are also called stickies. The main sources for stickies are recycled paper, waxes, and soft adhesives. Stickies cause quality problems or other serious problems similar to pitch, and these problems result in loss of runnability and high costs for papermakers (Sarja 2007).

Conventional ways of controlling pitch from wood chips include seasoning of raw materials before pulping. However, seasoning of wood chips is often unacceptable because of yield loss, decreased brightness because of biological deterioration, and lack of storage space (Scheepers 2000). To deal with this problem, various methods have been adopted in paper mills, including chemical and enzymatic treatments (Hata et al 1996; Bobacka et al 1999; Sui et al 2015). Enzymatic control is a method of removing triglyceride, which is a pitch component present in wood, through enzymatic hydrolysis. However, it is sensitive to temperature and heat because of the nature of enzyme activity.

The general measure used to control or prevent tacky substances during papermaking is the use of additives, and the best way to deal with stickies include avoiding them by selecting the kind of pulp source. The additives used in a pulp suspension to reduce the negative effects of pitch or stickies can be organic or inorganic (Putz 2000; Vahasalo and Holmbom 2006). They can also be used to a certain degree directly at the paper machine, where they help to prevent problems with deposits (Putz 2000; Vahasalo and Holmbom 2006). One way to prevent anionic pitch or sticky particles from accumulating in process water is to use a cationic polymer to fix these particles to anionic fibers so that they come out together with the end products (Putz 2000). The effect of these fixing agents is highly dependent on how they interact with the surface of the tacky particles (Sarja 2007). Cationic polyacrylamide (C-PAM) is very commonly used as a flocculant for retention (Sarja 2007). Poly-diallyl-dimethyl ammonium chloride (poly-DADMAC) together with acrylic acid or acrylamide is patented for deposit control (Song et al 2006; Sarja 2007) High polymer dosages contribute not only to good retention of stickies, but also to good fiber fines and filler retention (Fogarty 1993; Putz 2000). Another common method to control pitches or stickies is the addition of inorganic minerals to the recycled pulp slurry or thermomechanical pulp (TMP) stock. Adsorption of the minerals to the surface of pitch or sticky particles can reduce the tackiness of these harmful substances. For detackification of pitches and stickies, talc has been most widely used since the 1960s (Putz 2000). Usually, surfactant-based dispersants with a hydrophilic head and a hydrophobic tail tend to direct the hydrophobic tail part toward the pitch deposits and the head toward the water phase, thereby imparting a repulsive force between the pitch deposits (Hanu 1993; Hubbe et al 2006). The most widely used dispersant is an anionic surfactant. There is also a concern that, because of poor control of dispersants, dispersed tacky particles may cause another deposit problem, but in some cases, it has helped papermakers to overcome certain problems from pitches and stickies (Allen 1980; Grönfors et al 1991; Carter and Hyder 1993; Wågberg 2000; Hubbe et al 2006).

It is not easy to evaluate the effect of several types of pitch- or stickies-control agents with different mechanisms. Most mills verify their effects through trouble analysis, which occurs during the process after adding the control agents. BASF has developed a device that can measure the number and size of resin particles by dispersing the resin particles contained in the process water, dyeing them with a fluorescent dye, and detecting the optical signal excited by a laser light (Champ et al 2006). As this device cannot detect particles smaller than 0.8 microns, they are counted after making fine resin particles into large aggregates with a polymer coagulant. Gupta and Hodgson (1998) used various dyes to quantify only the hydrophobic sticky particles among old corrugated containers, and confirmed that Sudan IV showed the best selective dyeing effect among them. Nam et al (2015) developed a method for measuring the number and area of pitch particles after selectively dyeing the hydrophobic and tacky particles in sheets and white water by applying Gupta and Hodgson's method.

In this study, the pitch control effect was compared using various pitch control agents having three mechanisms, namely dispersion, fixation, and detackification, to control the pitch particles contained in TMP. For this purpose, the pitch quantification method applied by Nam et al (2015) was used.

MATERIALS AND METHODS

Raw Materials

TMP stock collected in Jeonju Paper Co., Ltd. in Korea was used to evaluate the effect of the pitch control agents. TMP was manufactured from Korean red pine (*Pinus densiflora*).

Pitch Control Agents Used for Pitch Control

Pitch control agents currently supplied to pulp and paper mills in Korea were collected to investigate the effect of pitch control in TMP stock. The chemical suppliers were Kemira Co., Ltd., Nalco Co., Ltd., BASF Co., Ltd., Solenis Co., Ltd., and Buckman Co., Ltd. The exact product names of the chemicals provided by each supplier are not disclosed by the request of the company, and only the types of chemicals, defined by their mechanism of action, are described, as shown in Table 1. The amount added for each agent was based on the application range recommended by the suppliers.

Procedure of Pitch Analysis

The stepwise procedure of dyeing the transferred pitch particles on the paper sheet with the furnish is shown in Figure 1. This process has already been described in previously published papers (Nam et al 2015). First, a dye solution was prepared by dissolving 0.7 g of Sudan IV in 100 mL of ethylene glycol. It was dissolved using a magnetic stirrer at 100°C for several minutes. The hot dye solution was filtered twice through Whatman No. 2 filter paper. The handsheet with a basis weight of 50 g/m^2 was immersed into the dye solution at about 40°C and was stained for about 5 min. The dyed handsheet was transferred to 85% propylene or ethylene glycol in water and gently agitated for about 30 s to wash away the excess stain. The stained handsheet was briefly rinsed with distilled water and mounted on a slide in 30% glycerin in water.

The stepwise procedure of preparing specimens for observing the pitches contained in white water is shown in Figure 2. First, TMP stock was decanted into a Büchner funnel in which 100 mesh wire was placed, and only white water was filtered out. White water was filtered again through

Table 1. Addition amounts for different pitch control agents.

Chemical types	Symbol	Supplier's recommendation (ppm)	Applied amount for each agent (ppm)		
Fixative (polyamine type)	F1	500-1000	500	750	1000
Fixative (poly-DADMAC type)	F2	500-1000	500	750	1000
Fixative (poly-DADMAC type)	F3	1000	1000		2000
Fixative (aliphatic polyamine type)	F4	1000↑	1000		2000
Fixative (PEI type)	F5	1000↑	1000		2000
Fixative (Polyvinylamine type)	F6	1000↑	1000		2000
Detackifier (Talc)	DT1	500-1500	500	1000	1500
Detackifier (Talc & bentonite)	DT2	1000-2000	1000	1500	2000
Dispersive (nonionic surfactant)	DP1	200-1000	200	600	1000
Dispersive (anionic surfactant)	DP2	200-1000	200	600	1000

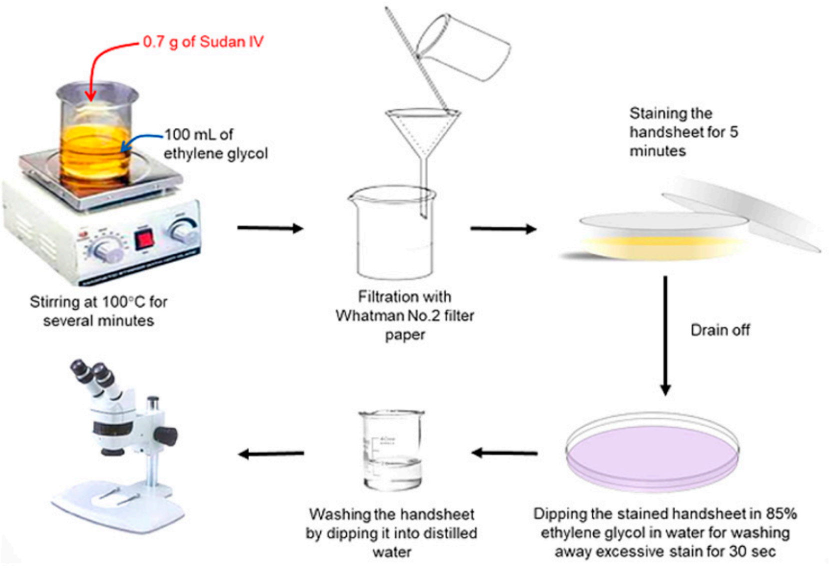

Figure 1. Stepwise procedure for staining paper specimens contaminated by pitch.

Whatman filter paper No.2 to collect only pitch particles. The pitch particles filtered onto the paper were dyed according to the method described in Figure 1.

Image analysis. Pitch images (×15, total area 63.21 mm^2) were acquired using a stereomicroscope (Leica, Japan) to measure the number and area of pitches on the dyed specimens (refer to Figure 3[a]), which were automatically quantified using Axiovision software (ver. 4.4, Carl Zeiss, Germany) under certain conditions. The pixel value of the pitch image was converted to mm or µm to measure the actual area of the pitch through the captured image. As shown in Figure 3(b), after measuring the number and area of pitches, the pitch data were compared using MS Excel. The final analyzed sample image is shown in

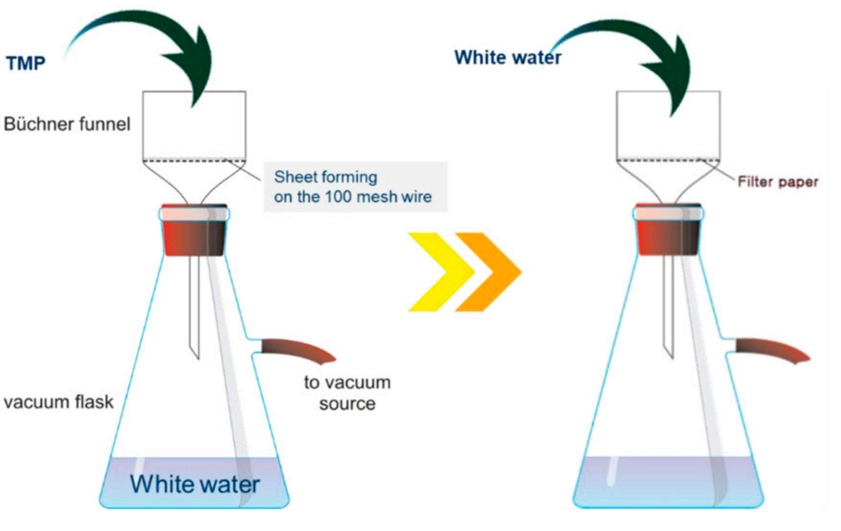

Figure 2. Stepwise procedure for staining pitches contained in white water.

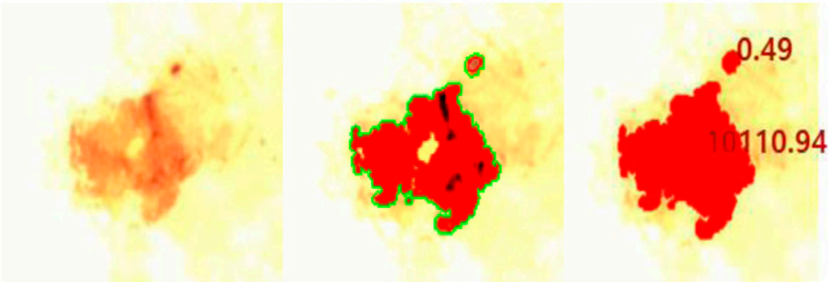

Figure 3. Stepwise procedure for analyzing pitch deposits.

Figure 3(c), the number of each pitch was counted and the area of each pitch was thus obtained. The images were automatically analyzed under certain settings during image analysis so that subjective judgment by any operator did not intervene.

RESULTS AND DISCUSSION

Pitch Controlling Effect by Fixation

Chemicals that remove pitches by fixation make colloidal substances into aggregates in the stock, adhere to fibers or fines, and come out with the final paper sheet (refer to Figure 4). Therefore, since very tiny pitch particles are aggregated and transferred into the sheet with the addition of the fixing agent, a large number of pitches should be detected on the sheet and the number of pitches included in the white water might decrease. Typical chemicals include polyDADMAC, polyethyleneimine (PEI), polyacrylamide, diamine polymer, and dicyanoamide polymers. Unlike retention aids, these polymers have a smaller molecular weight and are supplied in an aqueous solution (Hubbe et al 2006).

Before the addition of a fixing agent, the colloidal tacky particles were dispersed in a very small size in pulp suspension. As shown in Figure 4, when the fixing agent is added, the tacky particles are coagulated to form large particles and fixed onto the fiber surface. If the pitches are not properly controlled, these tacky particles can agglomerate and form very large deposits, causing problems with sheets and dryer felts.

Figure 5 shows the red-stained images of the pitch deposits detected in the sheet and white water before the fixing agent was treated. The pitch particles were coagulated and a large area of the deposits was detected in both the sheet and

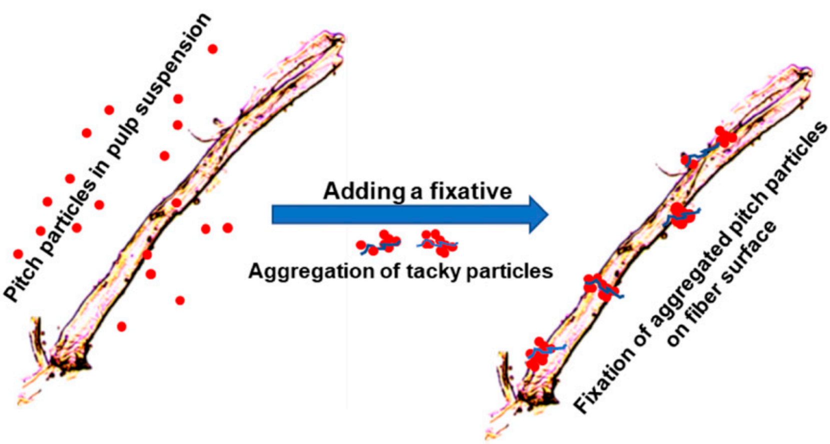

Figure 4. Conceptual diagram of a fixative that fix tacky particles onto a fiber.

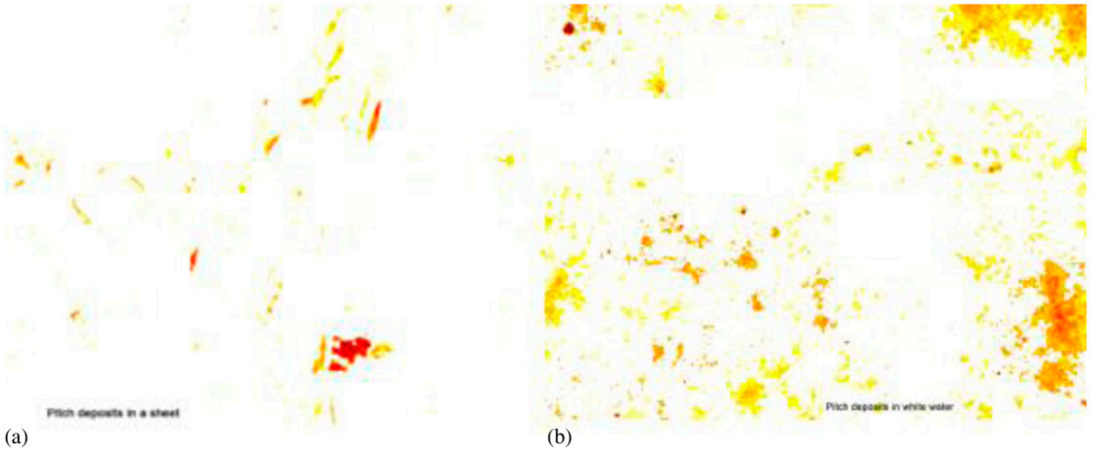

Figure 5. Images of stained pitch deposits transferred to a sheet and white water before a fixative treatment. (a) Pitch deposits in a sheet and (b) Pitch deposits in white water.

the white water. If the fixative was not added, the pitch particles were easily aggregated and deposited during the drying process of the sheet, and then transferred to the sheet or came out with white water and stuck to the pipe.

Before the fixatives were added, the number of pitches that escaped with the white water as the sheet was formed was detected much more than in the sheet (refer to Figure 6). However, the number of pitches per unit area on the sheet and in white water was remarkably reduced with the addition of the fixatives compared with the control. It was believed that the number of tacky particles in TMP suspension and white water was sharply reduced because the fixatives to coagulate the colloidal particles were bound to the fibers. In the end, since the fixatives caught many tacky

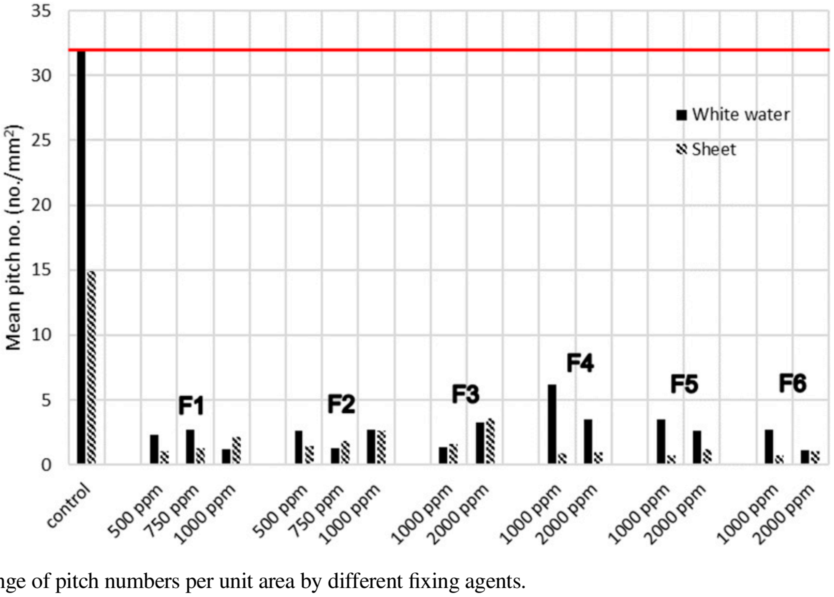

Figure 6. Change of pitch numbers per unit area by different fixing agents.

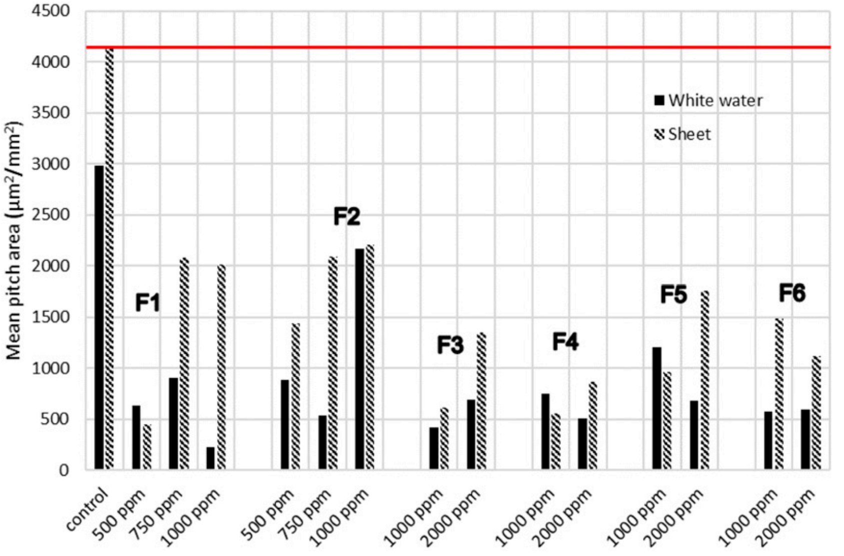

Figure 7. Change of pitch area per unit area by different fixing agents.

particles and caused them to be discharged together with the fibers, it also contributed to the reduction of the mean area of pitch deposits detected in sheets and white water (see Figure 7). When the amount of the adhesive was increased, the number of pitches detected in the sheet increased as the number of tacky particles transferred to the sheet increased. In particular, there were significant differences in F1, F2, and F3, which were polyamine- and poly-DADMAC-type agents. Figures 8 and 9 are diagrams showing the mechanism of action of the detackifier on tacky particles.

In conclusion, it was confirmed that polyamine-, poly-DADMAC-, and PEI-based fixatives had a positive effect on reducing the number and area of pitch deposits in both sheets and white water.

Pitch Controlling Effect by Detackifier

In Figure 10 and 11, when detackifiers were added, the number and the area of pitches per unit area in white water and on the sheet were compared. Both DT1 and DT2 significantly reduced the number of pitches compared with the control. Before the detackifier is added, tacky materials are dispersed in the furnish and are converted into large and small deposits as they combine themselves during the papermaking process. Contaminants that are not transferred to the dryer felt or sheet are discharged into white water and cause another problem. However, the addition of the detackifiers (DT1 and DT2) contributed to reducing the number of deposits by attaching tiny tacky particles to the surface of the detackifying particles or enclosing large tacky particles. Figures 12

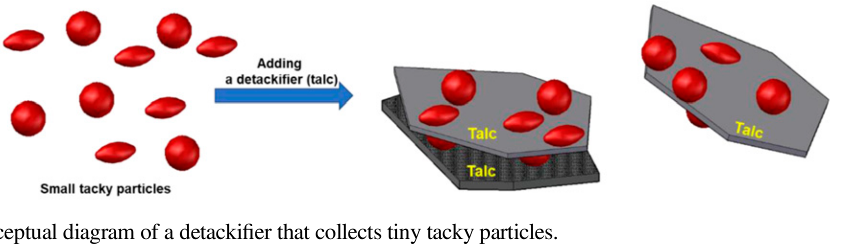

Figure 8. Conceptual diagram of a detackifier that collects tiny tacky particles.

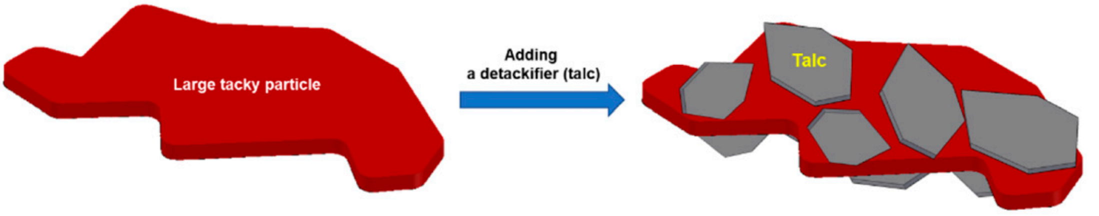

Figure 9. Conceptual diagram of a detackifier that collects large tacky particles.

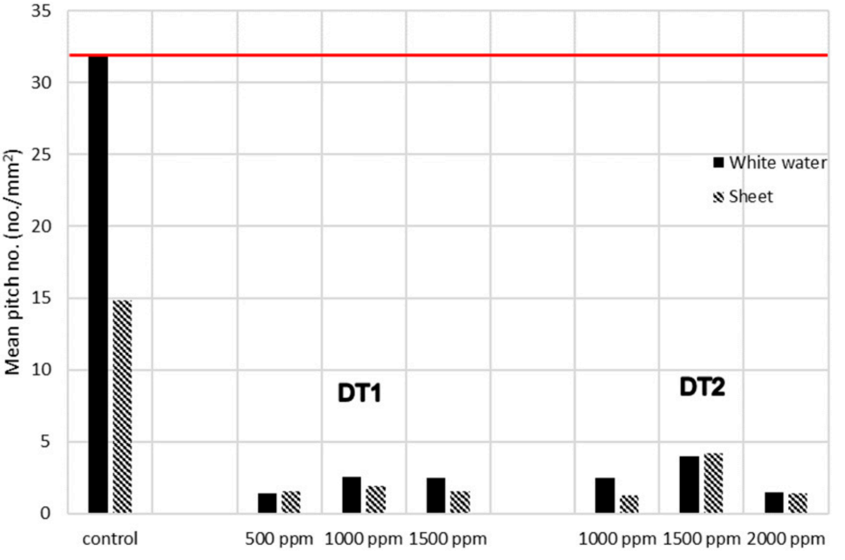

Figure 10. Change of pitch numbers per unit area by two different detackifiers.

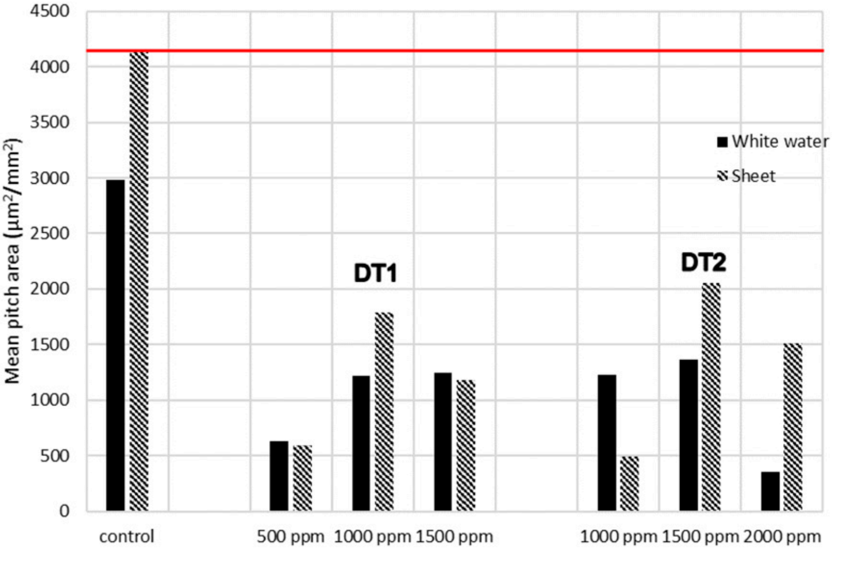

Figure 11. Change of pitch area per unit area by two different detackifiers.

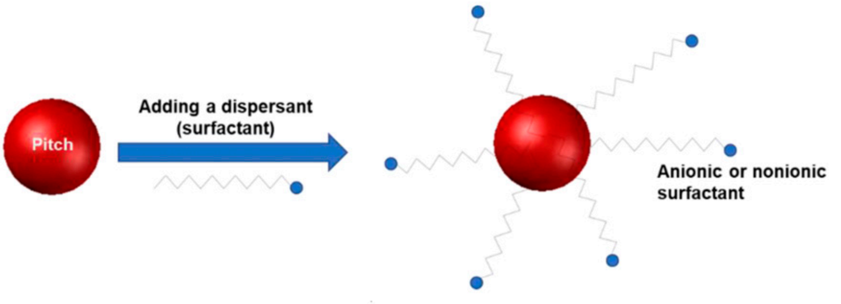

Figure 12. Conceptual diagram of a dispersant surrounding a tacky particle.

is a diagram showing the mechanism of action of the dispersant on tacky particles. It was difficult to find a meaningful difference because of the change in the amount of the detackifiers added.

Pitch Controlling Effect by Dispersant

Figure 13 shows the number of pitch particles per unit area before and after adding the dispersants. Since the addition of DT1 and DT2 left tacky particles as small particles in the furnish, the number of pitch particles detected in the sheet and the white water was remarkably reduced. Also, as shown in Figure 14, the area of tacky particles detected in the sheet and the white water was greatly reduced compared with the control because the dispersants prevented the formation of pitch deposits. As the addition amount of DT1 and DT2 increased, the number of pitch particles also tended to decrease, but the area of the pitch particles was not significantly affected by the change in the amount of dispersant added. Nevertheless, it was found that the dispersant showed a better effect in reducing the number or area of pitches observed in sheets and white water, unlike the fixatives and the detackifiers.

In the end, the pitch control effect of the dispersant could be confirmed through the application of the image analysis through dyeing, but it would

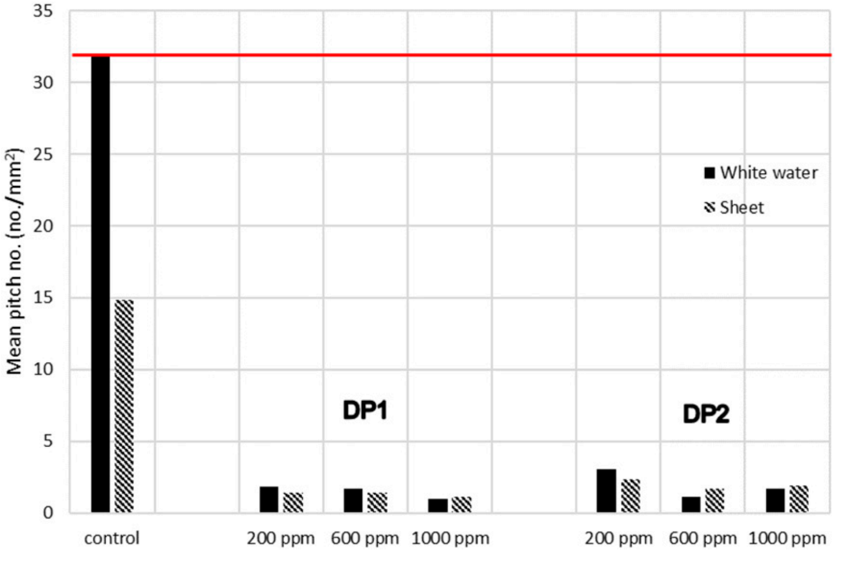

Figure 13. Change of pitch numbers per unit area by two different dispersants.

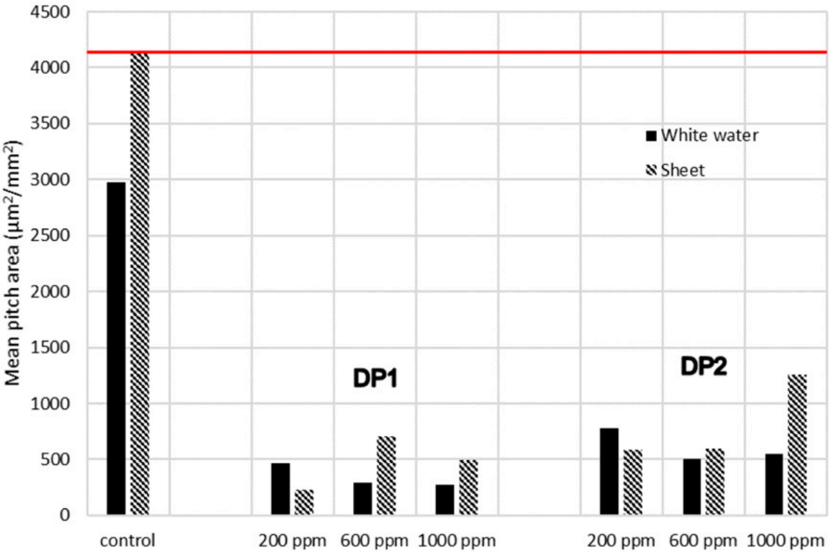

Figure 14. Change of pitch area per unit area by two different dispersive chemicals.

be difficult to find a significant difference in both sheets and white water based on the amount of the dispersants added.

CONCLUSIONS

Problems arising from pitches are known to be the most common issue in the pulp and papermaking process. In this study, the effect of pitch control was confirmed through image analysis after selectively dyeing hydrophobic pitch particles in red. The pitch control effects present in the TMP were compared using the pitch control agents acting through three different mechanisms, namely fixation, detackification, and dispersion. All pitch control agents contributed to the reduction of the number and area of pitch deposits in the sheet and white water when compared with the control. However, unlike fixatives, detackifiers and dispersants made it difficult to clearly distinguish the pitch control effect of changes in the amount of these chemicals through image analysis after staining.

In conclusion, it was confirmed that the use of a dispersant to control TMP pitches showed the most efficient effect in preventing the formation of pitch deposits in sheets or white water by reducing the coagulation of pitch particles.

ACKNOWLEDGMENTS

This work was supported by the Program for Forest Convergence Professional Manpower Pro motion, funded by Korea Forest Service in 2021 (FTIS Grant No. 2020186A00-2022-AA02).

REFERENCES

Allen LH (1980) Mechanisms and control of pitch deposition in newsprint mills. TAPPI J 63(2):81.

Bobacka V, Kreutzman N, Eklund D (1999) The use of a fixative in combination with cationic starch in peroxide-bleached TMP. J Pulp Paper Sci 25(3):100-103.

Carter RD, Hyder J (1993) Treated kaolin combines effective pitch control with handling ease. Pulp & Paper 67(11):87-90.

Champ S, Hughes D, Lee WS, Esser A, Kaub HP (2006) The BASF laser optical pitch particle counter-current applications and future developments. Pages 73-78 *in* Proceedings of the Korea Technical Association of the Pulp and Paper Industry Conference, Korea Technical Association of the Pulp and Paper Industry.

Fogarty TJ (1993) Cost-effective, common sense approach to stickies control. TAPPI J 76(3):161-167.

Guéra N, Schoelkopf J, Gane PA, Rauatmaa I (2005) Comparing colloidal pitch adsorption on different talcs. Nord Pulp Paper Res J 20(2):156-163.

Gupta P, Hodgson KT (1998) Characterization of stickie contamination from OCC recycle mills. Pages 25-29 *in* TAPPI Pulping Conference, Montreal, Quebec, Canada, October.

Gutiérrez A, José C, Martínez ÁT (2004) Chemical analysis and biological removal of wood lipids forming pitch deposits in paper pulp manufacturing. Pages 189-202 *in* Environmental microbiology. Humana Press, Totowa, NJ.

Hanu WM (1993) Dispersants. Pages 293-311 *in* Kirk-Othmer Encyclopedia of Chemical Technol, 4th edition. Vol. 8, Wiley-Interscience, NY.

Hata K, Matsukura M, Taneda H, Fujita Y (1996) Mill-scale application of enzymatic pitch control during paper production. Pages 280-296 *in* Enzymes for Pulp and Paper Processing. Vol. 655, ACS Publications, Washington, DC.

Hubbe MA, Rojas OJ, Venditti RA (2006) Control of tacky deposits on paper machines: A review. Nord Pulp Paper Res J 21(2):154-171.

Nam H, Kim CH, Lee JY, Park H, Kwon S (2015) Optimization technology of thermomechanical pulp made from *Pinus densiflora* (II)-quantification of pitch contents in TMP. J Korea TAPPI 47(5):33-42.

Putz HJ (2000) Stickies in recycled fiber pulp. Papermaking Science and Technology Book 7. Recycled Fiber and Deinking. Fapet Oy, Helsinki, Finland. pp. 441-498.

Sarja T (2007) Measurement, nature, and removal of stickies in deinked pulp. PhD thesis, University of Oulu, Finland.

Scheepers GC (2000) Enzymatic pitch control in the kraft pulping and bleaching of *Eucalyptus* spp. PhD thesis, Stellenbosch University.

Song Z, Ford P, Roy V, Grimsley S, Satcher K, Blazey M, Pelbois R (2006) U.S. Patent Application No. 11/158,845.

Sui L, Zhao G, Li X (2015) Pitch control of recycled whitewater from papermaking by *Aspergillus oryzae*. BioResources 10(4):7232-7241.

Vahasalo LJ, Holmbom BR (2006) White pitch deposition and styrene-butadiene-rubber binder content in paper mill process waters. Appita: Technology, innovation, manufacturing. Environment 59(3):213-217.

Wågberg L (2000) Polyelectrolyte adsorption onto cellulose fibers: A review. Nord Pulp Paper Res J 15(5): 586-597.

WOOD-BASED PREPREG FOR COMPOSITE LAMINATES

M. Mohammadabadi
Assistant Professor
Department of Sustainable Bioproducts
Mississippi State University
Starkville, MS 39762-5724
E-mail: mm5132@msstate.edu

V. Yadama†
Professor
Department of Civil and Environmental Engineering
Composite Materials and Engineering Center
Washington State University
Pullman, WA 99164
E-mail: vyadama@wsu.edu

L. V. Smith
Professor
School of Mechanical and Materials Engineering
Washington State University
Pullman, WA 99164
E-mail: lvsmith@wsu.edu

(Received January 2022)

Abstract. A wood-based prepreg was formed using vacuum-assisted resin transfer molding (VARTM) and a low-viscosity thermoplastic resin. Wood strands were assembled to make a porous mat for resin injection. The resin filled most of the cavities inside the wood cells resulting in a void volume fraction of 7%. The Young's modulus and strength of the saturated wood strands were 38% and 124% higher, respectively, than those of wood strands prior to resin infusion. Flat laminates were produced by thermoforming prepreg plies at 180°C and 830 kPa, for 25 min. The Young's modulus and strength of flat 12-ply laminates were 73% and 20% higher, respectively, than a wood-strand panel produced using compression resin transfer molding (CRTM) and epoxy resin. Wood prepreg shows promise as an alternative to traditional wood composite forming processes, with the potential to simplify the manufacture of complex shapes, while improving the properties of the natural material.

Keywords: Wood prepreg, liquid thermoplastic resin, vacuum-assisted resin transfer molding, thermoforming; natural fiber panels, compression molding.

INTRODUCTION

Synthetic fibers are strong and stiff with lower density than metals and are in use in almost every type of advanced engineering structure from aerospace, marine, and automotive to sport and biomedical (Masuelli 2013). However, in addition to being expensive, they do not degrade at the end of their life. Although a small fraction of these synthetic composites are crushed into powder and used as filler or incinerated to obtain energy in the form of heat, most of them are not recycled and end up in land-fills (Mitra 2014). Environmental issues have motivated governmental actions in the form of environmental regulations to protect the environment for future generations. To increase the biodegradation and recyclability of products, and reduce the use of petroleum sources, natural fibers have received considerable attention from both academia and industry. Since natural fibers are renewable, degradable, carbon negative, nonabrasive, less emission of toxic

* Corresponding author
† SWST member

Wood and Fiber Science, 54(2), 2022, pp. 122-133
https://doi.org/10.22382/wfs-2022-13

fumes, and abundant, there has been an increase in natural fiber composites (NFCs) research (Saheb and Jog 1999; Westman et al 2010; Ahmad et al 2015; Pickering et al 2016) for a variety of applications including aerospace (John et al 2008; Haris et al 2011; Boegler et al 2015) and automotive (Drzal et al 2001; Huda et al 2008; Hill et al 2012; Verma and Sharma 2017). Due to these advantages, NFCs are a realistic alternative to synthetic composites that meet the requirements of the automotive industry for both exterior and interior applications (Holbery and Houston 2006). However, one challenge with NFC utilization in the automotive sector is the capital requirements and risk averse philosophy associated with high production processes (Hill et al 2012). Also, typically thermoset resins have been used to produce NFCs for automotive applications due to poor fiber-matrix interaction.

Among the natural fibers, wood has the highest annual production (Antov et al 2017). Healthy forests play a vital role in meeting the climate change/global warming challenge through carbon sequestration in trees and wood products. The practice of thinning is an effective method to improving the overall health and value of a forest, mitigating fire risk, and optimizing forest management regimes. However, the biggest challenge with thinned materials is that they are generally left on the forest floor or stacked and burned (Hunt and Winandy 2002). Therefore, high-value markets can not only efficiently use these low-quality materials, but can also recover the cost of thinning and management processes.

Liquid molding technology (Nedanov and Advani 2000; Umer et al 2007), commonly used for synthetic fibers, provides an opportunity to develop a sustainable manufacturing infrastructure. Properly developed, it has the potential to convert underutilized lignocellulosic fiber from forest thinning for hazardous fuel reduction and fast growing short-rotation plantations into net shape composite products for niche markets such as the automotive, marine, and aviation industry. Resin transfer molding (RTM) (Fong and Advani 1998; Rouison et al 2004, 2006; Verrey et al 2006), vacuum-assisted resin transfer molding (VARTM) (Grimsley et al 2001; Kang et al 2001; Dai et al 2004), and compression resin transfer molding (CRTM) (Bhat et al 2009; Idicula et al 2009; Verleye et al 2011) are some variations of liquid molding technology for production of composites with complex geometries and large curvatures. Liquid molding, such as RTM, has been used in the aerospace and automotive industries due to its cost-effectiveness and dimensional stability. While natural (jute and sisal) and synthetic fibers (glass and carbon) are commonly used, the authors have shown that low-cost wood strands can be formed with controlled orientation and consolidated using RTM to yield high-performance thin flat panels (Yang 2014; Gartner et al 2022).

One method to increase the use of NFCs and enable sustainable forest management is to adapt underutilized wood into material forms that have successfully been used with synthetic composites. Synthetic fiber (ie carbon or glass fiber) thermoset or thermoplastic prepregs are growing in popularity among all segments of the composites industry at 10% per year since 2002 (Stewart 2009). The demand for thermoplastic composites is strong as they can be recycled and their market size is estimated to grow from USD 22.2 billion in 2020 to USD 31.8 billion by 2025 (Garofalo and Walczyk 2021).

Considering theses aspects, however, the composite industry lacks a natural fiber-based prepreg, analogous to a synthetic fiber prepreg (such as carbon fiber prepreg), with a thermoplastic or a thermoset matrix. The innovation described in this paper is a natural fiber prepreg using wood strands that has been developed with a thermoplastic resin for use as feedstock for fabricating laminated composite materials, flat or profiled, by compression molding for a variety of applications including automotive interior and exterior panels. Wood strands have an advantage over other natural fibers and wood fiber as they enable production of higher performance composite panel products with complex geometries and large curvatures for more demanding applications as needed in the automotive and aerospace industries. Lightweight and renewable materials are of interest to several industries including aerospace and automotive; the automotive industry is pivoting toward bio-based materials for interior and exterior body parts. Meeting the requirements, such a prepreg can be introduced by current consumers of the synthetic prepreg to their fabrication line without any disturbance to the manufacturing process. Due to development of low-viscosity liquid thermoplastic resin (Kinvi-Dossou et al 2019), in this study, a thermoplastic wood-based prepreg was developed using a VARTM process. Processing parameters to thermoform flat laminates from the prepreg were investigated. Production process of wood strand prepreg and a composite laminate using prepregs is depicted in Fig 1.

MATERIALS

Thin wood strands measuring 146 × 19 × 0.36 mm were produced from small diameter trees (ponderosa and lodgepole pine logs ranging in diameter from 191 to 311 mm) and dried to approximately 1% MC. Wood strand mats were assembled using strips of tacky paper (Super 77 Multipurpose Adhesive by 3M), as shown in Fig 2(a). The preform was placed under peel ply and vacuum bagged using VARTM as shown in Fig 2(b). Spiral tubes under the bagging film on both ends of the preform were attached to the resin inlet and outlet for an even flow of resin. A low-viscosity resin (Elium® 150, Arkema, Prussia, PA) was mixed with 3% initiator (Luperox® AFR40 benzoyl peroxide) prior to injection. Elium® is a thermoformable, infusible, and recyclable acrylic thermoplastic resin and has high mechanical properties and compatibility with conventional thermoset processes (Nash et al 2018; Arkema 2021). Fiber-reinforced Elium® resin can be thermoformed with heat and pressure as the resin undergoes a radical polymerization to produce a thermoplastic matrix after injection and the curing process. Resin-injected prepregs were then allowed to cure at room temperature. At room temperature, the resin system has a viscosity of 100 cps, open time of 20 min, and cure time of 40 min. A finished wood prepreg with an average thickness of 0.43 mm is shown in Fig 2(c) and (d).

EXPERIMENTS

Strands and Prepregs

To determine the level of resin saturation, unprocessed plain wood strands were compared with the prepreg under a scanning electron microscope (SEM). The effect of VARTM was determined by comparing the mechanical properties of unprocessed strands to those that are resin saturated (shown in Fig 3[a] and [b]) using the mechanical test coupons described in Table 1. To examine the effect of fiber discontinuity, the mechanical properties of the prepreg were evaluated by testing large samples cut in the longitudinal direction as shown in Fig 3(c).

Since fiber content is a key factor for prepregs and composite materials, the following procedure was used to determine fiber, resin, and void volume fractions of the wood prepreg. The weight difference of the wood strand preform (Fig 2[a]) before resin injection (M_F) and the prepreg after cure (M_C) (Fig 2[c] and [d]) were used to obtain the resin weight (M_R). Wood strands are composed

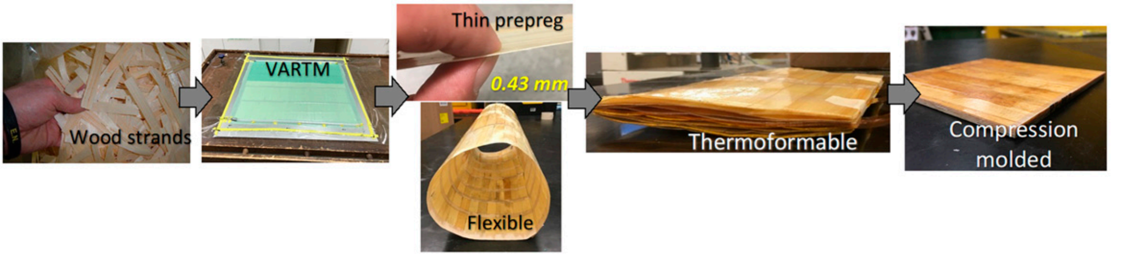

Figure 1. A brief pictorial summary of wood strand prepreg and composite laminate process.

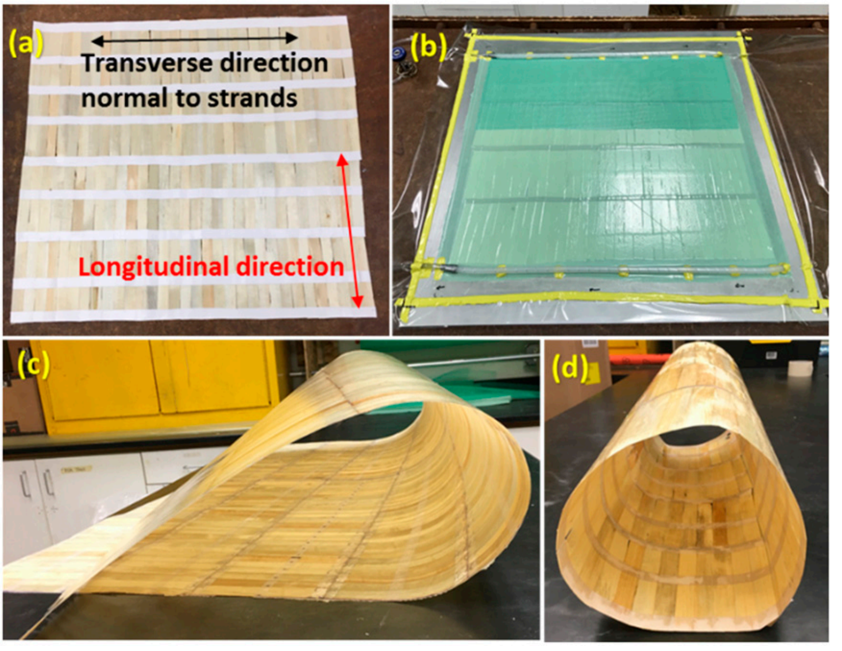

Figure 2. Prepreg development (a) wood strand mat indicating longitudinal and transverse directions (b) preform under vacuum bagging (c, d) thin and flexible prepreg.

of wood fibers that include the cell wall material (assumed to include the interfibrillar and cell wall void as well) and the fiber lumen (void in the fiber core). The wood fiber volume, V_F, was found from the wood cell wall density, ρ_W, (1524 kg/m^3; Kellogg and Wangaard 1969) as

$$V_F = M_F/\rho_W \quad (1)$$

Knowing the volume of the composite (V_C) by measuring the dimensions of the wood prepreg, the void volume, V_V, was found from

$$V_V = V_C - V_F - V_R = V_C - \frac{M_F}{\rho_W} - \frac{M_R}{\rho_R} \quad (2)$$

where V, M, and ρ are volume, mass, and density, and subscripts C, F, R, W refer to composite, fiber, resin, and wood cell wall, respectively. Knowing the volume of fiber, resin, and void, the volume fractions were computed with respect to the volume of the composite.

Composite Laminates

To laminate layers of prepreg into a composite laminate, the prepreg thermoforming temperature must be higher than its glass transition temperature (T_g) and lower than its thermal degradation temperature. Dynamic mechanical analysis (DMA) and thermogravimetric analysis (TGA) tests were conducted to find these temperature limits. For the DMA test, both single prepreg plies and 6-ply laminates were evaluated, while 12 g prepreg samples were used for the TGA analysis.

To achieve good bonding between the prepreg plies, a suitable temperature and pressure for thermoforming were determined. Twelve plies of prepreg were hot-pressed at different temperatures and pressures to make flat laminates and tested using the shear block test (ASTM 2021) to evaluate the bonding between prepreg plies. To have specimens with the desired thickness for shear block tests, samples cut from laminates were sandwiched between two layers of a wood-strand panel. The midplane of the 12-layer-prepreg

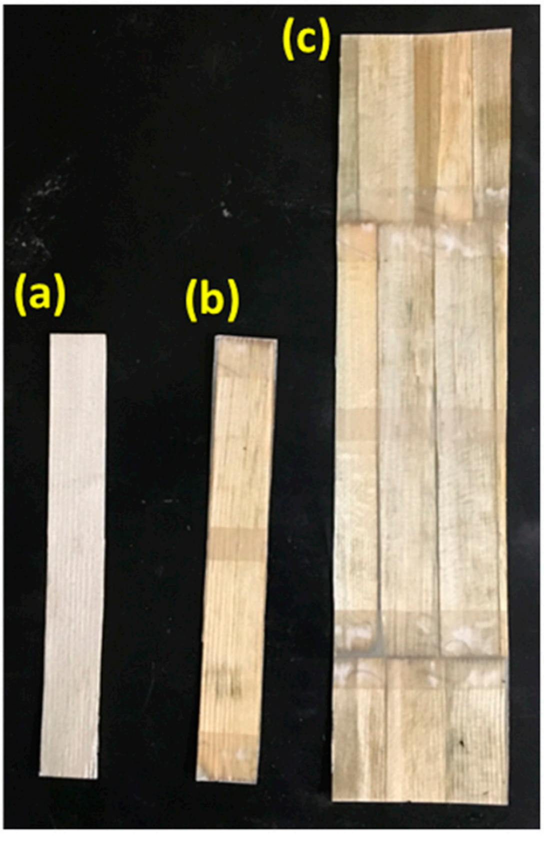

Figure 3. Tensile coupons (a) plain strand, (b) resin-saturated strand, and (c) large coupons having fiber discontinuity cut from wood prepreg in longitudinal direction.

laminate was the plane subjected to shear by compression loading.

Composite laminates consisting of 12 plies of wood strand prepreg were produced under the predetermined conditions for mechanical testing. Specimens cut from these laminates were submitted to tensile, bending, and water absorption (WA) and thickness swelling (TS) tests (ASTM 2020). The dimensions of these specimens are given in Table 1.

RESULTS AND DISCUSSION

Strand Impregnation

The average thickness of the prepreg was 0.43 mm with COV of 5%. Three samples, fully resinated, partially resinated, and plain strands shown in Fig 4(a) were evaluated under SEM to see how resin permeates throughout wood strands. Partially resinated samples were cut from regions where one side of the strand was wetted by resin whereas the other side was dry. This method resulted in good quality prepreg and partially resinated only occurred in two prepreg samples in regions close to the resin outlet. Empty lumens can be seen in Fig 4(b) for plain strands. It can be seen how fiber lumens of fully saturated strands shown in Fig 4(d) and (e) have been filled with resin. For partially resinated strands, where the resin could reach just one side of the strands, only half of the fiber lumens have been filled as shown in Fig 4(c). Unlike thermoplastic polymers such as polypropylene and polyethylene which only encapsulate the wood particles (López et al 2018) when used in wood thermoplastic composites, SEM images demonstrate that the low-viscosity thermoplastic resin used in this study can not only encapsulate the wood fibers,

Table 1. Dimensions of specimens used for mechanical testing (all are in mm).

Material	Test	Details such as size, shape, and direction		#	Length: Total	Length: Active[a]	Width	Thickness
Plain strand	Tensile	Rectangle-longitudinal		15	146	96	19	0.40
Prepreg	Tensile	Strand size	Rectangle-longitudinal	33	146	96	19	0.43
		Large Coupon	Rectangle-longitudinal	35	255	166	51	0.45
Laminate	Tensile[b]	Dog bone-longitudinal		6	255	166	39[c]	5
	Bending	Rectangle-longitudinal		5	185	140	51	5
	WA-TS	Square		5	153	—	153	5

[a] Active length is the length between two grips for tensile and two supports for bending specimens.
[b] Fillet radius was 76 mm and gauge length was 51 mm.
[c] This dimension is width of the reduced section.

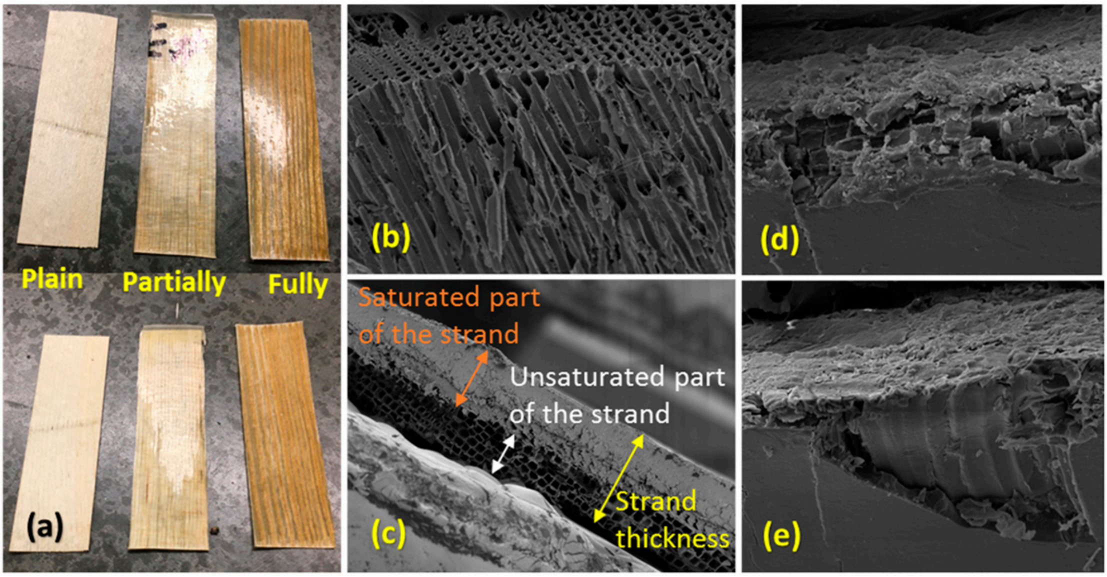

Figure 4. Scanning electron microscope evaluation (a) both sides of plain, partially, and fully resinated, (b) plain strands, (c) partially resinated, (d, e) fully resinated strands.

but can also penetrate the fiber lumens within the strands of the prepreg. In addition, the effect of penetration of high-density polyethylene (HDPE) in different wood species (lodgepole pine, grand fir, and Douglas fir) was evaluated using vacuum bagging (Gacitua 2008), and the results showed that the penetration parallel to resin flow varies between 0.04 and 0.1 mm for both earlywood and latewood. However, the low-viscosity thermoplastic resin in this study was able to penetrate the whole thickness of the wood strands (0.4 mm), which was normal to resin flow.

Experimental Mechanical Properties of Prepreg

Saturated strands, cut from prepreg, along with plain strands, were submitted to tensile tests to compare the effect of VARTM on strand mechanical properties, as shown in Table 2. The average Young's modulus and strength of saturated strands increased by 38% and 124% compared with those of plain strands, respectively.

Since the wood strands in the prepreg are not continuous, larger specimens (shown in Fig 3[b]) were cut from the prepreg in the longitudinal direction and tensile tested. Because of the discontinuity between the strands, the mechanical properties of these specimens given in Table 2 are lower than those of saturated strands having no discontinuity.

Analytical Mechanical Properties of Prepreg

Fiber, resin, and void volume fractions of the prepreg were found to be 25%, 68%, and 7%, respectively. Knowing these properties, the rule of mixtures (Gibson 2016) can be used to predict ideal continuous fiber material properties of saturated strands by

$$E_{SS} = \nu_F E_F + \nu_R E_R \text{ and } U_{SS} = \nu_F U_F + \nu_R U_R \tag{3}$$

where E and U are Young's modulus and strength, ν is the volume fraction, subscript SS refers to saturated strand, subscript F refers to fiber, and subscript R refers to resin. The stiffness and strength of plain strands depend on the strand fiber volume fraction (ν_{PS}) as

$$E_{PS} = \nu_{PS} E_F \text{ and } U_{PS} = \nu_{PS} U_F \tag{4}$$

Table 2. Mechanical properties of Elium®, plain strands, saturated strands, and coupons cut from wood prepreg (COV is mentioned in parenthesis).

			Saturated strands		
	Elium® (Bair 2020)	Plain strands	Experiment	Rule of mixtures	Longitudinal prepreg specimens
Young modulus (GPa)	3.3	9.82 (28%)	13.58 (13%)	12.92	10.03 (20%)
Strength (MPa)	76	46 (45%)	103 (20%)	102	32 (47%)

where *PS* stands for plain strand and ν_{PS} is the average fiber volume fraction in plain strands which using Eq 1 and physical properties of the plain strands (dimensions and mass) was found to be 0.23. The measured and predicted saturated strand modulus and strength are compared in Table 2. Good agreement was found (within 5% for Young's modulus and 1% for strength) due to uniform resin penetration into the fiber lumens.

Thermoforming Variables

The glass transition and thermal degradation temperatures were found to be 132°C and 257°C, respectively. Since hemicelluloses, a primary constituent of the wood cell wall, begins to degrade at around 220°C (Waters et al 2017), a temperature of 200°C was used as the upper thermoforming limit. The effect of the processing temperature (140, 160, and 180°C), pressure (380, 555, 690, 830 kPa), and thermoforming duration (15 and 25 min) were evaluated using the shear block test (ASTM 2021).

A thermocouple was placed at the mid plane of 12-ply laminates to monitor temperature, which, on average, required 6 min to reach the target temperature. Laminates were left under pressure for an additional 19 min (25 min thermoforming duration). The laminates cooled under pressure to 80°C at which point the laminate was unloaded and removed from the press. The shear strength of six specimens cut from each laminate is reported in Table 3, which tended to increase with temperature and pressure (except for 555 kPa and 180°C). The fiber and matrix demonstrated good adhesion with increasing the temperature and pressure as specimens failed due to fiber failure rather than adhesion. Different types of shear failure are shown in Fig 5 (the bonding area of shear block specimens is indicated by dashed line).

Table 3 includes the effect of the cooling process and pressing time on shear strength. Laminates pressed at 180°C and 830 kPa were removed from the press prior to cool. For a 25 min press time the shear strength decreased by 56% by removing the cooling step. Reducing the pressing time from 25 to 15 min decreased the shear strength by 20%. These results show that bond strength depends strongly on the hot-press duration and the cooling process. In the following, laminates were formed at 180°C and 830 kPa for 25 min, and cooled to 80°C under the target pressure of 830 kPa as these specified thermoforming variables resulted in an excellent bonding between prepreg plies as shown in Fig 5(c).

Laminate Mechanical Testing

The results of laminate bending and tensile tests are given in Fig 6. The tensile Young's modulus of the wood prepreg laminate was 66% and 22% larger than the wood prepreg and the saturated strands, respectively, as shown in Fig 6(a). The laminate tensile strength (Fig 6[b]) was 150% higher than the prepreg and 22% smaller than the saturated strands. Fiber discontinuity and different densities between specimens cut form the prepreg and laminate likely cause the differences. The average density for wood prepreg was 1026 kg/m^3, while it increased by 12% and reached 1151 kg/m^3 for flat laminates.

The prepreg laminate is compared in Fig 6 with that of similar composites fabricated from wood strands but using different manufacturing techniques and resins (Gartner 2017; Mohammadabadi et al 2020). RTM with external pressure is known as CRTM and was used to manufacture wood-strand-based composites with Derakane 411-350 epoxy vinyl ester resin (Gartner 2017). The thickness and fiber volume fraction for this composite

Table 3. Maximum shear stress in samples made under different temperature and pressures and submitted to shear block test.

Laminates under target temperature for 25 min but under target pressure until cool down									
Target pressure (kPa)		380		555		690		830	
Target temp. (°C)	140	160	180	160	180	160	180	160	180
Shear strength (kPa) (COV %)	1793 (52)	2868 (34)	4675 (46)	2992 (74)	4199 (43)	3027 (32)	5716 (13)	4730 (45)	7308 (12)
Laminate under target temperature and pressure for specified pressing time with no cooling									
Target pressure (kPa)								830	
Target temp. (°C)								180	
Press time (min)								15	25
Shear strength (kPa) (COV %)								2551 (15)	3206 (30)

were 6.35 mm and 37%, respectively. Densifying the wood strand mat by applying pressure during resin injection and injecting resin with high pressure resulted in fiber compaction and higher fiber volume fraction and less void content compared with the prepreg laminate developed in this study. Another composite was produced by hot-pressing wood strands with a low percentage of phenol formaldehyde resin (8% of the oven-dry weight of the wood strands) (Weight and Yadama 2008a 2008b; Mohammadabadi et al 2020). The thickness and density of the hot-pressed wood strand composite were 6.35 mm and 640 kg/m^3, respectively. The fiber volume fraction of the composite was about 40%. Even though the laminate developed in this study had a lower fiber content

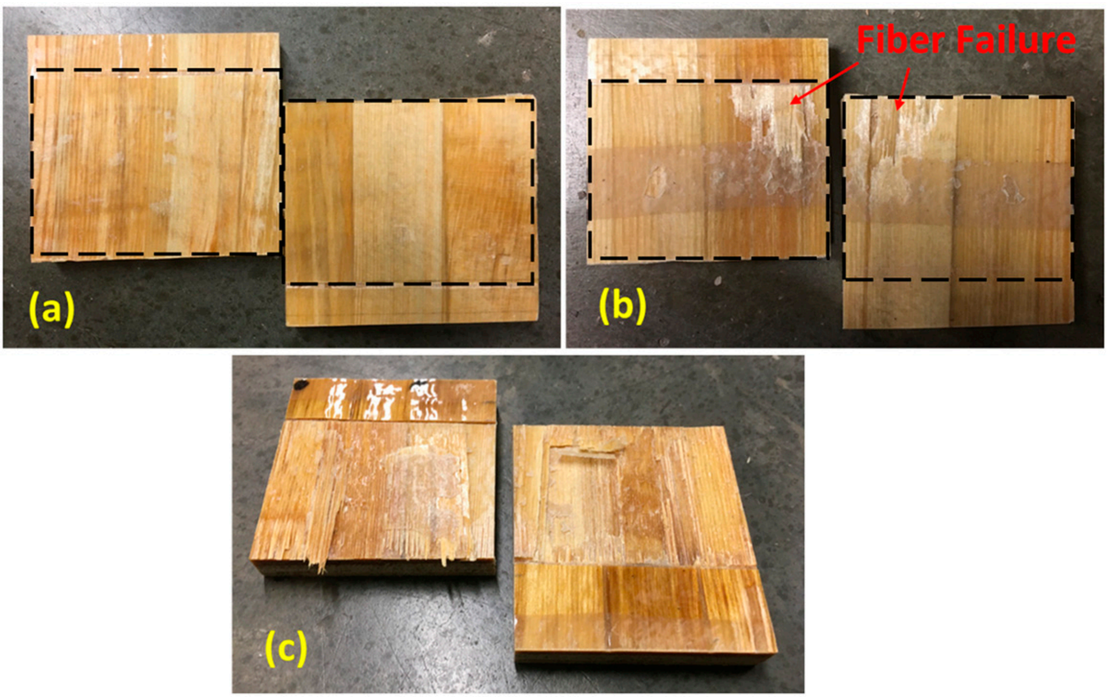

Figure 5. Different types of shear failure (a) pure adhesion failure, (b) partial fiber failure, and (c) pure fiber failure.

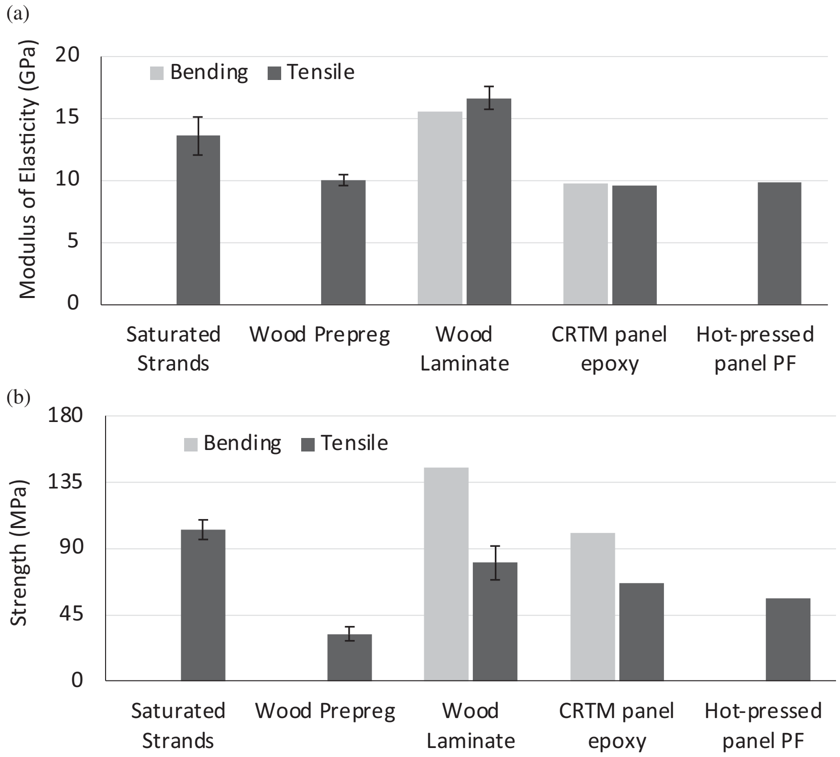

Figure 6. Results of mechanical testing (a) modulus of elasticity and (b) strength compared with other studies and similar materials.

compared with the other composites, its modulus of elasticity and strength in tension and bending were noticeably higher. For the bending test, the modulus of elasticity of the laminate was 60% higher than that of the CRTM panel and in tension, it was 73% and 69% larger than CRTM and hot-pressing panels, respectively. The modulus of rupture of the laminate was 44% higher than that of CRTM and its tensile strength was 20% and 42% higher than that of CRTM and hot-pressing panels, respectively. Fiber orientation is one reason for this difference as all wood strands were oriented in the longitudinal direction to make the prepreg as shown in Fig 2(a). For CRTM and hot-pressed panels, however, strands were oriented within ±35 degrees with respect to the longitudinal direction. Compared with CRTM specimens with a higher fiber volume fraction of 37%, the laminates yield better mechanical properties which could be due to higher mechanical properties of the thermoplastic resin or improved interaction between the thermoplastic resin and wood strands compared with the low-viscosity thermoset resins used for the CRTM specimens.

WA and TS of the wood prepreg laminate after 2 and 24 h are shown in Fig 7 and are compared with the wood strand composites produced (using CRTM and hot press) and tested by Gartner (2017) and Weight and Yadama (2008a, 2008b). The laminate and CRTM panel showed similar behavior in the presence of water. The wood prepreg laminates showed much better performance compared with hot-pressed panels as the low-viscosity resin during the VARTM process was mostly able to fill all the cavities or fiber lumens within the wood strands. These superior moisture resistant properties are important for automotive applications where shape stability and durability are critical.

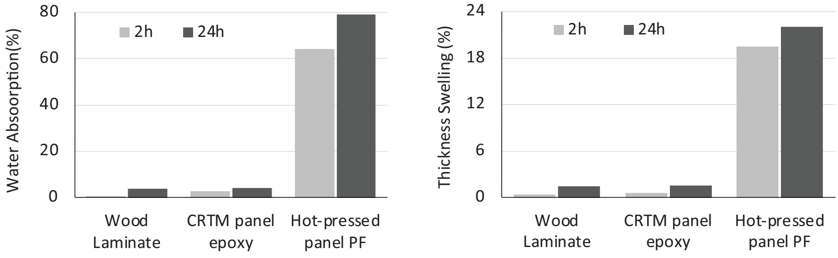

Figure 7. Comparison between water absorption and thickness swelling of wood prepreg laminate with other bio-based composites.

CONCLUSIONS

A natural fiber-based thermoplastic prepreg similar to a synthetic prepreg has been developed to manufacture molded and shaped interior panels for a variety of applications, including automotive. Wood strands from small diameter timber were used to develop a wood-based prepreg using a novel thermoplastic resin and VARTM technique. Unlike the traditional thermoplastic resins which penetrate only a few microns into the wood structure, the low-viscosity thermoplastic resin in this study easily penetrated the fiber lumens. This resulted in a low void volume fraction and a high-performance thin wood strand prepreg. The interlaminar shear strength of laminates produced from the wood prepreg increased with the thermoforming duration and cooling under pressure. Due to reprocessability of the wood-based prepregs, they can be used to produce flat or shaped composite laminates, with high strength, stiffness, water resistant, and dimensional stability.

ACKNOWLEDGMENTS

The study was funded by Agriculture and Food Research Initiative grant no. 2016-67021-24413 from the USDA National Institute of Food and Agriculture. Arkema for supplying Elium® resin.

REFERENCES

Ahmad F, Choi HS, Park MK (2015) A review: Natural fiber composites selection in view of mechanical, light weight, and economic properties. Macromol Mater Eng 300(1):10-24.

Antov P, Savov V, Neykov N (2017) Utilization of agricultural waste and wood industry residues in the production of natural fiber-reinforced composite materials. International Journal–Wood, Design, and Technology 6: 64-71.

Arkema (2021) Liquid thermoplastic resin for tougher composites. Colombes Cedex, France. www.elium-composites.com.

ASTM (2020) D 1037-12. Standard test methods for evaluating properties of wood-base fiber and particle panel materials. American Society for Testing and Materials, West Conshohocken, PA.

ASTM (2021) D 905-08. Standard test method for strength properties of adhesive bonds in shear by compression loading. American Society for Testing and Materials, West Conshohocken, PA.

Bair J (2020) Investigation of resin infusion consumable effect on fusion bond strength in the manufacture of a thermoplastic vertical axis wind turbine prototype. MS thesis, Colorado State University, Fort Collins, CO.

Bhat P, Merotte J, Simacek P, Advani SG (2009) Process analysis of compression resin transfer molding. Compos, Part A Appl Sci Manuf 40:431-441.

Boegler O, Kling U, Empl D, Isikveren AT (2015) Potential of sustainable materials in wing structural design. Deutsche Gesellschaft für Luft-und Raumfahrt-Lilienthal-Oberth eV.

Dai J, Pellaton D, Hahn HT (2004) A comparative study of vacuum-assisted resin transfer molding (VARTM) for sandwich panels. Polym Compos 24:672-685.

Drzal LT, Mohanty AK, Misra M (2001) Bio-composite materials as alternatives to petroleum-based composites for automotive applications. Magnesium 40(60):1-3.

Fong L, Advani SG (1998) Resin transfer molding. Handbook of composites. Springer, Boston, MA. pp. 433-455.

Gacitua EW (2008) Influence of wood species on properties of wood/HDPE composites. PhD thesis, Washington State University, Pullman, WA. 120 pp.

Garofalo J, Walczyk D (2021) In situ impregnation of continuous thermoplastic composite prepreg for additive manufacturing and automated fiber placement. Compos, Part A Appl Sci Manuf 147:106446.

Gartner BS (2017) Effects of preform architecture and processing parameters on the production of wood strand reinforced resin transfer molded composite panels. MS thesis, Washington State University, Pullman, WA.

Gartner BS, Yadama V, Smith LV (2022) Resin transfer molding of wood strand composite panels. Forests 13(2):278.

Gibson RF (2016) Principles of composite material mechanics. CRC Press, Boca Raton, FL. 700 pp.

Grimsley BW, Hubert P, Song X-L, Cano RJ, Loos AC, Pipes RB (2001) Flow and compaction during the vacuum assisted resin transfer molding process. Int. SAMPE Technol. Conf. 33:140-153.

Haris MY, Laila D, Zainudin ES, Mustapha F, Zahari R, Halim Z (2011) Preliminary review of biocomposites materials for aircraft radome application. Key Eng Mater 471-472:563-567.

Hill K, Swiecki B, Cregger J (2012) The bio-based materials automotive value chain. Center for Automotive Research, Ann Arbor, MI. p. 82. https://www.cargroup.org/wp-content/uploads/2017/02/The-Bio_Based-Materials-Automotive-Value-Chain.pdf.

Holbery J, Houston D (2006) Natural-fiber-reinforced polymer composites in automotive applications. JOM 58(11):80-86.

Huda MS, Drzal LT, Ray D, Mohanty AK, Mishra M (2008) Natural-fiber composites in the automotive sector. *in* Properties and performance of natural-fibre composites. Woodhead Publishing, Oxford, UK. pp. 221-268.

Hunt JF, Winandy JE (2002) 3D engineered fiberboard: A new structural building product. Pages 106-117, *in* Proc Sixth Panel Products Symposium, October 1-11, 2002, Llandudno, Wales, UK. Bangor, Gwynedd, UK: The BioComposites Centre, UWB, 2002.

Idicula M, Sreekumar PA, Joseph K, Thomas S (2009) Natural fiber hybrid composites—A comparison between compression molding and resin transfer molding. Polym Compos 30:1417-1425.

John MJ, Anandjiwala RD, Wambua P, Chapple SA, Klems T, Doecker M, Erasmus LD (2008) Bio-based structural composite materials for aerospace applications. Pages 14-16 *in* 2nd South African International Aerospace Symposium, September, Cape Town, South Africa.

Kang MK, Lee WI, Hahn HT (2001) Analysis of vacuum bag resin transfer molding process. Compos, Part A Appl Sci Manuf 32:1553-1560.

Kellogg RM, Wangaard FF (1969) Variation in the cell-wall density of wood. Wood Fiber Sci 1(3):180-204.

Kinvi-Dossou G, Boumbimba RM, Bonfoh N, Garzon-Hernandez S, Garcia-Gonzalez D, Gerard P, Arias A (2019) Innovative acrylic thermoplastic composites versus conventional composites: Improving the impact performances. Compos Struct 217:1-13.

López YM, Paes JB, Rodríguez EM, Gustave D, Gonçalves FG (2018) Wood particleboards reinforced with thermoplastics to improve thickness swelling and mechanical properties. Cerne 24:369-378.

Masuelli MA (2013) Introduction of fibre-reinforced polymers− polymers and composites: Concepts, properties and processes. *In* Fiber reinforced polymers-the technology applied for concrete repair. IntechOpen. http://dx.doi.org/10.5772/54629.

Mitra BC (2014) Environment friendly composite materials: Biocomposites and green composites. Def Sci J 64(3):244-261.

Mohammadabadi M, Jarvis J, Yadama V, Cofer W (2020) Predictive models for elastic bending behavior of a wood composite sandwich panel. Forests 11(6):624.

Nash N, Sirerol CB, Manolakis I, Comer AJ (2018) Thermoplastic infusible resin systems: Candidates for the marine sector? Pages 24-28 *in* 18th European Conference on Composite Materials, June 7, Athens, Greece.

Nedanov P, Advani SG (2000) Mold filling simulation of sandwich composite structures manufactured by liquid molding: A parametric study. J Sandw Struct Mater 2:117-130.

Pickering KL, Efendy MA, Le TM (2016) A review of recent developments in natural fibre composites and their mechanical performance. Compos, Part A Appl Sci Manuf 83:98-112.

Rouison D, Sain M, Couturier M (2004) Resin transfer molding of natural fiber reinforced composites: Cure simulation. Compos Sci Technol 64:629-644.

Rouison D, Sain M, Couturier M (2006) Resin transfer molding of hemp fiber composites: Optimization of the process and mechanical properties of the materials. Compos Sci Technol 66:895-906.

Saheb DN, Jog J (1999) Natural fiber polymer composites: A review. Adv Polym Technol 18:351-363.

Stewart R (2009) New prepreg materials offer versatility, top performance. Reinforced Plastics 53(5):28-33.

Umer R, Bickerton S, Fernyhough A (2007) Characterising wood fibre mats as reinforcements for liquid composite moulding processes. Compos, Part A Appl Sci Manuf 38:434-448.

Verleye B, Walbran WA, Bickerton S, Kelly PA (2011) Simulation and experimental validation of force controlled compression resin transfer molding. J Compos Mater 45(7):815-829.

Verma D, Sharma S (2017) Green biocomposites: A prospective utilization in automobile industry. Pages 167-191 *in* M Jawaid, MS Salit, OY Alothman, eds. Green Biocomposites. Springer, Cham, Switzerland.

Verrey J, Wakeman MD, Michaud V, Månson JAE (2006) Manufacturing cost comparison of thermoplastic and thermoset RTM for an automotive floor pan. Composites Part A 37:9-22.

Waters CL, Janupala RR, Mallinson RG, Lobban LL (2017) Staged thermal fractionation for segregation of lignin and cellulose pyrolysis products: An experimental study of residence time and temperature effects. J Anal Appl Pyrolysis 126:380-389.

Weight SW, Yadama V (2008a) Manufacture of laminated strand veneer (LSV) composite. Part 1: Optimization and characterization of thin strand veneers. Holzforschung 62(6):718-724.

Weight SW, Yadama V (2008b) Manufacture of laminated strand veneer (LSV) composite. Part 2: Elastic and strength properties of laminate of thin strand veneers. Holzforschung 62(6):725-730.

Westman MP, Fifield LS, Simmons KL, Laddha S, Kafentzis TA (2010) Natural fiber composites: A review. PNNL-19220, Pacific Northwest National Laboratory, Richland, WA. 10 pp.

Yang W (2014) Resin Transfer Molding (RTM) of wood-strand reinforced composite panels. MS thesis, Department of Civil and Environmental Engineering, Washington State University, Pullman, WA. 105 pp.

WOOD PROPERTIES OF NINE ACETYLATED TROPICAL HARDWOODS FROM FAST-GROWTH PLANTATIONS IN COSTA RICA

*Róger Moya**†

Professor
E-mail: rmoya@itcr.ac.cr

Johanna Gaitán-Álvarez

Research Scientist
E-mail: jgaitan@itcr.ac.cr

Alexander Berrocal

Professor
Escuela de Ingeniería Forestal
Instituto Tecnológico de Costa Rica
Apartado 159-7050 Cartago, Costa Rica
E-mail: aberrocal@itcr.ac.cr

Claudia B. Cáceres

Former Research Associate
E-mail: claudia.caceres@mffp.gouv.qc.ca

Roger E. Hernández†

Professor
Département des Sciences du Bois et de la Forêt
Centre de Recherche sur les Matériaux Renouvelables
Université Laval, 2425 Rue de la Terrasse
Québec, Canada G1V 0A6
E-mail: roger.hernandez@sbf.ulaval.ca

(Received March 2022)

Abstract. The treatment of acetylation on tropical woods is influenced by their different levels of permeability and how these affect the weight percentage gain (WPG) in acetylated wood. The objective of this study was to identify the effect of acetylation on physical properties, hygroscopic and dimensional stability, wetting rate, and durability of nine tropical species of hardwoods used for commercial reforestations in Costa Rica. The results showed that WPG varied from 2.2% to 16.8% among species. Positive significant correlations were observed between WPG and two parameters of dimensional and hygroscopic stability, whereas a negative correlation was observed with water absorption (WA). For species with a WPG of over 10% (*Vochysia ferruginea*, *Vochysia guatemalensis*, *Cordia alliodora*, and *Enterolobium cyclocarpum*) wetting rate, hygroscopic stability, and resistance to biological attack showed an increase while swelling, and WA decreased. For these species, the best behaviors were obtained with an acetylation time of 2.5 h. The same properties of wood in species with a WPG under 5% were found to be less affected by the different acetylation times and showed little difference in relation to untreated wood. Finally, the analysis showed that the dimensional stability obtained was attributed to the reduction of the absorptive capacity of the acetylated wood.

Keywords: Moisture absorption, wood properties, tropical wood, fast-growth plantation, dimensional stability.

* Corresponding author
† SWST member

https://doi.org/10.22382/wfs-2022-14

INTRODUCTION

Wood has several commercial and noncommercial uses, and as an industrial material, it is easily degraded or affected in presence of moisture (Adebawo et al 2016). Components of wood (ie lignin, cellulose, and hemicellulose) contain free hydroxyl radicals (Rowell 2012) that adsorb and release water depending on changes in temperature and RH conditions. This, in turn, causes the cell walls to adjust to the presence (or absence) of moisture, thereby, provoking changes in the dimensions of lumber (Giridhar et al 2017).

Recent research has studied chemical modifications to wood toward decreasing water absorption (WA) and, thus, to improve dimensional stability (Mantanis 2017), without altering other properties (Rowell 2006). Among these chemical treatments, most common is the use of acetic anhydride (Hill 2006; Rowell 2006), wherein the OH^- anion group of the wood components becomes chemically bound to a residue of the acetate (CH_3COO) of an acetic anhydride molecule $(CH_3CO)_2$. This treatment is known as the acetylation process where the OH^- anion group is reduced, which decreases the wood hygroscopicity and increases its dimensional stability (Adebawo et al 2016). Other important wood properties take benefit from acetylation (Gérardin 2016; Mantanis 2017), notably: natural resistance to fungi and insects (Fojutowski et al 2014; Rowell 2016); resistance to marine conditions; reduced wettability (Bongers et al 2016) and wood swelling (Kozarić et al 2016); and increased wood hardness (Rowell 2006).

Polymer composition and distribution in hardwood species differ from those of softwood species (Engelund et al 2013), and, as such, the acetylation produces varied effects (Rowell 2016). In hardwood species, hydroxyl groups are reported to be present at proportions of 2.0% to 4.5%, whereas in softwoods these vary from 0.5% to 1.7% (Rowell 2016). This difference is attributed to the hemicellulose and lignin compositions, ie in hardwood species, hemicelluloses include glucuronoxylan, xyloglucan, and glucomannan, while softwood hemicellulose is primarily composed of xyloglucan, arabinoglucuronoxylan, and galactoglucomannan, as well as lignin in a lesser proportion (Wang et al 2017).

Studies have indicated that acetylated hardwoods achieve lesser weight percentage gain (WPG) compared with acetylated softwood species (Rowell 2016). Nonetheless, compared with softwoods, hardwoods contain a higher content of xylans, which do not contain a primary hydroxyl group in which to react (Rowell 2014). Moreover, softwood species contain a greater percentage of lignin, the component where the higher percentage of acetylation has been demonstrated (Rowell 2016).

In addition to the difference in the type and proportion of hemicellulose, the anatomical structure differs significantly between both wood species groups, eg hardwoods are characterized by the presence of conducting elements such as vessels, whereas softwoods are made of tracheids (Gibson 2012). This distinction causes the flow of liquid to vary between both groups (Gaitán-Álvarez et al 2020), therefore affecting the acetylation process, which is associated with liquid flow in wood (Kozarić et al 2016).

Despite these differences and the studies conducted on softwoods, relatively lesser research on hardwoods has been carried out, including Matsunaga et al (2016) and Gaitán-Álvarez et al (2021). WPG for tropical hardwoods ranges from 4% to 18%, values lower than those observed in softwood species (Gaitán-Álvarez et al 2021). This difference can be attributed mostly to the flow of liquid in wood, regulated by its permeability, which is determined by the anatomical elements involved in the flow of liquids (Emaminasab et al 2017). In these initial studies, the change in wood properties due to acetylation remains unknown, which has not allowed expanding the uses of hardwood species (Bollmus et al 2015).

In Central America, Costa Rica has implemented reforestation programs with fast-growth plantations that use a variety of hardwood species for lumber production (Adebawo et al 2019). In these programs, early-age tree harvesting yields juvenile wood, which is characterized by dimensional instability (Moya 2018). In line with this gap, a series of treatments have been implemented to improve lumber properties (Gaitán-Álvarez et al 2020, 2021; Tenorio and Moya 2021) and reduce the problems surrounding the durability and dimensional stability of these species (Moya et al 2017; Gaitán-Álvarez et al 2020). In such situations, acetylation provides an opportunity to improve dimensional stability, durability, and other wood properties of hardwood species (Mantanis and Young 1997; Rowell 2006, 2016; Adebawo et al 2016). Given that plantation species in tropical regions represent a great opportunity for production, it is very important to increase wood durability and dimensional stability to render added value to the products (Kojima et al 2009).

Therefore, the objective of the study was to evaluate the effect of three different acetylation times with acetic anhydride on nine hardwood species commonly used in commercial reforestation in Costa Rica. The effects of the acetylation on physical properties, hygroscopic stability, dimensional stability, wetting rate, and durability were thus evaluated.

METHODOLOGY

Materials

The species studied were *Cedrela odorata*, *Cordia alliodora*, *Enterolobium cyclocarpum*, *Gmelina arborea*, *Hieronyma alchorneoides*, *Samanea saman*, *Tectona grandis*, *Vochysia ferruginea*, and *Vochysia guatemalensis.* The wood of these species presents generally good permeability (Tenorio et al 2016) and has shown potential behavior for wood modification (Gaitán-Álvarez et al 2020). Gaitán-Álvarez et al (2020, 2021) presented the characteristics and origin of these woods in great detail. The wood samples were dried to achieve a MC ranging between 12% and 15% and comprised mostly of sapwood, to insure that juvenile wood is used. The reagents used were: acetic anhydride $(CH_3CO)_2O$ at 98% concentration, commercial brand J.T. Baker (Madrid, Spain) (https://www.fishersci.es/es/es/brands/IPF8MGDA/jt-baker.html); and glacial acetic acid CH_3COOH at 99% concentration, distributed by Químicos Holanda Costa Rica S.A. (Costa Rica) (https://www.brenntag.com/locations/en/brenntag-locations/loc-809-qu%C3%ADmicos-holanda-costa-rica-s-a.jsp).

Acetylation Process

For each species, three groups of 15 samples of 50 mm (R) × 50 mm (T) × 20 mm (L) in oven-dry condition (at 103°C for 24 h) were treated with different acetylation times per group. Another group of 15 samples were left untreated (control) to be compared with the acetylated material. A detailed description of the acetylation process is given in Gaitán-Álvarez et al (2020). The process consisted in applying vacuum for 15 min at −70 kPa (gauge mark), after which the solution of acetic anhydride and glacial acetic acid was introduced, in a 92:8 proportion, respectively. Once inside, the contents were subjected to a 690 kPa pressure for 30 min, after which, the excess liquid solution was extracted and nitrogen gas was injected to serve as the inert medium to control the internal temperature of wood samples. For the reaction, the temperature was fixed at 120°C and three different acetylation times were applied per species: 1.0, 2.5, and 4.0 h, labeled 1 h-acetylation-time, 2.5 h-acetylation-time, and 4 h-acetylation-time, respectively. Then, the acetylated samples were again oven-dry at 103°C for 24 h. Finally, the oven-dry weight of all samples was measured before placing them in a conditioning chamber at 20°C and 65% of RH until reaching a constant weight.

Evaluation of the Acetylation Process

The dimensions (ie length, width, and thickness) and oven-dry weight of the acetylated samples were measured before and after the treatment. The acetylation process was evaluated by determining the uptake of the solution (uptake) (Eq 1) and by the WPG (Eq 2) considering the oven-dry weight before acetylation as the initial weight.

$$\text{Uptake}\left(\frac{\text{liters}}{\text{m}^3}\right) = \left(\frac{\text{Weight}_{\text{after acetylation}}(\text{g}) - \text{Weight}_{\text{before acetylation}}(\text{g})}{\text{Volume of sample (cm}^3)}\right) \times \frac{1\ \text{liter}}{1000\text{g}} \quad (1)$$

$$\text{Weight percentage gain (WPG)} = \frac{\text{Weight}_{\text{after acetylation}}(\text{g}) - \text{Weight}_{\text{before acetylation}}(\text{g})}{\text{Weight}_{\text{before acetylation}}(\text{g})} \times 100 \quad (2)$$

Wettability Measurement

The contact angle was determined with an FTÅ ° D200 imaging goniometer (Folio Instruments Inc., Ontario, Canada) at 20°C. One drop (6 mL) of pure water was added to wood surfaces with an injection microsyringe. Measurements were carried out in the longitudinal direction. The contact angle was calculated as a mean of both sides of the drop to compensate for any horizontal variations. The procedure used by Cool and Hernández (2011) was followed in this study. Two contact angles were measured, ie the initial contact angle ($\theta_{initial}$) and the contact angle at 30 s (θ_{30s}). Afterward, the wetting rate was calculated as the variation of the contact angle ($\theta_{initial} - \theta_{30s}$) over the first 30 s of wetting to assess the spreading and penetration of pure water. This procedure was performed on five samples per treatment, for all wood species studied.

Physical Properties

Partial tangential swelling (TS) was determined by the changes in dimensions of samples occurring between 65% and 85% RH, at 22°C (Eq 3). Thus, the dimensions and weight of treated and untreated samples were first measured once conditioned at 65% RH. The samples were then equilibrated at 22°C and 85% RH according to ASTM D4933-16 standard (ASTM 2021). After conditioning, the dimensions and weight of samples were again measured. This hygrothermal condition was chosen because the Atlantic and some Pacific areas in Costa Rica present high RH, where wood can reach equilibrium moisture contents up to 18% MC. The sorption ratio (S) was used to evaluate the hygroscopic stability of wood. This ratio characterizes the sensitivity of changes in EMC (ΔEMC) to changes in RH (ΔRH) and is defined according to Eq 4 (Hernández 2007a). However, the differential TS ratio (G_T) was used to assess the dimensional stability of wood, which is defined according to Eq 5. These parameters (S and G_T) assume a linear relationship between EMC and RH and between TS and EMC, respectively (Hernández 2007b). Therefore, S and G_T values were calculated between 65% and 85% RH as follows:

$$\text{Partial tangential swelling (\%)} = \frac{\text{dimension at 85\% RH (mm)} - \text{dimension at 65\% RH (mm)}}{\text{dimension at 65\% RH (mm)}} * 100 \quad (3)$$

$$S\,\text{ratio factor} = \frac{\Delta\text{EMC}}{\Delta\text{RH}} = \frac{\text{EMC}_{\text{at 85\%}} - \text{EMC}_{\text{at 65\%}}}{85 - 65\%} \quad (4)$$

$$\text{Differential tangential swelling ratio (GT)} = \frac{\text{Partial tangential swelling from 65\% to 85\% (\%)}}{\text{MC}_{\text{at 85\%}} - \text{MC}_{\text{at 65\%}}} \quad (5)$$

Besides these wood properties, three other parameters were evaluated: 1) the difference in ΔMC between acetylated and untreated wood, 2) the difference in S ratio between acetylated and untreated wood, and 3) the difference in G_T between acetylated and untreated wood. These factors were determined according to Eq 6.

$$\text{Difference in } \Delta\text{MC, S ratio or GT } \Delta\text{MC, S ratio or GT}_{\text{untreated wood}} - \Delta\text{MC, S ratio or GT}_{\text{acetylated wood}} \quad (6)$$

(WA was also determined by immersion in cold distilled water for 24 h. For this, another set of 60 samples (ie 15 samples untreated and 15 samples for each time of acetylation, 1.0, 2.5, and 4.0 h) per species were weighed before and after the immersion in water. WA was calculated using Eq 7, following the ASTM D1037-12 standard (ASTM 2020).

$$\text{Water absorption} = \frac{\text{Weight}_{\text{atfer submersion for 24 h C}}\ (\text{g}) - \text{Weight}_{\text{oven-dry}}\ (\text{g})}{\text{Weight}_{\text{oven-dry}}\ (\text{g})} * 100 \quad (7)$$

Durability

The accelerated laboratory test of natural decay resistance was carried out according to the ASTM D-2017-81 standard (ASTM 2014). For each treatment and species, 30 samples measuring 2 cm wide, 2 cm long, and 2 cm thick were prepared. Two types of fungi were tested, namely, *Trametes versicolor* and *Lenzites acuta*, which correspond to white- and brown-rot fungi, respectively. For each type of fungus, 15 samples were exposed to fungal degradation per species and treatment.

Statistical Analysis

Data were tested for normality and homogeneity, and outliers of the variables evaluated were removed. For each species and treatment, the mean, standard deviation, and coefficient of variation were determined for each property studied. A variance analysis (ANOVA) was performed for each species, where wood properties were the dependent variables and time of acetylation was the source of variation, but for WGP was performed two-way ANOVA, where species, time of acetylation and the specie*time integrations were independent variables and WPG as dependent variable. The statistical significance level of $p < 0.05$ was applied to determine the effect of acetylation time. Moreover, Tukey's test was used to determine the statistical significance of the difference between the means of the properties. This analysis was performed with the SAS 9.4 program (SAS Institute Inc., Cary, NC). After, the effect of acetylation of wood, measured by WPG, on wood properties was established by Pearson correlation coefficient, where all properties were cataloged as a dependent variable and WPW as an independent variable.

RESULTS

Evaluation of the Acetylation Process

The evaluation of WPG by two-way ANOVA showed that species, time of acetylation and the interaction were statistically significant with F-values of 256.6, 6.9, and 4.8, all these valued statistically significant at *P*-value less than 0.05. The WPG varied between 2.2% and 16.8% (Fig 1). No statistical differences existed in the WPG among acetylation times for *V. ferruginea*, *V. guatemalensis*, *C. alliodora*, *C. odorata*, *G. arborea*, and *T. grandis*. However, significant statistical differences among acetylation times were observed in *E. cyclocarpum*, *S. saman*, and *H. alchorneoides*. Moreover, *E. cyclocarpum* and *S. saman* showed the highest WPG after 2.5 h-acetylation-time, whereas *H. alchorneoides* showed it after 1 h-acetylation-time (Fig 1). In relation to species, it was found that *V. ferruginea*, *V. guatemalensis*, *C. alliodora*, and *C. odorata* wood had the same performance of WPG in three times tested (Fig 2[a]-[c]), but the differences between species varied in the relation to time of acetylation for other species (*E. cyclocarpum*, *C. odorata*, *G. arborea*, *S. saman*, *H. alchorneoides*, and *T. grandis*), (Fig 2).

Wettability Measurement

The acetylation process decreased the wetting rate in *V. ferruginea* (Fig 3[a]), *V. guatemalensis* (Fig 3[b]), *S. saman* (Fig 3[e]), and *T. grandis* (Fig 3[i]). Untreated samples presented a significantly higher value compared with all acetylated samples and no statistical differences were observed among acetylation times, in these species. No statistical difference was found in *G. arborea* and *C. odorata* between untreated and acetylated samples and between acetylation times (Fig 3[g] and [h]). The acetylation did not affect the wetting rate in relation to the untreated samples and the 4.0 h-acetylation-time in *E. cyclocarpum* (Fig 3[c]), in 1.0 h-acetylation-time of *C. alliodora*, in 2.5 h- and 4.0 h-acetylation-time for *H. alchorneoides* (Fig 3[f]). A significant decrease in wetting rate was found for 2.5 h-acetylation-time for *E. cyclocarpum* (Fig 3[c]), for 2.5 h- and 4.0 h-acetylation-time for *C. alliodora* (Fig 3[d]), and 1.0 h-acetylation-time for *H. alchorneoides* (Fig 3[f]).

Physical Properties

The main physical properties for untreated and treated wood samples are presented in Table 1.

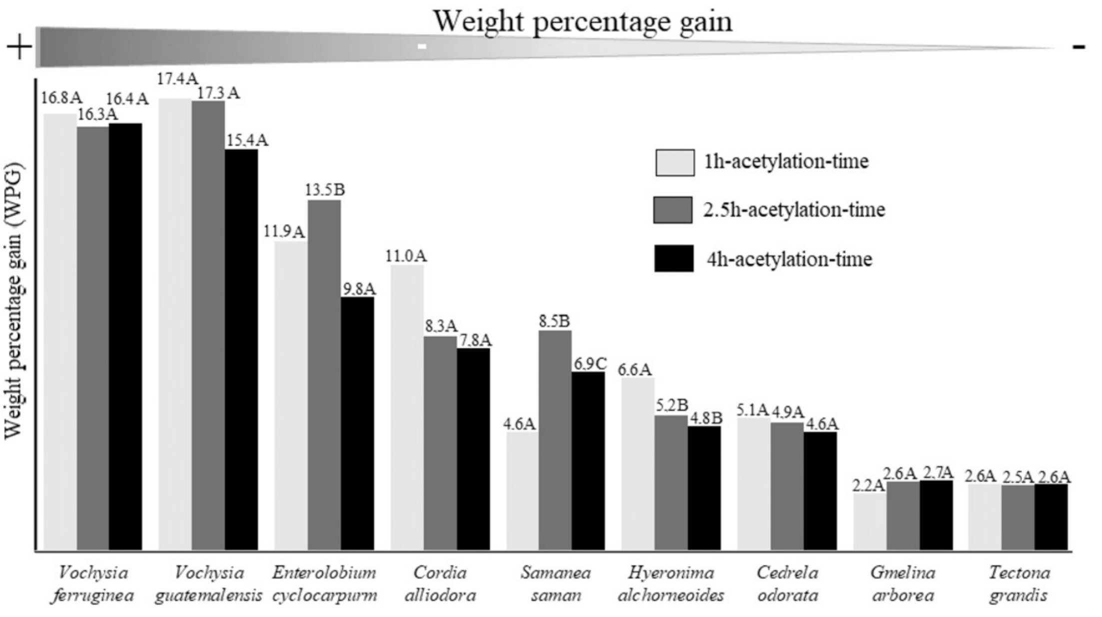

Figure 1. Weight percentage gain of nine fast-growth tropical species of Costa Rica for treated samples with three acetylation times. Legend: Different letters between acetylation times for a given parameter indicate statistical differences at 99%.

Wood density for original (untreated) woods at 65% RH varied between 349 kg/m^3 for *C. odorata* and 577 kg/m^3 for *H. alchorneoides.* Because this property is directly related to wood porosity, this could affect the WPG as discussed later. As expected, density generally increased after the acetylation process since that samples absorbed the chemical components. In some cases, density decreased after treatment, which however was attributed to differences in the initial density among the untreated group and the three treated groups of samples studied.

The MC at 65% RH for the untreated samples varied between 11.3% for *V. ferruginea* and 13.4% for *S. saman* (Table 1). These differences in EMC for a same RH could be due to the different amounts of extractives between the hardwoods studied (Hernández 2007a). As a result, comparisons on the effect of acetylation on hygroscopicity for the nine species becomes difficult. For this, comparisons of ΔMC and sorption ratio were more appropriate.

After wood samples were conditioned at 85%, the ΔMC values from 65% to 85% RH were all lower than those of untreated samples. The effect of the time of acetylation on ΔMC was generally not statistically significant, except for *S. saman*, where ΔMC means were different among different times of acetylation (Table 1). The sorption ratio (S) showed a similar behavior compared with ΔMC values, S decreased with the acetylation treatment, and some statistical differences were found among acetylation times (*S. saman*, *H. alchorneoides*, *G. arborea*, *C. odorata*; Table 1). Moreover, it was observed that the differences between the values of ΔMC and S factor of acetylated wood with untreated wood were lower in the species with lower WPG.

The partial TS significantly decreased after acetylation for all species (Table 1). There were no statistical differences between the acetylation times for *V. ferruginea*, *C. alliodora*, *H. alchorneoides*, *G. arborea*, and *C. odorata*. The highest partial TS among treatments was measured for 4.0 h-acetylation-time of *V. ferruginea*, *E. cyclocarpum*, *S. saman*, and *T. grandis* (Table 1). The differential TS ratio (G_T) was not affected by the acetylation in *V. ferruginea*, *V. guatemalensis*,

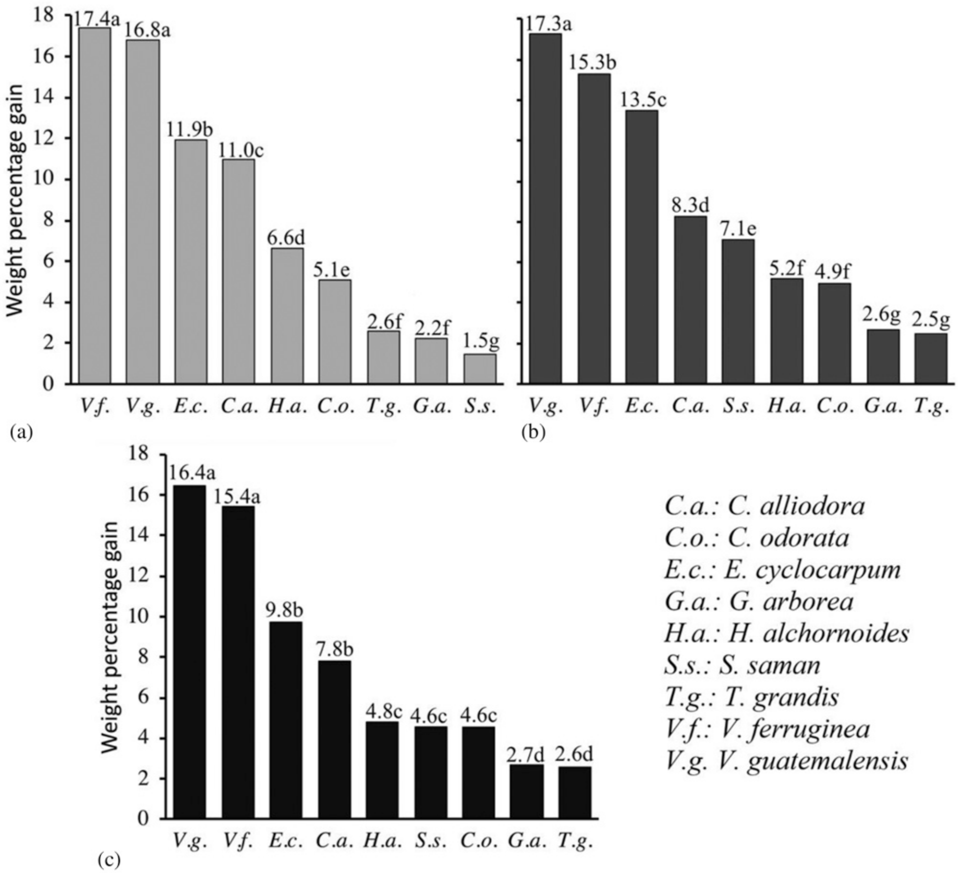

Figure 2. Weight percentage gain for (a) 1 h-acetylation, (b) 2.5 h-acetylation, and (c) 4 h-acetylation of nine fast-growth tropical species of Costa Rica. Legend: Different letters between acetylation times for a given parameter indicate statistical differences at 99%.

E. cyclocarpum, *C. alliodora*, *G. arborea*, *C. odorata*, and *T. grandis* but some acetylation time affected G_T parameter in *S. saman* and *H. alchorneoides*.

The acetylation did not affect the WA in *H. alchorneoides* and *G. arborea* in relation to untreated samples. However, WA decreased after acetylation in the three-time tested in relation to untreated samples for *V. guatemalensis*, *V. ferruginea*, *C. alliodora*, *S. saman*, and *T. grandis*. Also, this parameter (WA) decreased in 2.5 h-acetylation-time in *E. cyclocarpum* and 2.5 h- and 4.0 h-acetylation-time in *C. odorata*. In relation to different times of acetylation, no differences were found in *V. guatemalensis*, *H. alchorneoides*, and *G. arborea.* The lowest values of WA were found in 1.0 h-acetylation-time in *S. saman*, in 2.5 h-acetylation-time of *E. cyclocarpum* and *C. alliodora*, 2.5 h- and 4.0 h-acetylation-time of *C. alliodora*, in 4.0 h-acetylation-time of *V. ferruginea* and *T. grandis*, and 2.5 h- and 4.0 h-acetylation-time of *C. odorata* (Table 1).

Decay Resistance

In general, the acetylation process increased the resistance to decay, especially in species with higher values of WGP (Fig 4). For *L. acuta*, the acetylation treatments in all tested times did not

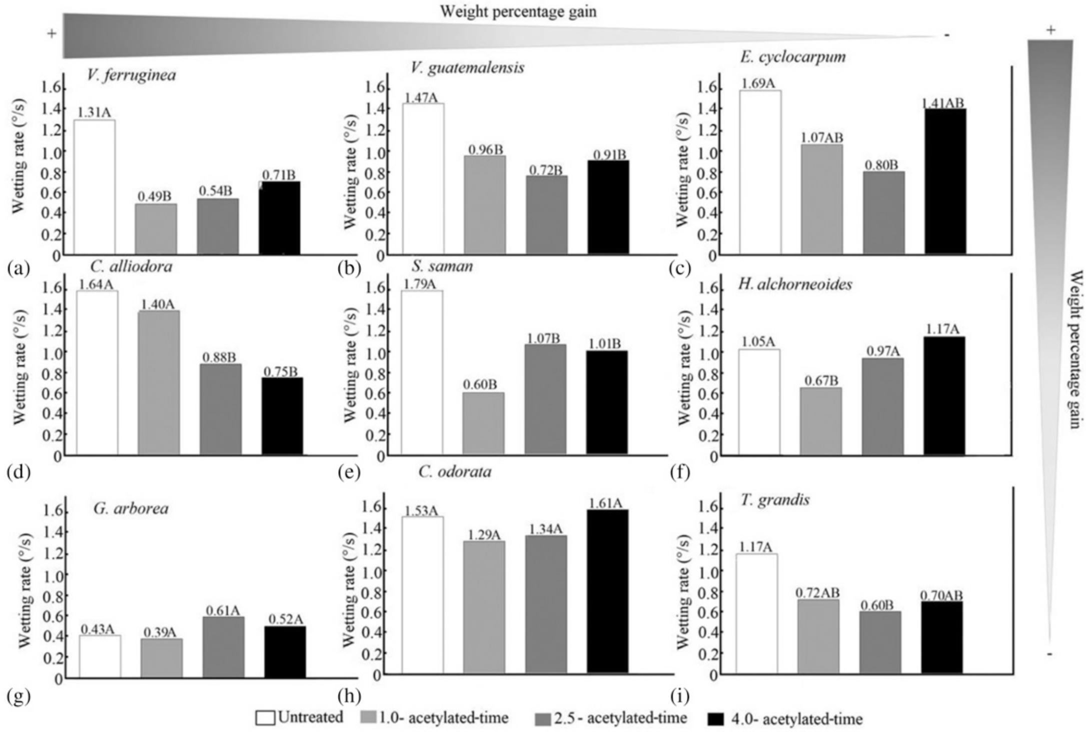

Figure 3. Wetting rate of nine fast-growth tropical species of Costa Rica for untreated and treated samples with three acetylation times. Legend: Different letters between acetylation times indicate statistical differences at 99% for each species.

affect weight loss in *H. alchorneoides* and *G. arborea*, in relation to the untreated samples. Weight loss decreased after acetylation three times in relation to untreated samples for *V. guatemalensis*, *V. ferruginea*, *C. odorata*, and *S. saman*. The lowest weight loss in three acetylation times was presented in *V. guatemalensis* and *S. saman*, in 2.5 h-acetylation-time in *V. ferruginea*, *E. cyclocarpum*, and *C. alliodora*, and in 4.0 h-acetylation-time in *T. grandis*. In relation to different times of acetylation, no differences were found in *V. guatemalensis*, *H. alchorneoides*, and *G. arborea.* The lowest values of weight loss of *L. acuta* fungus were found in 2.5 h-acetylation-time of *V. ferruginea*, *E. cyclocarpum*, *C. odorata*, and *C. alliodora*, 4.0 h-acetylation-time of *C. alliodora*, *T. grandis*, and *C. odorata* (Fig 4).

For *T. versicolor* (Fig 4), the acetylation process decreased the weight loss of this fungus in relation to untreated samples in *V. guatemalensis*, *V. ferruginea*, *S. saman*, *G. arborea*, and *C. odorata.* But this process affected *E. cyclocarpum*, *C. alliodora*, and *T. grandis* in 2.5 h-acetylation-time and for 4.0 h-acetylation-time of *C. alliodora*. For different time of acetylation, no affection was found in *V. guatemalensis*, *H. alchorneoides*, *G. arborea*, and *C. odorata*; also, the lowest weight loss was measured in 1.0 h- and 2.5 h-acetylation-time of *V. ferruginea*, in 2.5 h-acetylation-time of *E. cyclocarpum* and *T. grandis*, in 2.5 h- and 4.0 h-acetylation-time for *C. alliodora* and in 1.0 h-acetylation-time of *S. saman* (Fig 4).

Correlation Between WPG and Wood Properties of Acetylated Wood

A statistically positive correlation was observed between the WPGs, while a statistically negative correlation appeared in WPG with WA, Conversely, no correlation was found among wetting

Table 1. Density, MC at 65% RH, ΔMC, S ratio, partial tangential swelling (TS), differential TS, and water absorption (WA) of nine fast-growth tropical species of Costa Rica for untreated and treated samples with three acetylation times.

	Species	Acetylation time (h)	Density at 65% (kg/m³)	MC at 65% RH	ΔMC from 65% to 85% RH	S ratio	Partial TS from 65% to 85% RH (%)	Differential TS (G_T)	WA after immersion for 24 h (%)
Weight percentage gain	*Vochysia ferruginea*	Untreated	317.6^{A}	11.3^{A}	6.91^{A}	0.35^{A}	1.79^{A}	0.26^{A}	67.2^{A}
		1.0	330.5^{A}	8.32^{B}	3.48^{B}	0.17^{B}	0.85^{B}	0.25^{A}	40.8^{B}
		2.5	340.4^{A}	8.31^{B}	3.35^{B}	0.16^{B}	0.85^{B}	0.25^{A}	40.4^{B}
		4.0	327.0^{A}	9.16^{B}	3.58^{B}	0.17^{B}	1.15^{C}	0.32^{A}	47.4^{C}
	Vochysia guatemalensis	Untreated	303.6^{A}	11.86^{A}	7.61^{A}	0.38^{A}	1.49^{A}	0.21^{A}	62.8^{A}
		1.0	317.1^{A}	8.5^{B}	4.32^{B}	0.22^{B}	0.88^{B}	0.21^{A}	48.8^{B}
		2.5	316.5^{A}	8.02^{C}	4.00^{B}	0.20^{B}	0.92^{B}	0.23^{A}	50.3^{B}
		4.0	355.7^{B}	9.12^{BC}	4.27^{B}	0.21^{B}	1.03^{B}	0.24^{A}	49.5^{B}
	Enterolobium cyclocarpum	Untreated	461.4^{A}	12.16^{A}	6.39^{A}	0.29^{A}	1.41^{A}	0.22^{A}	30.8^{A}
		1.0	466.5^{A}	9.09^{B}	3.57^{B}	0.18^{B}	0.67^{B}	0.19^{A}	29.9^{A}
		2.5	446.1^{A}	8.16^{C}	3.00^{B}	0.15^{B}	0.60^{B}	0.20^{A}	26.6^{B}
		4.0	479.9^{A}	9.56^{B}	3.74^{B}	0.19^{B}	0.90^{C}	0.24^{A}	30.9^{A}
	Cordia alliodora	Untreated	378.5^{A}	12.02^{A}	6.27^{A}	0.28^{A}	1.63^{A}	0.26^{A}	51.9^{A}
		1.0	388.4^{A}	9.86^{B}	3.67^{B}	0.17^{B}	0.81^{B}	0.24^{A}	35.8^{B}
		2.5	421.7^{B}	8.21^{C}	3.53^{B}	0.15^{B}	0.87^{B}	0.26^{A}	25.5^{C}
		4.0	381.6^{A}	8.70^{CD}	3.27^{B}	0.14^{B}	0.76^{B}	0.24^{A}	30.6^{B}
	Samanea saman	Untreated	522.9^{A}	13.36^{A}	6.47^{A}	0.32^{A}	1.74^{A}	0.27^{A}	35.1^{A}
		1.0	539.2^{A}	8.64^{B}	2.80^{B}	0.13^{B}	0.43^{B}	0.16^{B}	20.3^{C}
		2.5	546.8^{A}	10.77^{C}	3.89^{C}	0.19^{C}	0.99^{C}	0.25^{A}	39.4^{B}
		4.0	570.5^{B}	9.96^{D}	3.59^{D}	0.16^{B}	1.14^{C}	0.33^{C}	33.4^{B}
	Hieronyma alchorneoides	Untreated	556.7^{A}	12.52^{A}	6.20^{A}	0.31^{A}	1.93^{A}	0.31^{A}	28.1^{A}
		1.0	590.4^{B}	12.65^{A}	4.07^{B}	0.18^{B}	1.28^{B}	0.32^{A}	25.1^{A}
		2.5	526.3^{C}	12.60^{A}	4.33^{B}	0.22^{C}	1.19^{B}	0.27^{B}	26.1^{A}
		4.0	543.4^{C}	12.40^{A}	4.31^{B}	0.22^{C}	1.23^{B}	0.29^{AB}	25.4^{A}
	Gmelina arborea	Untreated	422.3^{A}	11.77^{A}	6.06^{A}	0.30^{A}	1.41^{A}	0.23^{A}	18.3^{A}
		1.0	397.7^{B}	10.96^{A}	4.42^{B}	0.22^{B}	1.00^{B}	0.23^{A}	24.1^{A}
		2.5	466.4^{C}	10.74^{A}	3.85^{B}	0.19^{C}	1.08^{B}	0.28^{A}	22.7^{A}
		4.0	409.1^{A}	9.71^{B}	4.37^{B}	0.22^{B}	1.07^{B}	0.24^{A}	25.9^{A}
	Cedrela odorata	Untreated	317.1^{A}	12.10^{A}	7.86^{A}	0.31^{A}	1.67^{A}	0.21^{A}	56.8^{A}
		1.0	286.2^{A}	10.79^{B}	5.98^{B}	0.30^{B}	1.14^{B}	0.19^{A}	53.3^{A}
		2.5	297.8^{A}	11.02^{B}	5.43^{B}	0.27^{C}	0.92^{B}	0.17^{A}	40.6^{B}
		4.0	282.7^{A}	10.50^{B}	5.44^{B}	0.25^{C}	0.90^{B}	0.17^{A}	41.2^{B}
	Tectona grandis	Untreated	495.4^{A}	11.88^{A}	5.96^{A}	0.27^{A}	1.00^{A}	0.17^{A}	35.6^{A}
		1.0	538.0^{AB}	9.23^{B}	4.75^{B}	0.24^{B}	0.68^{B}	0.14^{A}	22.6^{B}
		2.5	528.8^{AB}	8.58^{B}	4.50^{B}	0.23^{B}	0.87^{C}	0.19^{AB}	21.2^{B}
		4.0	549.2^{B}	9.3^{B}	4.45^{B}	0.22^{B}	1.03^{C}	0.23^{B}	17.1^{C}

Same letters are not statistically different at the 1% probability level for different acetylation time, for each species separately.

rate, wood density, MC, partial TS, ΔMC from 65% to 85% and S factor, differential TS ratio, and weight loss by *L. acuta* and *T. versicolor* (Table 2). In the relation to the new parameter derived of ΔMC, factor S, and GU, the difference of these parameters between acetylated and untreated wood, correlation coefficient showed that there was a positive correlation of these parameters with WPG for each species (Fig 5).

DISCUSSION

The absorption of liquids in hardwoods is related to the permeability of the wood species (Ahmed and Chun 2011), which varies as a function of their anatomical structure. In hardwoods, liquid flow occurs mainly along lumina vessels in the longitudinal axis of tree (Ahmed and Chun 2009), but this flow can be interrupted by the presence of tyloses or gum in the vessels (Ahmed and Chun

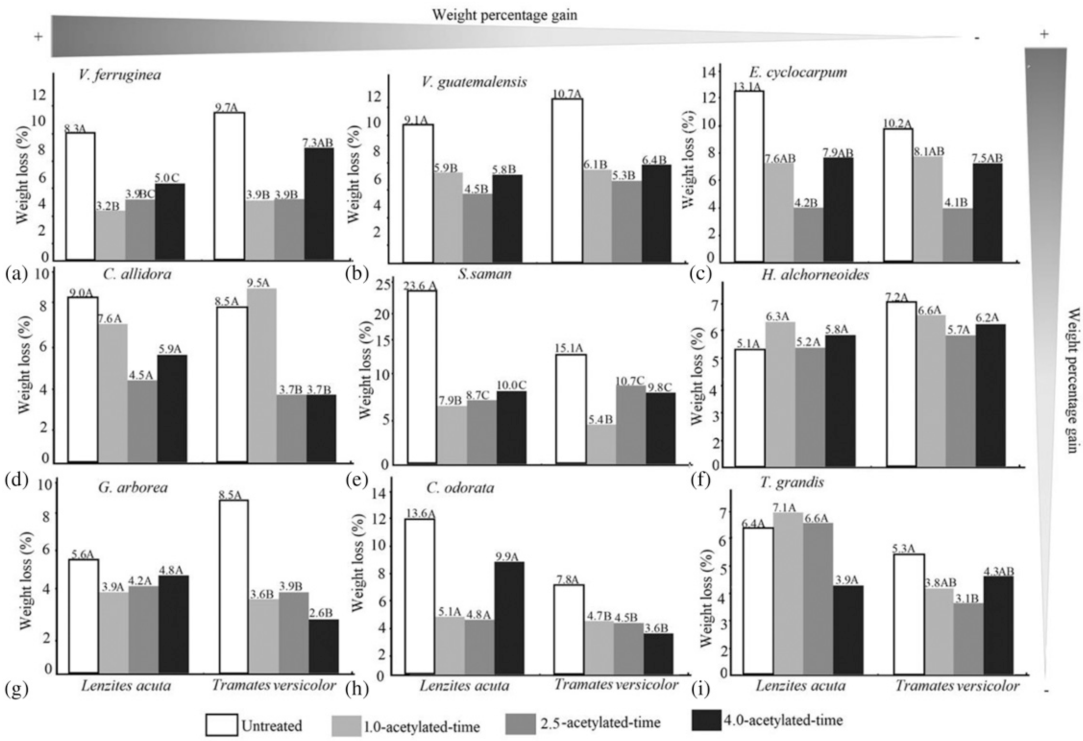

Figure 4. Weight loss due to fungal decay by *Lenzites acuta* and *Trametes versicolor* of nine fast-growth tropical species of Costa Rica for untreated and treated samples with three acetylation times. Legend: Different letters between acetylation times for a given fungal decay indicate statistical differences at 99%.

2011). Vessels connect longitudinal and radial parenchyma across wall pits, so liquids can subsequently flow through the ray lumina (Ahmed and Chun 2009). This flow is favored when the rays are composed of either over 3 series in width or a greater abundance of parenchyma is demonstrated (Ahmed and Chun 2011). Variations in the anatomy of the species tested in acetylation have been extensively discussed by Gaitán-Álvarez et al (2020). These authors reported that *E. cyclocarpum*, *H. alchorneoides*, *S. saman*, *V. ferruginea*, and *V. guatemalensis* present anatomical features of greater dimensions, specifically vessels' diameter (ie over 120 μm), rays' width (ie from 2 to 10 series of cells or over 252 μm) and their frequency of over 5 rays/mm^2, as well as various types of parenchyma (Table 3). These anatomical features are conducive to the flow of acetic anhydride and glacial acetic acid solutions, per the present study, in which these species present higher absorption and WPG values (Fig 1) and presented same variation of acetylation time (Fig 2). Conversely, species showing the lower absorption and WPG values were *C. odorata*, *G. arborea*, and

Table 2. Pearson correlation between weight percentage gain and the different properties of acetylated wood from nine fast-growth hardwoods in Costa Rica.

Wood properties	Correlation coefficient
Wetting rate	-0.04^{NS}
Wood density (kg/cm^3)	0.06^{NS}
MC at 65% of HR	-0.31^{NS}
ΔMC from 65% to 85%	-0.42^{NS}
S ratio	-0.38^{NS}
Differential TS ratio	0.19^{NS}
TS (%)	-0.27^{NS}
WA	−0.83**
Weight loss by *Lenzites acuta*	0.04^{NS}
Weight loss by *Trametes versicolor*	0.16^{NS}

NS, not statistically significant.

** Statistically significant at 0.01 probability level.

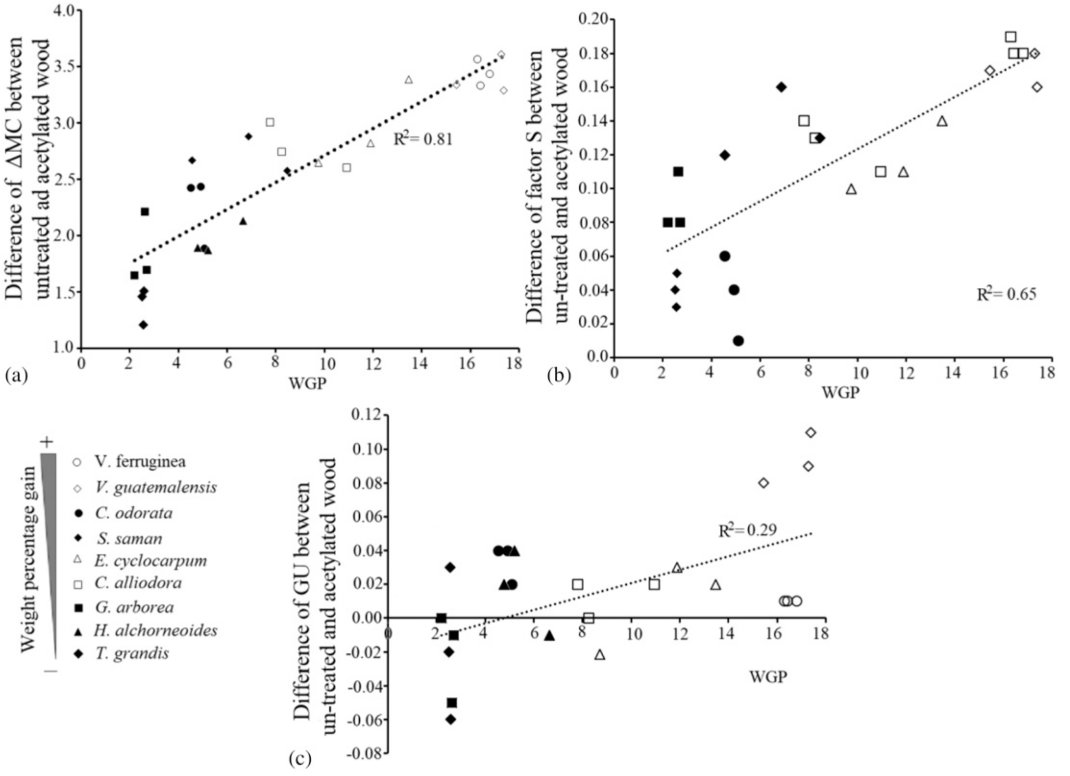

Figure 5. Relationship between weight percentage gain and the difference of ΔMC (a), S factor (b), and GU (c) of acetylated wood and untreated wood.

T. grandis (Fig 1), due to anatomical structure less favorable to liquid flow, such as smaller and less-frequent rays, deposits in vessels such as gum and tyloses, as well as few vessel-associated parenchyma (Table 3). Then the effects of acetylation varied with time, for some species, eg *T. grandis* presented higher WPG than *G. arborea* and *S. saman* at 1 h-acetylation-time (Fig 2[a]), but WPG was lowest values in 2.5 h-acetylation-time and 4 h-acetylation-time (Fig 2[b] and [c]).

In many of the species, the acetylation time did not have an effect on the absorption except for *E. cyclocarpum*, *S. saman*, and *H. alchorneoides* or partial TS, which the 4 h-acetylation-time treatment yielded a significantly lower absorption (Fig 1) or higher partial TS (Table 2). This decrease, for these species, may be attributed to the completion of the acetylation reaction well before the time limit. After some time, the reaction slows down and levels off, indicating that the reaction was "complete" (Rowell and Ibach 2018). After which, once acetylation is fulfilled, degradation of the acetic anhydride may have taken place, since the temperature used for the process (120°C) was close to the boiling temperature of this compound (139°C). As such, this result suggests that a longer acetylation time resulted appropriated for *E. cyclocarpum*, *S. saman*, and *H. alchorneoides*.

The wetting rate determines indirectly surface tension and the elation of the surface energy of the solid material (Gindl et al 2001) and, in the case of wood, these parameters are related to water adsorption (Collett 1972). In this way, in some species, namely *V. ferruginea* (Fig 3[a]), *V. guatemalensis* (Fig 3[b]), and *S. saman* (Fig 3[e]), these properties were influenced with acetylation in relation to untreated samples, because

Table 3. Anatomical characteristics of nine fast-growth tropical species in Costa Rica.

	Species	*C. odorata*	*C. alliodora*	*E. cyclocarpum*	*G. arborea*	*H. alchorneoides*	*S. saman*	*T. grandis*	*V. ferruginea*	*V. guatemalensis*
	FP (vessel mm^{-2})	9	7	6	5	17	4-5	4	2-3	3
	DV (μm)	125	166	167	189	116	152	150	145	169
	Deposits	G	T	G	T	G	G	G	—	—
	DPI	3	3	3	5	10	4	6	4	3
Radial	Ray height	104	870	252	270	560	250	440	580	229
parenchyma	Cells in ray width	4-10	2-6	1-3	1-3, 4-10	2-4	2-3	1-3, 4-10	1-3	1-3, 4-10
	Ray frequency	2	3	6-7	6	7	6-7	5	5	3
Axial	PA	−	−	−	−	+	+	−	−	−
parenchyma	PP	+	+	+	+	+	+	+	+	+
	PB	−	+	−	−	−	−	+	−	+

FP, pore frequency; LV, vessel length; DV, vessel diameter; T, tyloses; G, gums; DIP, intervascular punctuation diameter; PA, apotracheal parenchyma; PP, paratracheal parenchyma; PB, banded parenchyma.

wetting rate values showed a decrease, therefore these species were more affected by acetylation. In addition, the decrease in the wetting rate indicates a change in polarity of the surface for the different tropical wood species (Adebawo et al 2016). This is especially true in species with a high degree of acetylation (high WPG). Adebawo et al (2016) indicate that upon acetylation there comes incorporation of acetyl groups into the cell walls, thereby making the wood surface hydrophobic (Sandberg et al 2017). This performance was confirmed with the ΔMC values between 65% and 85% RH for the different species, where acetylated wood presented significantly lower ΔMC than untreated wood (Table 2). Another aspect of this relationship between wetting rate and WPG is that there are fewer differences between untreated and acetylated wood in species with low WPG, such as *G. arborea*, *C. odorata*, or *T. grandis* (Fig 3[g] and [h]). In contrast, no correlation was revealed between wetting rate and WPG (Table 3), probably due to fact that the wetting rate is related to other parameters of the wood that are not affected by the acetalization (Collett 1972).

Each acetylation time yields different values of WPG (Fig 1) and, of course, different surface effects which may or may not be compatible with water molecules (Gindl et al 2001). Among the different tropical species presented in this study, in those with a high WPG value, specifically *V. ferruginea*, *V. guatemalensis*, and *E. cyclocarpum* (Fig 3[a]-[c]), the 4 h-acetylation-time yields similar values of contact angles and T_{final} compared with untreated samples, suggesting better acetylation in 1 h-acetylation-time and 2.5 h-acetylation-time for those species. Meanwhile, in species with a lower WPG value, acetylation time from 1 to 4 h will not produce variation in contact angles and their final stabilization time (Fig 3[d]-[i]).

As expected, physical properties related to WA (MC, ΔMC, TS, S factor, GU, and WA) in most species presented lower values after acetylation treatment (Table 1). However, although the acetylation process affected wood properties in all species, the effect of this treatment is greater in species with higher WPG. The relationships between WPGs and the difference of ΔMC, TS, S ratio, G_T between acetylated and untreated wood is positive (Fig 5). Therefore, wood species with low WPG (such as *G. arborea* and *T. grandis*) showed less gain in dimensional and hygroscopic stabilities than those species with high WPGs, such as *V. guatemalensis* or *V. ferruginea* (Fig 5).

In fact, the lower acetylation and its effect on physical properties related to WA can also be observed in the correlation analysis shown for MC, TS, and WA, in which these presented a negative correlation with WPG (ie a decrease in each parameter with increasing WPG); however, only for WA, the physical properties showed statistical significance (Table 2). The presence and amount of hydroxyl groups, capable of forming hydrogen bonds with water molecules, is important to hygroscopic and dimensional stability and they are mainly present in hemicelluloses, followed by cellulose and lignin (Engelund et al 2013). During WA in these sites, the water molecule with two full-strength covalent bonds may become bound by two relatively strong H-bonds with a pair of nearby OH groups of the amorphous polysaccharide polymers in low MC. Meanwhile, the cooperativity in the H-bond network increases with increasing MC, gradually allowing the coalescence of water vapor molecules with already adsorbed water molecules to form a water dimer (Willems 2018). Thus, this gain in moisture makes wood dimensionally and hygroscopically unstable as the lumber gains weight. With acetylation, however, the OH^- anion group in wood components becomes chemically bound to a residue of the acetate (CH_3COO) of an acetic anhydride molecule $(CH_3CO)_2$ (Mantanis 2017). In this process, the OH^- anion group is reduced, decreasing the hygroscopicity of the wood and resultantly, increasing its dimensional stability (Adebawo et al 2016). Although the acetylation affected the hygroscopic S and dimensional stability of wood, the results showed that this treatment affected the former relatively more than the latter. The S ratio, which measures hygroscopic stability, decreased in all species (Table 1) and presented higher correlation coefficients (Fig 5[a] and [b]) than those obtained for G_T (dimensional stability, in Fig 5[c]). G_T in fact did not show a significant difference between acetylated wood and untreated wood (Table 1). Therefore, these results indicate that the changes in tangential dimensions for acetylated wood were caused by the reduction of the sorption capacity of wood.

However, according to Rowell (2016), acetylation of wood prevents its biological degradation by three possible mechanisms: 1) the first one consists in modifying the composition and physical configuration of the substrate where the specific enzymatic attack may take place, 2) the second one where the acetyl group forms a covalent bond, therefore it is no longer available for an enzymatic attack, and 3) the third theory based on the physical blockage of micropores of the cellular wall, rendering enzymatic penetration impossible. As confirmed in this study, susceptibility to fungal attack is related to WPG (Fojutowski et al 2014; Rowell 2014); however, this is a negative correlation, indicating that an increasing WPG decreases the loss of mass by the two fungi tested (Table 3). Therefore, differences between acetylated and untreated samples were found to be less or almost null in those species with lower WPG (Fig 4[b] and [f]-[h]). This effect can be attributed to low acetylation, which eases fungal enzymes' access to hydroxyl groups (Fojutowski et al 2014; Rowell 2014). There were no effects on resistance to decay related to the length of acetylation times, indicating that in shorter times acetyl groups have already been taken by the acetate group (CH_3COO), leaving little opportunity for fungal attack (Pawar et al. 2013).

CONCLUSIONS

The acetylation treatment of tropical hardwoods is achieved with varying levels of WPG, which is more directly related to the type of species and less to the length of the acetylation time. This clearly evidences that differences between the species are attributed to liquid flow inside the wood, or permeability, which depends on the anatomical features of the species. This variation in WPG per species produces various effects on the properties of wood. When species presented WPG values over 10%, eg *V. ferruginea*, *V. guatemalensis*, *C. alliodora*, or *E. cyclocarpum*, thermal stability and wetting rate, but the advantage that there was a decrease in the value of parameters related to water adsorption (ie swelling, MC, MC variation, ΔMC from 65% to 85%, S ratio, and G_T) and a favorable increase in resistance to biological degradation. Other important results were that species with low WPG values (ie low acetylation level), showed less gain in the dimensional or hygroscopic stability of the wood than those species with high WPG. It was also clear that gain in the dimensional stability was due to the better hygroscopic stability after acetylation. In addition, results showed that the 2.5 h time is an appropriate acetylation time.

ACKNOWLEDGMENTS

The authors wish to thank Vicerrectoría de Investigación y Extensión, of the Instituto Tecnológico de Costa Rica (ITCR, Cartago, Costa Rica) for the project financial support. This research project was carried out in cooperation with Département des Sciences du Bois et de la Forêt of the Université Laval, Québec, Canada.

REFERENCES

Adebawo FG, Naithani V, Sadeghifar H, Tilotta D, Lucia LA, Jameel H, Ogunsanwo OY (2016) Morphological and interfacial properties of chemically-modified tropical hardwood. RSC Adv 6:6571-6576. doi: 10.1039/C5RA19409A.

Adebawo F, Sadeghifar H, Tilotta D, Jameel H, Liu Y, Lucia L (2019) Spectroscopic interrogation of the acetylation selectivity of hardwood biopolymers. Starke 71: 1900086. doi: 10.1002/star.201900086.

Ahmed SA, Chun SK (2009) Observation of liquid permeability related to anatomical characteristics in *Samanea saman*. Turk J Agric For 33(2):155-163. doi: 10.3906/tar-0807-13.

Ahmed SA, Chun SK (2011) Permeability of *Tectona grandis* L. as affected by wood structure. Wood Sci Technol 45(3):487-500. doi: 10.1007/s00226-010-0335-5.

ASTM (2014) Standard test method of accelerated laboratory test of natural decay resistance of woods. D-2017-05. Annual Book 04.09. ASTM Standard. American Society for Testing and Materials, West Conshohocken, PA. 8 pp.

ASTM (2020) Standard test methods for evaluating properties of wood-base fiber and particle panel materials. D-1037-12. Annual Book 04.10. ASTM Standard. American Society for Testing and Materials, West Conshohocken, PA. 37 pp.

ASTM (2021) Standard guide for moisture conditioning of wood and wood-based materials. D-4933-16. Annual Book 04.10. ASTM Standard. American Society for Testing and Materials, West Conshohocken, PA. 8 pp.

Bollmus S, Bongers F, Gellerich A, Lankveld C, Alexander J, Militz H (2015) Acetylation of German hardwoods. Pages 164-173 *in* Proc 8th European Conference on Wood Modification, Helsinki, Finland.

Bongers F, Meijerink T, Lütkemeier B, Lankveld C, Alexander J, Militz H, Lehringer C (2016) Bonding of acetylated wood. Int Wood Prod J 7(2):102-106. doi: 10.1080/20426445.2016.1161944.

Collett BM (1972) A review of surface and interfacial adhesion in wood science and related fields. Wood Sci Technol 6(1):1-42. doi: 10.1007/BF00351806.

Cool J, Hernández RE (2011) Improving the sanding process of black spruce wood for surface quality and water-based coating adhesion. Forest Prod J 61(5):372-380. doi: 10.13073/0015-7473-61.5.372.

Emaminasab M, Tarmian A, Oladi R, Pourtahmasi K, Avramidis S (2017) Fluid permeability in poplar tension and normal wood in relation to ray and vessel properties. Wood Sci Technol 51(2):261-272. doi: 10.1007/s00226-016-0860-y.

Engelund ET, Thygesen LG, Svensson S, Hill C (2013) A critical discussion of the physics of wood-water interactions. Wood Sci Technol 47(1):141-161. doi: 10.1007/s00226-012-0514-7.

Fojutowski A, Koziróg A, Kropacz A, Noskowiak A (2014) The susceptibility of some acetylated hardwood species to mould fungi attack—An attempt to objectify the assessment. Int Biodeterior Biodegrad 86(Part B 86):60-65. doi: 10.1016/j.ibiod.2013.08.007.

Gaitán-Álvarez J, Berrocal A, Mantanis G, Moya R, Araya F (2021) Acetylation of tropical hardwood species from forest plantations in Costa Rica: An FTIR spectroscopic analysis. J Wood Sci 66:49-59. doi: 10.1186/s10086-020-01898-9.

Gaitán-Álvarez J, Moya R, Berrocal A, Araya F (2020) In-situ mineralization of calcium carbonate of tropical hardwood species from fast-grown plantations in Costa Rica. Fresenius Environ Bull 29(10):9184-9194.

Gérardin P (2016) New alternatives for wood preservation based on thermal and chemical modification of wood—A review. Ann Sci 73(3):559-570. doi: 10.1007/s13595-015-0531-4.

Gibson LJ (2012) The hierarchical structure and mechanics of plant materials. J R Soc Interface 9(76):2749-2766. doi: 10.1098/rsif.2012.0341.

Gindl M, Sinn G, Gindl W, Reiterer A, Tschegg S (2001) A comparison of different methods to calculate the surface free energy of wood using contact angle measurements. Colloids Surf A Physicochem Eng Asp 181 (1-3):279-287. doi: 10.1016/S0927-7757(00)00795-0.

Giridhar BN, Pandey KK, Prasad BE, Bisht SS, Vagdevi HM (2017) Dimensional stabilization of wood by chemical modification using isopropenyl acetate. Maderas Cienc Tecnol 19(1):15-20. doi: 10.4067/S0718-221X2017005000002.

Hernández RE (2007a) Moisture sorption properties of hardwoods as affected by their extraneous substances, wood density and interlocked grain. Wood Fiber Sci 39(1):132-145.

Hernández RE (2007b) Swelling properties of hardwoods as affected by their extraneous substances, wood density, and interlocked grain. Wood Fiber Sci 39(1): 146-158.

Hill C (2006) Wood modification: Chemical, thermal and other processes. John Wiley & Sons, Ltd., Chichester, UK. 219 pp.

Kojima M, Yamamoto H, Okumura K, Ojio Y, Yoshida M, Okuyama T, Ona T, Matsune K, Nakamura K, Ide Y, Marsoem S, Sahri M, Hadi Y (2009) Effect of the lateral growth rate on wood properties in fast-growing hardwood species. J Wood Sci 55(6):417-424. doi: 10.1007/s10086-009-1057-x.

Kozarić L, Kukaras D, Bešević M, Prokić A, Đurić N (2016) Acetylated wood in constructions. Transilvania University of Braşo 9(58):81-86.

Mantanis GI (2017) Chemical modification of wood by acetylation or furfurylation: A review of the present scaled-up technologies. BioResources 12(2):4478-4489.

Mantanis GI, Young RA (1997) Wetting of wood. Wood Sci Technol 31(5):339-353. doi: 10.1007/BF01159153.

Matsunaga M, Hewage DC, Kataoka Y, Ishikawa A, Kobayashi M, Kiguchi M (2016) Acetylation of wood using supercritical carbon dioxide. J Trop For Sci 28 (2):132-138.

Moya R (2018) La producción de madera de especies nativas en plantaciones comerciales: Una opción real. Ambientico 267(6):32-36.

Moya R, Rodriguez-Zuñiga A, Berrocal A, Vega-Baudrit J (2017) Effect of silver nanoparticles synthetized with NPsAg-ethylene glycol ($C_2H_6O_2$) on brown decay and white decay fungi of nine tropical woods. J Nanosci Nanotechnol 17(8):5233-5240. doi: 10.1166/jnn.2017.13814.

Pawar PMA, Koutaniemi S, Tenkanen M, Mellerowicz EJ (2013) Acetylation of woody lignocellulose: Significance and regulation. Front Plant Sci 4:118. doi: 10.3389/fpls.2013.00118.

Rowell RM (2006) Acetylation of wood: Journey from analytical technique to commercial reality. Forest Prod J 56(9):4-12.

Rowell RM (2012) Handbook of wood chemistry and wood composites. Pages 537-598 *in* RM Rowell, ed. Handbook of wood chemistry and wood composites, 2nd edition. CRC Press, Boca Raton, FL.

Rowell RM (2014) Acetylation of wood—A review. Int J Lignocellulosic Prod 1(1):1-27.

Rowell RM (2016) Dimensional stability and fungal durability of acetylated wood. Drewno 59(197):139-150. doi: 10.12841/wood.1644-3985.C14.04.

Rowell RM, Ibach RE (2018) Stable and durable wood products based on molecular modification. J Trop For Sci 30:488-495.

Sandberg D, Kutnar A, Mantanis G (2017) Wood modification technologies—A review. IForest (Viterbo) 10(6): 895-908. doi: 10.3832/ifor2380-010.

Tenorio C, Moya R (2021) Development of a thermo-hydro-mechanical device for wood densification adaptable to universal testing machines and its evaluation in a tropical species. J Test Eval 49(4):20180760. doi: 10.1520/JTE20180760.

Tenorio C, Moya R, Salas C, Berrocal A (2016) Evaluation of wood properties from six native species of forest plantations in Costa Rica. Rev Bosque 37(1):71-84. doi: 10.4067/S0717-92002016000100008.

Wang S, Dai G, Yang H, Luo Z (2017) Lignocellulosic biomass pyrolysis mechanism: A state-of-the-art review. Prog Energy Combust Sci 62:33-86. doi: 10.1016/j.pecs.2017.05.004.

Willems W (2018) Hygroscopic wood moisture: Single and dimerized water molecules at hydroxyl-pair sites? Wood Sci Technol 52(3):777-791. doi: 10.1007/s00226-018-0998-x.

EVALUATION OF XYLEM MATURATION PROCESS AND EFFECTS OF RADIAL GROWTH RATE ON CELL MORPHOLOGIES IN WOOD OF BALSA (*OCHROMA PRYAMIDALE*) TREES

Y. A. B. Pertiwi

Lecturer
Faculty of Agriculture
Sebelas Maret University
Surakarta, 57126, Indonesia
E-mail: yus_andhini@staff.uns.ac.id

F. Ishiguri†

Associate Professor
School of Agriculture
Utsunomiya University
Utsunomiya 321-8505, Japan
E-mail: ishiguri@cc.utsunomiya-u.ac.jp

I. Nezu

PhD Student
United Graduate School of Agricultural Science
Tokyo University of Agriculture and Technology
Fuchu, Tokyo 183-8509, Japan
E-mail: s216739w@st.go.tuat.ac.jp

H. Aiso

Assistant Professor
E-mail: aiso.haruna@spua.ac.jp

Y. Hiraoka

Associate Professor
Faculty of Agricultural Production and Management
Shizuoka Professional University of Agriculture
Iwata, Shizuoka 438-8577, Japan
E-mail: hiraoka.yuichiro@spua.ac.jp

S. N. Marsoem

Professor
Faculty of Forestry
Gadjah Mada University
Yogyakarta, Indonesia
E-mail: snmarsoem@ugm.ac.id

J. Ohshima

Associate Professor
E-mail: johshima@cc.utsunomiya-u.ac.jp

* Corresponding author
† SWST member

Wood and Fiber Science, 54(2), 2022, pp. 149-159
https://doi.org/10.22382/wfs-2022-15

S. Yokota
Professor
School of Agriculture
Utsunomiya University
Utsunomiya 321-8505, Japan
E-mail: yokotas@cc.utsunomiya-u.ac.jp

(Received March 2022)

Abstract. The radial variations of cell morphologies (cell lengths, vessel diameter, vessel frequency, and cell wall thickness of wood fibers) were investigated for 7-yr-old *Ochroma pyramidale* trees planted in East Java, Indonesia, by developing the linear or nonlinear mixed-effects models. In addition, xylem maturation process based on the cell morphologies and effects of radial growth rate on cell morphologies were discussed. The mean values of cell morphology were as follows: vessel element length 0.59 mm, fiber length 2.16 mm, vessel diameter 221 μm, and fiber wall thickness 1.03 μm. Radial variations of cell length and vessel diameter were well explained by Michaelis–Menten equation: values increased from pith to certain position and then it became almost stable. Vessel frequency, wood fiber diameter, and wood fiber wall thickness was expressed by the formula of logarithmic formula, quadratic formula, and linear formula, respectively. Variance component ratio of category was 66.8%, 46.1%, 31.4%, 1.5%, and 33.7% for vessel element length, wood fiber length, vessel diameter, vessel frequency, and wood fiber wall thickness, respectively, whereas the model for wood fiber diameter was not converged. These results suggested that many cell morphologies were influenced by the radial growth rate. Smaller values of mean absolute error obtained in the models in relation to distance from pith were found in all cell morphologies, except for vessel frequency and wood fiber diameter. Thus, xylem maturation of this species depended on diameter growth rather than cambial age. Boundary of core wood and outer wood was 5-10 cm from pith in which increasing ratio of cell length reached <0.3%. Core wood was characterized as lower wood density and mechanical properties with shorter cell lengths and thinner wood fiber walls, whereas outer wood was characterized as higher wood density and mechanical properties with longer cell length and thicker wood fiber walls.

Keywords: Balsa, radial growth rate, radial variation, xylem maturation process.

INTRODUCTION

Balsa (*Ochroma pyramidale* [Cav.] Urban., Syn. *O. lagopus* Swartz) is a pioneer tropical fast-growing tree species in wet tropical lowlands which produces exceptionally low and wide range wood density (0.04-0.31 g/cm^3) (Easterling et al 1982; Midgley et al 2010; Rueda and Williamson 1992; Sosef et al 1998; Wiemann and Williamson 1988; Williamson and Wiemann 2010). This species is also used as plantation species in tropics (Midgley et al 2010; Pertiwi et al 2017a; Sosef et al 1998).

Xylem maturation process both in the tropical and temperate hardwood species has been evaluated by the radial variations of cell morphologies and wood properties (Bhat et al 2001; Honjo et al 2005; Kojima et al 2009a,b; Pertiwi et al 2018; Tsuchiya and Furukawa 2009a,b). The concept of "juvenile wood and mature wood" or "core wood and mature wood" is based on the radial variations of wood properties and cell morphologies in relation to xylem maturation process: juvenile wood or core wood is the wood with unstable properties, and mature wood or outer wood is the wood with stable properties (Erdene-Ochir et al 2021; Makino et al 2012; Nezu et al 2020, 2022; Wahyudi et al 2014). On the other hand, we previously reported that basic density and mechanical properties of 7-yr-old *O. pyramidale* trees planted in Indonesia were almost constant up to 8 cm from pith and then increased toward the bark (Pertiwi et al 2017a): core wood was stable but lower strength properties, and outer wood was unstable but higher strength properties. The concept of core wood and outer wood in relation to xylem maturation process in *O. pyramidale* might be different from other tropical and temperate hardwood species. Thus, detailed xylem maturation process should be clarified for this species.

Mixed-effects models are primary used to describe relationships between a response variable and some covariates in data that are grouped according to one or more classification factors (Pinheiro and Bates 2000). Examples of such grouped data include longitudinal data, repeated measures data, multilevel data, and block designs (Pinheiro and Bates 2000). By using these characteristics, radial variations of wood properties and cell morphologies in softwoods were evaluated by developing linear or nonlinear mixed-effect models models (Auty et al 2013; Dahlen et al 2018; Fujimoto and Koga 2010). Recently, we evaluated xylem maturation process of cell morphologies in a tropical tree species, *Shorea macrophylla*, planted in Malaysia by using mixed-effects models (Nezu et al 2022). In the study, the mixed-effects models with fixed-effect parameter of distance from pith and random-parameter of individual trees was used, resulting that radial variation patterns of cell morphologies could be evaluated with a consideration of variations of individuals. However, application of mixed-effect models is still limited for tropical hardwoods to evaluate the radial variations of wood properties and cell morphologies.

Evaluation of effects of radial growth rate on the wood properties is one of the interesting topics in commercial tropical fast-growing tree species (Aiso-Sanada et al 2019; Hidayati et al 2017; Ishiguri et al 2016; Kojima et al 2009a,b; Makino et al 2012; Pertiwi et al 2017a,b, 2018; Wahyudi et al 2016) because many forest managers considered that trees with fast-growing characteristics may produce wood with lower quality. We previously reported that fast-growing characteristics did not always produce the lower quality wood in several fast-growing tree species, such as *Acacia mangium, Eucalyptus camaldulensis, Gmelina arborea*, and others (Aiso-Sanada et al 2019; Hidayati et al 2017; Ishiguri et al 2016; Makino et al 2012; Pertiwi et al 2017a,b; Wahyudi et al 2016). Thus, the effect of radial growth rate on cell morphologies and wood properties should be clarified for plantation grown *O. pyramidale*.

The objectives of this study were to evaluate the xylem maturation process and effects of the radial growth rate on cell morphologies in *O. pyramidale*. Radial variations of cell morphologies were measured in 7-yr-old *O. pyramidale* trees grown in Probolinggo, East Java, Indonesia, and were evaluated by developing linear or nonlinear mixed-effect models. In addition, characteristics of core wood and outer wood in this species were also discussed.

MATERIALS AND METHODS

Samples Collection

A 10-cm thick disk strips were obtained from the disks collected at 1.2-1.3 m above the ground from the 7-yr-old balsa (*O. pyramidale* [Cav.] Urban.) at the plantation forest located in Krucil, Probolinggo, East Java, Indonesia (07°58′ S, 113°29′ E, *ca.* 1053 m in altitude). In the present study, to evaluate the effect of radial growth rate on the cell morphologies, trees were categorized into three groups based on its stem diameter (slow-, medium-, and fast-growth) as described by Pertiwi et al (2017a). The mean values and detail information on the tree growth characteristics and wood properties were reported in our previous study (Table 1, Pertiwi et al 2017a).

Cell Morphologies

Due to indistinct growth rings, the radial variation in fiber and vessel element lengths were determined at 1-cm intervals from the pith to the bark. Small pieces of wood were macerated in Schulze's solution (100 mL of 35% nitric acid with 6 g potassium chlorate). Macerated samples were washed with distilled water several times. The macerated samples were placed on glass slides, mounted with 75% glycerol, and covered with cover slips. Fiber and vessel element lengths were measured by using a profile projector (V-12B, Nikon, Tokyo, Japan) and a digital caliper (CD-30C, Mitutoyo, Kawasaki, Japan). Wood fiber and vessel element lengths were measured according to our previous paper (Pertiwi et al 2017a). A total 50 wood fibers and 30 vessel elements were measured for each position.

The radial variations of anatomical characteristics were examined by using specimens (ca. 1 cm [L] by 1 cm [R] by 1 cm [T]) collected from the pith

Table 1. Mean and standard deviation of tree characteristics and wood properties of nine selected *Ochroma pyramidale* used in the present study (Pertiwi et al 2017a).

Character	Slow growth (n = 3)	Medium growth (n = 3)	Fast growth (n = 3)	Total (n = 9)
D (cm)	22.7 ± 1.7	31.1 ± 0.2	40.8 ± 2.1	31.5 ± 8.0
TH (m)	20.0 ± 4.7	25.8 ± 4.2	26.0 ± 5.4	24.0 ± 5.1
BD (g/cm^3)	0.12 ± 0.01	0.14 ± 0.01	0.15 ± 0.02	0.14 ± 0.02
CS (MPa)	9.5 ± 1.6	9.3 ± 0.5	11.9 ± 1.5	10.3 ± 1.7

n, number of trees; D, stem diameter at 1.3 m above the ground; TH, tree height; BD, basic density; CS, compressive strength parallel to grain. Values are mean ± standard deviation.

to the bark. Transverse sections of 20-30 μm in thickness were obtained by a sliding microtome (REM 710, Yamatokoki, Saitama, Japan). The transverse sections were stained with 1% safranin, dehydrated, mounted, and covered with cover slip. The images of *O. pyramidale* wood transverse sections were captured by a digital camera (E-P3, Olympus, Tokyo, Japan) attached to a light microscope (BX51, Olympus, Tokyo, Japan). Then, the digital images were transferred to the personal computer and analyzed with ImageJ software (National Institute of Hearth, Bethesda, MD). The diameters and frequency of vessels and cell wall thickness of wood fibers were measured according to our previous report (Pertiwi et al 2017a).

Statistical Analysis

For the statistical analysis, R software version 4.0.3 (R Core Team 2020) was used. For evaluation of radial variations of cell morphologies, the following four mixed-effects models (Table 2) were developed by using the lmer function in the lme4 packages (Bates et al 2015) and the nlme function in the nlme package (Pinheiro and Bates 2000). The model with the minimum Akaike Information Criterion (AIC, Akaike 1998) was considered as the best fitted model among four models (Eqs 1-4 in Table 2).

The following intercept-only linear mixed-effects model was also developed to evaluate the effects of radial growth rate on cell morphologies:

$$y_{ij} = \mu + Category_j + e_{ij} \quad (5)$$

where y_{ij} is the ith measured values of the jth category, μ is general mean, $Category_j$ is random effect of category, and e_{ij} is residual.

For evaluating the xylem maturation process, estimated cambial age at a certain radial position was calculated by the radius (stem diameter at 1.3 m above the ground/2) dividing by tree age (Chowdhury et al 2009b). By using the best fitted

Table 2. Model form and comparison of AIC in each model for radial variation of each cell morphology in relation to distance from pith.

Function	Eq	Model	AIC					
			VEL	WFL	VD	VF	WFD	WFWT
Linear	(1)	$y_{ij} = \beta_0 x_{ij} + \beta_1 + u_{1j} + e_{ij}$	—	—	—	—	—	**−198.70**
Logarithmic	(2)	$y_{ij} = \beta_0 \ln x_{ij} + \beta_1 + u_{1j} + e_{ij}$	−519.64	−81.03	—	**448.24**	592.34	−191.11
Quadratic	(3)	$y_{ij} = \beta_0 x_{ij}^2 + \beta_1 x_{ij} + \beta_2 + u_{2j} + e_{ij}$	−526.28	−121.07	1140.46	464.51	**564.43**	−177.13
Michaelis–Menten	(4)	$y_{ij} = \beta_0 x_{ij} / (\beta_1 + x_{ij}) + \beta_2 + u_{2j} + e_{ij}$	**−532.68**	**−156.98**	**1106.41**	488.50	—	—

Eq, equation number; AIC, Akaike information criterion; VEL, vessel element length; WFL, wood fiber length; VD, vessel diameter; VF, vessel frequency; WFD, wood fiber diameter; WFWT; wood fiber wall thickness; y_{ij}, measured value for the ith radial position from the pith of the jth individual tree; x_{ij}, the ith radial position from the pith of the jth individual tree; β_0, β_1, and β_2, fixed-effect parameters; u_{1j} and u_{2j}, random-effect parameters of β_1 and β_2 at the individual level; e_{ij}, residual. Bold indicates minimum AIC among four models in each cell morphology. Hyphen indicates that the formula was not converged.

model from Eqs (1) to (4) in each cell morphology, radial variation of the cell morphology in relation to cambial age (the *i*th estimated cambial age was used instead of the *i*th radial distance from pith in the selected equation for radial variation of cell morphologies) were also evaluated. Then, mean absolute error (MAE) was calculated for both models (explanatory variables: radial distance from pith or estimated cambial age) by the method described in our previous report (Nezu et al 2022). In addition, normality of residuals in the both models was visually confirmed by quantile–quantile (Q–Q) plot. After that, the model with minimum MAE was considered as the best model for explaining the xylem maturation process.

Boundary of core wood and outer wood was determined by increasing ratio of cell length (Honjo et al 2005). Cell lengths were estimated at 1 mm interval up to 250 mm from pith by using the selected models with only fixed-effect parameter for cell length. Increasing ratio of cell length were calculated at 1 mm interval from pith.

RESULTS

Table 3 shows statistical values of cell morphologies. Mean value of nine trees was 0.59 mm in vessel element length, 2.16 mm in wood fiber length, 221 μm in vessel diameter, two vessels/mm^2 in vessel frequency, 35.5 μm in wood fiber diameter, and 1.03 μm in wood fiber wall thickness, respectively.

Results of model selection for radial variation of cell morphologies are shown in Table 2. Michaelis–Menten equation [Eq (4)] was fitted on radial variations of cell lengths and vessel diameter (Fig 1, Tables 2 and 4). Radial variation of vessel frequency, wood fiber diameter, and wood fiber wall thickness were well explained by logarithmic formula [Eq (2)], quadratic formula [Eq (3)], and linear formula [Eq (1)], respectively (Fig 1, Tables 2 and 4).

Table 5 shows variance components obtained by Eq (5) in each cell morphology. The model of wood fiber diameter was singular fitting. The Variance component ratio of category was 66.8%, 46.1%, 31.4%, 1.5%, and 33.7% for vessel element length, wood fiber length, vessel diameter, vessel frequency, and wood fiber wall thickness, respectively.

Values of MAE in selected models for radial variations of cell morphologies in relation to distance from pith or estimated cambial age were shown in Table 6. Smaller values of MAE obtained in the models in relation to distance from pith were found in all cell morphologies, except for vessel frequency and wood fiber diameter.

Figure 2 shows increasing ratio of cell length in relation to distance from pith. The values of distance from pith in which increase ratio of cell length became <1%, 0.5%, and 0.3% were 1.4, 5.8, and 10.4 cm in wood fiber length, and 0.8, 3.1, and 5.5 cm in vessel element length, respectively.

DISCUSSION

Cell Morphologies

The fiber length of *O. pyramidale* (2.16 mm, Table 3) was longer than those in other tropical

Table 3. Mean and standard deviation of each cell morphology for nine trees.

Cell morphology	Slow growth (n = 3)	Medium growth (n = 3)	Fast growth (n = 3)	Total (n = 9)
VEL (mm)	0.57 ± 0.02	0.58 ± 0.02	0.62 ± 0.00	0.59 ± 0.03
WFL (mm)	2.06 ± 0.07	2.16 ± 0.15	2.28 ± 0.06	2.16 ± 0.13
VD (μm)	218 ± 16	209 ± 20	236 ± 3	221 ± 18
VF (No./mm^2)	3 ± 1	3 ± 1	2 ± 0	2 ± 1
WFD (μm)	35.6 ± 1.5	35.5 ± 1.4	35.4 ± 1.7	35.5 ± 1.3
WFWT (μm)	0.96 ± 0.12	1.01 ± 0.04	1.12 ± 0.09	1.03 ± 0.10

n, number of trees; VEL, vessel element length; WFL, wood fiber length; VD, vessel diameter; VF, vessel frequency; WFD, wood fiber diameter; WFWT, wood fiber wall thickness. Values are mean ± standard deviation.

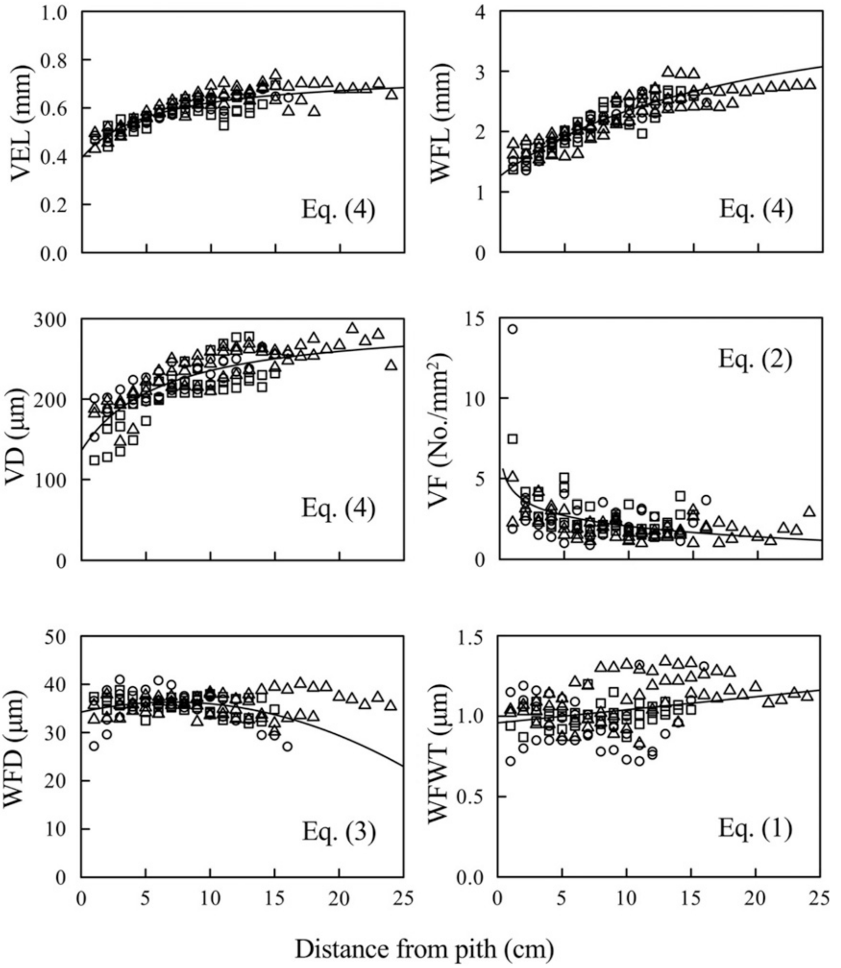

Figure 1. Radial variations of cell morphologies in relation to distance from pith. VEL, vessel element length; WFL, wood fiber length; VD, vessel diameter; VF, vessel frequency; WFD, wood fiber diameter; WFWT; wood fiber wall thickness. Eq (1), linear; Eq (2), logarithmic; Eq (3), quadratic; Eq (4), Michaelis–Menten (Table 2). Circle, triangle, and square indicate slow, medium, and fast growth, respectively. Solid line indicates regression line or curve based on the fixed parameters of the best model with smallest AIC in each cell morphology (Tables 2 and 4).

fast-growing trees, such as *A. mangium*, *A. auriculiformis*, *E. camaldulensis*, and *Falcataria moluccana* (Chowdhury et al 2009a; Honjo et al 2005; Ishiguri et al 2007; Nugroho et al 2012; Veenin et al 2005). However, the fiber length observed in the *O. pyramidale* in this study was similar to those of other species from the same family (Malvaceae), such as *Ceiba pentandra* (1.6-2.2 mm, Nordahlia et al 2016) and *Durio* spp. (1.4-2.3 mm, Ogata et al 2008). The vessel element length of *O. pyramidale* (0.59 mm, Table 3) was obviously longer than that of other tropical fast-growing tree species, such as *A. mangium* and *A. auriculiformis*, about 0.2 mm (Chowdhury et al 2009a; Honjo et al 2005) and other species in the same family such as *Heritiera* sp. (0.25 mm, Helmling et al 2018), *Abutilon stenopetalm* (0.22 mm), and *Bastardia viscosa* (0.19 mm) (Lindorf 1994). However, vessel element length of *O. pyramidale* was similar to that in *Durio* sp. (0.52 mm), which is the same family of *O. pyramidale* (Helmling et al 2018). As shown in Table 2 and Fig 1, Eq (4)

Table 4. Parameter estimates and associated standard errors (SE) and significance level of each parameter for the selected model in each cell morphology.

Cell morphology	Eq	Parameter	Estimates	SE	*t*-value	*p*-value
VEL	(4)	β_0	0.3704	0.0192	19.2660	<0.001
		β_1	7.0816	1.8745	3.7780	<0.001
		β_2	0.4066	0.0198	20.5330	<0.001
WFL	(4)	β_0	3.2383	0.3679	8.8023	<0.001
		β_1	19.6728	4.2111	4.6716	<0.001
		β_2	1.2640	0.0475	26.6338	<0.001
VD	(4)	β_0	162.49	11.91	13.64	<0.001
		β_1	6.37	1.68	3.78	<0.001
		β_2	136.18	9.16	14.86	<0.001
VF	(2)	β_0	−0.95	0.15	−6.39	<0.001
		β_1	4.26	0.31	13.57	<0.001
WFD	(3)	β_0	−0.042	0.009	−4.723	<0.001
		β_1	0.589	0.124	4.748	<0.001
		β_2	34.243	0.501	68.384	<0.001
WFWT	(1)	β_0	0.0081	0.0054	1.5020	0.247
		β_1	0.9584	0.0181	52.9810	<0.001

Eq, equation; SE, standard error; VEL, vessel element length; WFL, wood fiber length; VD, vessel diameter; VF, vessel frequency; WFD, wood fiber diameter; WFWT, wood fiber wall thickness. Eq (1), linear; Eq (2), logarithmic; Eq (3), quadratic; Eq (4), Michaelis–Menten. Equation of each cell morphology was selected as the best model in Table 2.

(Michaelis–Menten equations) was well fitted on the radial variations of cell length, suggesting that both wood fiber and vessel element lengths rapidly increased up to certain radial position from pith and then it became almost the stable. A distinct radial profile of vessel element length has been found in other tropical fast-growing tree species, such as *A. mangium* and *A. auriculiformis*: the vessel element length in these species is relatively constant from the pith toward the bark (Chowdhury et al 2009a; Honjo et al 2005). Thus, wood fiber and vessel element lengths in *O. pyramidale* showed relatively large elongation from the pith to the bark compared with those in other tropical fast-growing tree species, such as *Acacia* species.

Radial variation of vessel diameter was also well explained by Eq (4) (Michaelis–Menten equations, Table 2): vessel diameter showed rapid increase near the pith side and it gradually increased or become almost stable toward the bark side (Fig 1). The similar tendency in vessel diameter was also found in other fast-growing tree species, such as *Dysoxylum mollissimum* (Ishiguri et al 2016) and *Azadiracta excelsa* (Wahyudi et al 2016). Da Silva and Kyriakides (2007) reported

Table 5. Parameter estimates, standard errors (SE), and variance component for the models given by the Eq (5) for each cell morphology.

Cell morphology	Estimates	SE	Variance: Category	Variance: Residual	Variance component ratio of category (%)
VEL	0.590	0.015	0.00056	0.00028	66.8
WFL	2.164	0.063	0.00862	0.01005	46.1
VD	221.1	7.8	105.8	230.7	31.4
VF	2.5	0.2	0.0067	0.4478	1.5
WFWT	1.032	0.046	0.00390	0.00766	33.7

SE, standard error; VEL, vessel element length; WFL, wood fiber length; VD, vessel diameter; VF, vessel frequency; WFD, wood fiber diameter; WFWT, wood fiber wall thickness. Variance component ratio of category was calculated by dividing category variance by total variance (category + residual).

Table 6. Mean absolute error (MAE) for the developed models of radial variations for each cell morphology in relation to distance from pith or estimated cambial age.

		MAE	
Cell morphology	Eq	Distance from pith	Estimated cambial age
VEL	(4)	**0.025**	0.032
WFL	(4)	**0.139**	0.327
VD	(4)	**15.6**	18.4
VF	(2)	1.4	**1.0**
WFD	(3)	2.28	**1.90**
WFWT	(1)	**0.105**	0.109

Eq, equation listed in Table 2; VEL, vessel element length; WFL, wood fiber length; VD, vessel diameter; VF, vessel frequency; WFD, wood fiber diameter; WFWT, wood fiber wall thickness. Eq (1), linear; Eq (2), logarithmic; Eq (3), quadratic; Eq (4), Michaelis–Menten. Bold values indicate minimum MAE in each property.

that the vessel diameter in *O. pyramidale* was around 150-250 μm. In addition, the vessel diameter of *O. pyramidale* obtained in the present study was similar or slightly smaller than those of other species belonging to Malvaceae (Helmling et al 2018; Nordahlia et al 2016). Thereby, the vessel diameter values obtained in the present study were in accordance with those of the previous reports.

Da Silva and Kyriakides (2007) reported that the fiber wall thickness of *O. pyramidale* changed along with the density. As described in our previous study (Pertiwi et al 2017a), we found that the mean value of radial variation in basic density of *O. pyramidale* was almost constant from pith up to 8 cm and then increased toward the bark. The mean value of fiber wall thickness slightly increased from pith to the bark, which was well explained by Eq (1) (Table 2, Fig 1). Thus, the increase of basic density in *O. pyramidale* might be correlated with increase of the wood fiber wall thickness. The wood fiber wall thickness of *O. pyramidale* wood is very small, around 1.03 μm (Table 3). Earlier study on *O. pyramidale* wood was carried out by Easterling et al (1982). They reported that the double wall thickness of *O. pyramidale* wood was 1.5 μm. In addition, Ogata et al (2008) mentioned that the wood fiber wall thickness of *O. pyramidale* is very thin, even though they did not report its real value. The wood fiber wall thickness in some species belong to Malvaceae family is around 2-5 μm, such as *Bombax ceiba*, *Bombax anceps*, *Bombax valentonit*, and *C. pentandra* (Nordahlia et al 2016). Wiemann and Williamson (1988) reported that the genetic character of pioneer tree species produces the cells as many as possible, and there is almost no time for cell wall thickening during early-stage growth. Thus, characteristics of *O. pyramidale* as pioneer tree species in tropics might be lead that the *O. pyramidale* wood possess the thinnest cell wall in early-stage growth among these Malvaceae family.

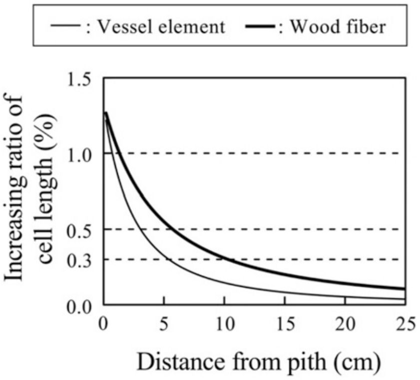

Figure 2. Radial variations of increasing ratio of cell lengths. Increasing ratio of cell lengths was determined by the best model with only fixed-effect parameters listed in Tables 2 and 4.

Effects of Radial Growth Rate on Cell Morphologies

Singular fitting on the model means that variances of one or more linear combinations of effects are (close to) zero (Bates et al 2015). The effect of the radial growth rate on wood fiber diameter was minimal in *O. pyramidale* because the developed model [Eq (5)] was singular fitting in wood fiber diameter. On the other hand, higher values of variance component ratio of growth category indicate that the measured properties may be affected by radial growth rate, suggesting that growth category influenced on the many cell morphologies in *O. pyramidale* (Table 5). However, fast-growth trees could be characterized by longer cell length, larger vessel diameter, and thicker cell wall of wood fiber (Table 3). In addition, the highest mean values of basic density and compressive strength were found in fast-growth trees among three growth categories (Table 1, Pertiwi et al 2017a). These characteristics in cell morphologies might not have negative impact for utilization of wood from this species as solid wood. It is concluded that the faster growth characteristics of this species did not always produce the lower quality of wood. Similar results were obtained in other tropical fast-growing tree species (Aiso-Sanada et al 2019; Hidayati et al 2017; Ishiguri et al 2016; Kojima et al 2009a,b; Makino et al 2012; Pertiwi et al 2017a,b; Wahyudi et al 2016). The characteristics of trees in fast-growth category in this study might be closely related with radial variations of cell morphologies (Fig 1): wood after about 10 cm from pith was longer cell lengths and thicker cell wall of wood fibers.

Xylem Maturation Process

Smaller values of MAE obtained in the models in relation to distance from pith were observed in all cell morphologies, except for vessel frequency and wood fiber diameter (Table 6), suggesting that radial variation of almost all cell morphologies in this species can be well-explained as function of distance from pith. It is thus concluded that the xylem maturation in *O. pyramidale* trees depends on the diameter growth rather than cambial age. Xylem maturation depending on diameter growth were also recognized in the many tropical fast-growing trees (Hidayati et al 2017; Honjo et al 2005; Ishiguri et al 2016; Kojima et al 2009a,b; Pertiwi et al 2018). Thus, characteristics of xylem maturation depending on diameter growth might be one of the characteristics in tropical fast-growing trees.

We previously reported that radial variations of basic density and mechanical properties of this species were almost constant up to 8 cm from pith and then sharply increased toward the bark (Pertiwi et al 2017a). As shown in Fig 2, the distance from pith in which increase ratio of cell length became $<$0.3% were 10.4 cm in wood fiber length, and 5.5 cm in vessel element length, respectively. Although the distance from pith showing increase ratio $<$0.3% was differed between wood fiber length and vessel element length, the boundary between core wood and outer wood judging from increase ratio of 0.3% was almost similar to the boundary determined by the radial variations of basic density and mechanical properties reported in a previous report (Pertiwi et al 2017a). Thus, it is considered that xylem maturation starts after 5-10 cm from pith (estimated age = 1.7-3.3 yr for 5 cm, and 3.4-6.5 cm for 10 cm) in this species.

Core wood (or sometimes referred as juvenile wood) in tropical hardwoods is characterized by lower wood density and strength properties with larger variations of cell morphologies and wood properties. On the other hand, higher wood density and strength properties with smaller variations of cell morphologies and wood properties are found in outer wood (or sometimes referred as mature wood) in hardwood species in tropics (Makino et al 2012; Wahyudi et al 2014). We previously reported that the value around pith area and near bark side was about 0.1 and 0.2 g/cm^3 in basic density, 10 and 20 MPa in compressive strength parallel to grain, 3 and 10 GPa in modulus of elasticity, and 15 and 40 MPa in modulus of rupture, respectively (Pertiwi et al 2017a). From the results obtained in the previous study and the present study, core wood (up to 5-10 cm from pith) and outer wood (after 5-10 cm from pith) can be characterized as follows: 1) core wood is lower basic density and mechanical properties with shorter cell length and thinner wood fiber wall but variations of basic density and mechanical properties are small, 2) outer wood is higher basic density and mechanical properties with longer cell length and thicker wood fiber wall but variations of basic density and mechanical properties are large. Thus, *O. pyramidale* trees might have different strategies of xylem maturation compared with other tropical fast-growing tree species. Further research is needed to clarify the relationships between xylem maturation process and tree survival strategies in pioneer species (eg sensitivity to light) in *O. pyramidale* as well as other tropical fast-growing tree species.

CONCLUSION

In the present study, the radial variations of anatomical characteristics were investigated for 7-yr-old

O. pyramidale trees with different radial growth rate by using linear or nonlinear mixed-effect models for clarifying xylem maturation process and effects of radial growth rate on the anatomical characteristics in this species. Results of model selection for radial variations of cell morphologies revealed that almost all cell morphologies, except for wood fiber diameter and wood fiber wall thickness, increased or decreased up to certain radial position from pith and then became almost stable. Variance component ratio of growth category showed relatively higher values in all cell morphologies except for vessel frequency and wood fiber diameter, suggesting that cell morphologies of this species were influenced by the radial growth rate. However, these characteristics in cell morphologies might not have negative impact for utilization of wood from this species as solid wood. It is concluded that the faster growth characteristics of this species did not always produce the lower quality of wood. Smaller values of MAE obtained in the models in relation to distance from pith were found in all cell morphologies, except for vessel frequency and wood fiber diameter. Thus, xylem maturation of this species mainly depended on diameter growth rather than cambial age. Boundary of core wood and outer wood was 5-10 cm from pith in which increasing ratio of cell length reached $<0.3\%$. Core wood was characterized as lower wood density and mechanical properties with shorter cell lengths and thinner wood fiber walls, whereas outer wood was characterized as higher wood density and mechanical properties with longer cell length and thicker wood fiber walls. In conclusion, radial growth promotion by intensive silvicultural treatments for plantation of this species will not always result in producing lower quality of wood.

ACKNOWLEDGMENTS

The authors express their sincere thanks to Mr. Setiyo Budi Nugroho, Parta Wood, Surabaya, Indonesia, for providing us wood materials, and to Mr. Soekmana Wedatama and Mr. Dany Mahardhika for helping us in the field experiments.

REFERENCES

Aiso-Sanada H, Ishiguri F, Diloksumpun S, Nezu I, Tanabe J, Ohshima J, Yokota S (2019) Effects of thinning on anatomical characteristics and wood properties of 12-year-old *Eucalyptus camaldulensis* trees planted in Thailand. Tropics 28:67-73.

Akaike H (1998) Information theory and an extension of the maximum likelihood principle. Pages 199-213 *in* E Parzen, K Tanabe, and G Kitagawa, eds. Selected papers of Hirotsugu Akaike. Springer series in statistics (Perspectives in statistics). Springer, New York.

Auty D, Gardiner BA, Achim A, Moore JR, Cameron AD (2013) Models for predicting microfibril angle variation in Scots pine. Ann Sci 70:209-218.

Bates D, Mächler M, Bolker BM, Walker SC (2015) Fitting linear mixed-effects models using lme4. J Stat Softw 67: 1-48.

Bhat KM, Priya PB, Rugmini P (2001) Characterisation of juvenile wood in teak. Wood Sci Technol 34:517-532.

Chowdhury MQ, Ishiguri F, Iizuka K, Hiraiwa T, Matsumoto K, Takashima Y, Yokota S (2009a) Wood property variation in *Acacia auriculiformis* growing in Bangladesh. Wood Fiber Sci 41:359-365.

Chowdhury MQ, Ishiguri F, Iizuka K, Takashima Y, Matsumoto K, Hiraiwa T, Ishido M, Sanpe H, Yokota S, Yoshizawa N (2009b) Radial variations of wood properties in *Casuarina equisetifolia* growing in Bangladesh. J Wood Sci 55:139-143.

Da Silva A, Kyriakides S (2007) Compressive response and failure of balsa wood. Int J Solids Struct 44:8685-8717.

Dahlen J, Auty D, Eberhardt TL (2018) Models for predicting specific gravity and ring width for loblolly pine from intensively managed plantations, and implications for wood utilization. Forests 9:292.

Easterling KE, Harrysson R, Gibson LJ, Ashby MF (1982) On the mechanics of balsa and other woods. Proc R Soc Lond A 383:31-41.

Erdene-Ochir T, Ishiguri F, Nezu I, Tumenjargal B, Sarkhad M, Ohshima J, Yokota S (2021) Within-tree and radial variations of wood properties in naturally regenerated trees of *Betula platyphylla* grown in Nikko, Japan. Int Wood Prod J 12:95-106.

Fujimoto T, Koga S (2010) An application of mixed-effects model to evaluate the effects of initial spacing on radial variation in wood density in Japanese larch (*Larix kaempferi*). J Wood Sci 56:7-14.

Helmling S, Olbrich A, Heinz I, Koch G (2018) Atlas of vessel elements: Identification of Asian timbers. IAWA J 39:249-352.

Hidayati H, Ishiguri F, Makino K, Tanabe J, Aiso H, Prasetyo VE, Marsoem SN, Wahyudi I, Iizuka K, Yokota S (2017) The effects of radial growth rate on wood properties and anatomical characteristics and an evaluation of the xylem maturation process in a tropical fast-growing tree species, *Gmelina arborea.* Forest Prod J 67:297-303.

Honjo K, Furukawa I, Sahri MH (2005) Radial variation of fiber length increment in *Acacia mangium.* IAWA J 26:339-352.

Ishiguri F, Aiso H, Hirano M, Yahya R, Wahyudi I, Ohshima J, Iizuka K, Yokota S (2016) Effects of radial growth rate on anatomical characteristics and wood properties of 10-year-old *Dysoxylum mollissimum* trees planted in Bengkulu, Indonesia. Tropics 25:23-31.

Ishiguri F, Eizawa J, Saito Y, Iizuka K, Yokota S, Priadi D, Sumiasri N, Yoshizawa N (2007) Variation in the wood properties of *Paraserianthes falcataria* planted in Indonesia. IAWA J 28:339-348.

Kojima M, Yamamoto H, Marsoem SN, Okuyama T, Yoshida M, Nakai T, Yamashita S, Saegusa K, Matsune K, Nakamura K, Inoue Y, Arizono T (2009a) Effects of the lateral growth rate on wood quality of *Gmelina arborea* from 3.5-, 7- and 12-year-old plantations. Ann Sci 66:507.

Kojima M, Yamamoto H, Yoshida M, Ojio Y, Okumura K (2009b) Maturation property of fast-growing hardwood plantation species: A view of fiber length. For Ecol Mgmt 257:15-22.

Lindorf H (1994) Eco-anatomical wood features of species from a very dry tropical forest. IAWA J 15:361-376.

Makino K, Ishiguri F, Wahyudi I, Takashima Y, Iizuka K, Yokota S, Yoshizawa N (2012) Wood properties of young *Acacia mangium* trees planted in Indonesia. Forest Prod J 62:102-106.

Midgley S, Blyth M, Howcroft N, Midgley D, Brown A (2010) Balsa: Biology, production and economics in Papua New Guinea. ACIAR Technical Reports No. 73. Australian Centre for International Agricultural Research, Canberra. 98 pp.

Nezu I, Ishiguri F, Aiso H, Hiraoka Y, Wasli ME, Ohkubo T, Ohshima J, Yokota S (2022) Secondary xylem maturation evaluated by modeling radial variations in anatomical characteristics and wood properties of *Shorea macrophylla* (De Vr.) Ashton planted in Sarawak, Malaysia. Trees (Berl) 36:659-668.

Nezu I, Ishiguri F, Aiso-Sanada H, Diloksumpun S, Ohshima J, Iizuka K, Yokota S (2020) Repeatability of growth characteristics and wood properties for solid wood production from *Eucalyptus camaldulensis* half-sib families growing in Thailand. Silvae Genet 69:36-43.

Nordahlia AS, Toraini T, Chung RCK, Lim SC, Nadiah I, Azahana NA, Solihani NS (2016) Comparative wood anatomy of three Bombax species and *Ceiba pentandra* (Malvaceae; Bombacoideae) in Malaysia. Malay Nat J 68:203-216.

Nugroho DW, Marsoem SN, Yasue K, Fujiwara T, Nakajima T, Hayakawa M, Nakaba S, Yamagishi Y, Jin H-O, Kubo T, Funada R (2012) Radial variations in the anatomical characteristics and density of the wood of *Acacia mangium* of five different provenances in Indonesia. J Wood Sci 58:185-194.

Ogata K, Fujii T, Abe H, Baas P (2008) Identification of the timbers of Southeast Asia and the Western Pacific. Kaiseisha Press, Ohtsu. 408 pp.

Pertiwi YAB, Aiso H, Ishiguri F, Marsoem SN, Yokota S (2018) Radial variation of wood properties in *Neolamarckia cadamba* trees from an East Java community forest. South For 80:351-359.

Pertiwi YAB, Aiso H, Ishiguri F, Ohshima J, Yokota S (2017a) Effect of radial growth rate on wood properties in balsa (*Ochroma pyramidale*) grown in East Java, Indonesia. Int Wood Prod J 8:227-232.

Pertiwi YAB, Aiso H, Ishiguri F, Wedatama S, Marsoem SN, Ohshima J, Iizuka K, Yokota S (2017b) Effect of radial growth rate on wood properties of *Neolamarckia cadamba.* J Trop For Sci 29:30-36.

Pinheiro JC, Bates DM (2000) Mixed-effects models in S and S-PLUS. Springer Verlag, New York. 528 pp.

R Core Team (2020) R: A language and environment for statistical computing. R Foundation for Statistical Computing, Vienna, Austria. https://www.R-project.org/ (28 October 2020).

Rueda R, Williamson GB (1992) Radial and vertical wood specific gravity in *Ochroma pyramidale* (Cav. Ex Lam.) Urb. (Bombaceae). Biotropica 24:512-518.

Sosef MSM, Hong LT, Prawirohatmodjo S (1998) Plant resources of South-East Asia No 5(3). Timber trees lesser-known timbers. Prosea Foundation, Bogor. 859 pp.

Tsuchiya R, Furukawa I (2009a) Radial variation in the size of axial elements in relation to stem increments in *Quercus serrata.* IAWA J 30:15-26.

Tsuchiya R, Furukawa I (2009b) Radial variation of vessel lumen diameter in relation to stem increment in 30 hardwood species. IAWA J 30:331-342.

Veenin T, Fujita M, Nobuchi T, Siripatanadilok S (2005) Radial variations of anatomical characteristics and specific gravity in *Eucalyptus camaldulensis* clones. IAWA J 26:353-361.

Wahyudi I, Ishiguri F, Aiso H, Istikowati WT, Sutiya B, Takashima Y, Ohkubo T, Iizuka K, Yokota S (2014) Anatomical characteristics and wood properties of *Melaleuca leucadendron* naturally growing in secondary forest in Indonesia. Aust For 77:168-172.

Wahyudi I, Ishiguri F, Makino K, Aiso H, Takashima Y, Ohshima J, Iizuka K, Yokota S (2016) Evaluation of xylem maturation and the effects of radial growth rate on anatomical characteristics and wood properties of *Azadirachta excelsa* planted in Indonesia. J Ind Acad Wood Sci 13:138-144.

Wiemann MC, Williamson GB (1988) Extreme radial changes in wood specific gravity in some tropical pioneers. Wood Fiber Sci 20:344-349.

Williamson GB, Wiemann MC (2010) Age-dependent radial increases in wood specific gravity of tropical pioneers in Costa Rica. Biotropica 42:590-597.

EDITORIAL AND PUBLICATION POLICY

Wood and Fiber Science as the official publication of the Society of Wood Science and Technology publishes papers with both professional and technical content. Original papers of professional concern, or based on research of international interest dealing with the science, processing, and manufacture of wood and composite products of wood or wood fiber origin will be considered.

All manuscripts are to be written in US English, the text should be proofread by a native speaker of English prior to submission. Any manuscript submitted must be unpublished work not being offered for publication elsewhere.

Papers will be reviewed by referees selected by the editor and will be published in approximately the order in which the final version is received. Research papers will be judged on the basis of their contribution of original data, rigor of analysis, and interpretations of results; in the case of reviews, on their relevancy and completeness.

As of January 1, 2022, Wood and Fiber Science will be an online only, Open Access journal. There will be no print copies. Color photos/graphics will be offered at no additional cost to authors. The Open Access fee will be $1800/article for SWST members and $2000/article for nonmembers. The previous five years of articles are still copyright protected (accept those that are identified as Open Access) and can be accessed through member subscriptions. Once a previous article has reached its 5th anniversary date since publication, it becomes Open Access.

Technical Notes

Authors are invited to submit Technical Notes to the Journal. A Technical Note is a concise description of a new research finding, development, procedure, or device. The length should be **no more than two printed pages** in WFS, which would be five pages or less of double-spaced text (TNR12) with normal margins on 8.5 x 11 paper, including space for figures and tables. In order to meet the limitation on space, figures and tables should be minimized, as should be the introduction, literature review and references. The Journal will attempt to expedite the review and publication process. As with research papers, Technical Notes must be original and go through a similar double-blind, peer review process.

On-line Access to *Wood and Fiber Science* Back Issues

SWST is providing readers with a means of searching all articles in *Wood and Fiber Science* from 1968 to present Articles from 1968 to 2017 are available to anyone, but in order to see 2017 to 2021 articles you must have an SWST membership or subscription. SWST members and subscribers have full search capability and can download PDF versions of the papers If you do not have a membership or subscription, you will not be able to view the full-text pdf.

Visit the SWST website at http://www.swst.org and go to Wood & Fiber Science Online. Click on either SWST Member Publication access (SWST members) or Subscriber Publication access (Institution Access). All must login with their email and password on the HYPERLINK "http://www.swst.org" www.swst.org site, or use their ip authentication if they have a site license.

As an added benefit to our current subscribers, you can now access the electronic version of every printed article along with exciting enhancements that include:

- IP authentication for institutions (only with site license)
- Enhanced search capabilities
- Email alerting of new issues
- Custom links to your favorite titles

(ISSN 0735-6161)
CODEN WOOFAJ

WOOD AND FIBER SCIENCE

JOURNAL OF THE SOCIETY OF WOOD SCIENCE AND TECHNOLOGY

VOLUME 54 APRIL 2022 NUMBER 2

CONTENTS

Articles

Volume 54, Number 2 WOOD AND FIBER SCIENCE April 2022